NASA CONTRACTOR REPORT

NASA CR-2391

NASA CR-2391

A FINITE ELEMENT SOLUTION ALGORITHM FOR THE NAVIER-STOKES EQUATIONS

by A. J. Baker

Prepared by
BELL AEROSPACE COMPANY
Buffalo, N.Y. 14240
for Langley Research Center

NATIONAL AERONAUTICS AND SPACE ADMINISTRATION • WASHINGTON, D. C. • JUNE 1974

1. Report No.	2. Government Accession No.	3. Recipient's Catalog No.
NASA CR-2391		

4. Title and Subtitle	5. Report Date
A Finite Element Solution Algorithm for the Navier-Stokes Equations	June 1974
	6. Performing Organization Code
7. Author(s)	8. Performing Organization Report No.
A.J. Baker	D9198-950001
9. Performing Organization Name and Address	10. Work Unit No.
Bell Aerospace Company P.O. Box One Buffalo, New York 14240	11. Contract or Grant No. NAS 1-11809
	13. Type of Report and Period Covered
12. Sponsoring Agency Name and Address	Contractor Report
National Aeronautics and Space Administration Washington, D.C. 20546	14. Sponsoring Agency Code

15. Supplementary Notes

Final Report

16. Abstract

A finite element solution algorithm is established for the two-dimensional Navier-Stokes equations governing the steady-state kinematics and thermodynamics of a variable viscosity, compressible multiple-species fluid. For an incompressible fluid, the motion may be transient as well. The primitive dependent variables are replaced by a vorticity-streamfunction description valid in domains spanned by rectangular, cylindrical and spherical coordinate systems. Use of derived variables provides a uniformly elliptic partial differential equation description for the Navier-Stokes system, and for which the finite element algorithm is established. Explicit non-linearity is accepted by the theory, since no psuedo-variational principles are employed, and there is no requirement for either computational mesh or solution domain closure regularity. Boundary condition constraints on the normal flux and tangential distribution of all computational variables, as well as velocity, are routinely piecewise enforceable on domain closure segments arbitrarily oriented with respect to a global reference frame.

A natural coordinate function description is established for the finite element approximation functions that renders matrix evaluation straightforward and accurate. The several explicitly non-linear terms in the equation system are shown to be expressible in terms of standard matrix forms. The consequence of integrating various terms by parts is thoroughly evaluated. The COMOC computer program system embodies the established finite element algorithm and matrix generator package built upon the natural function description. Numerical solutions for incompressible internal flow problems have illustrated solution accuracy, convergence, and versatility. Flow fields with imbedded regions of recirculation have been computed as well as transient solution domain closure shapes. Evaluation of pressure computations has been performed as well as extension to compressible flow field solutions.

17. Key Words (Selected by Author(s))	18. Distribution Statement
Finite Element Navier-Stokes Equations Natural Coordinate Functions Computer Program	Unclassified - Unlimited

19. Security Classif. (of this report)	20. Security Classif. (of this page)	21. No. of Pages	22. Price*
Unclassified	Unclassified	75	$3.75

*For sale by the National Technical Information Service, Springfield, Virginia 22151

Page Intentionally Left Blank

CONTENTS

ILLUSTRATIONS

TABLES

A FINITE ELEMENT SOLUTION ALGORITHM FOR THE NAVIER-STOKES EQUATIONS

By
A.J. Baker
Bell Aerospace Company

SUMMARY

A finite element solution algorithm is established for the two-dimensional Navier-Stokes equations governing the steady-state kinematics and thermodynamics of a variable viscosity, compressible multiple-species fluid. For an incompressible fluid, the motion may be transient as well. The primitive dependent variables are replaced by a vorticity-streamfunction description valid in domains spanned by rectangular, cylindrical and spherical coordinate systems. Use of derived variables provides a uniformly elliptic partial differential equation description for the Navier-Stokes system, and for which the finite element algorithm is established. Explicit nonlinearity is accepted by the theory, since no psuedo-variational principles are employed, and there is no requirement for either computational mesh or solution domain closure regularity. Boundary condition constraints on the normal flux and tangential distribution of all computational variables, as well as velocity, are routinely piecewise enforceable on domain closure segments arbitrarily oriented with respect to a global reference frame.

A natural coordinate function description is established for the finite element approximation functions that renders matrix evaluation straightforward and accurate. The several explicitly nonlinear terms in the equation system are shown to be expressible in terms of standard matrix forms. The consequence of integrating various terms by parts is thoroughly evaluated. The COMOC computer program system embodies the established finite element algorithm and matrix generator package built upon the natural function description. Numerical solutions for incompressible internal flow problems have illustrated solution accuracy, convergence, and versatility. Flow fields with imbedded regions of recirculation have been computed as well as transient solution domain closure shapes. Evaluation of pressure computations has been performed as well as extension to compressible flow field solutions.

INTRODUCTION

Numerical solution of a variety of field problems in mechanics has been made possible with the advent of the large digital computer. Development of solution procedures for specific disciplines has been highly problem oriented. As a result, little cross-fertilization has occurred that takes advantage of the uniform mathematical description for field problems in continuum mechanics. Specifically, finite difference methods have been almost universally employed for computational fluid mechanics, the electric analogy approach has been applied to heat conduction and seepage problems, while the finite element method has found wide acceptance for analysis of complex structural systems. Each of these approaches can now be viewed in a unifying manner as application of specific criteria within the Method of Weighted Residuals (MWR) (Reference 1), and satisfaction in a weighted average sense of the governing differential equations written on the discretized equivalent of the pertinent dependent variables. The select choice of weighting and approximation functions renders each approach identi-

fiable, including classical integral approaches like von Karman-Pohlhausen and Integral Method of Strips in boundary layer flow, and the many variations of Galerkin, Kantorovich and collocation methods.

Over the years, the finite element procedure has proven highly adaptable to solution of linear elliptic boundary value problems involving complex boundary conditions applied on irregularly shaped, non-coordinate surface solution domain closures. Its adaptation to quasilinear and/or nonlinear problem classes – for example, solution of the Navier-Stokes equations – has been held in abeyance, at least partially, by the common misconception that the method was constrained to problems having a differential equation description that could be equivalently cast into an extremization principle. This in turn led to derivation of a plethora of psuedo-variational statements for nonstationary field problems (see for example Reference 2) in an attempt to render the finite element method directly applicable to the broader problem class. Finite element solution of transient linear heat conduction in stationary continua drew much attention in the late 1960's (References 3, 4), and inclusion of implicit nonlinearity was eventually acceptable (Reference 5) within the constraints of "local" extremization. Extension to the Navier-Stokes equations using these concepts appeared theoretically difficult without gross assumptions on the concept of a local potential. However, about 1970 the connection between Galerkin criteria within MWR and equivalent extremization principles was established, the key items being performance of an integration by parts, identification of a numerical Lagrange multiplier, and Boolean assembly of the local finite element matrix equations into the global description. It could be readily proved that such a development, for a linear equation, produced a computational form that was identical to extremization of the equivalent stationary principle. However, since no linearity constraint existed in its derivation, the theory for finite element solution of nonlinear equations was established, especially for specific forms of the Navier-Stokes equations (References 6-8).

In this report, a finite element solution algorithm is established for the two-dimensional Navier-Stokes equations governing the kinematics and thermodynamics of a variable viscosity, compressible, multiple-species fluid. The primitive dependent variables are replaced by a vorticity-streamfunction description, which provides a uniformly elliptic differential equation system description for all computational variables. The preferred differential equation systems are established in rectangular, cylindrical and spherical Cartesian coordinate systems. The finite element algorithm is derived for the generalized, nonlinear elliptic boundary value problem of mathematical physics and contains no requirements for either computational mesh or solution domain closure regularity. Boundary condition constraints on the normal flux and tangential distribution of all computational dependent variables, as well as velocity, are routinely piecewise enforceable on domain closure segments arbitrarily oriented with respect to a global reference frame. The intrinsic finite element shapes for one-, two-, and three-dimensional domains spanned by linear approximation functions are the line, triangle and tetrahedron respectively. The area-coordinate concept of structural mechanics has been utilized to establish a natural coordinate function description for the finite element approximation to the Navier-Stokes equations. Adaptation of these functions represents a significant advance that has for the first time allowed analytical formulation of the complexly nonlinear matrix representations for specific terms in the equation system – in particular, the vorticity transport equation. The consequence of integration by parts of select nonlinear terms in the differential equation system is examined in detail, and the assumptive constraints are established according to which the generated surface integrals can be neglected or made to cancel. Establishment of the natural coordinate function description has allowed recognition of the many standard matrix forms that constitute the finite element algorithm for the nonlinear terms in the equation system and provides broad insight into the mechanics of the algorithm.

The finite element solution algorithm for the characteristic equation system has been embodied into the COMOC (Computational Continuum Mechanics) computer program system, specific variants of which have produced solutions in three-dimensional subsonic and supersonic viscous flow fields (References 9, 10) and nonlinear transient heat conduction (Reference 11) in addition to the Navier-Stokes solutions to be discussed. The COMOC system consists of four basic macro-modules, the first of which is Input wherein discretizations are formed and dependent variables initiated. The Geometry module establishes the non-standard element matrices for each finite element of the discretization and evaluates the matrix multipliers required for the standard matrices. All computations are performed in a local Cartesian coordinate system with automatic accounting for the lack of coordinate transformation invariance for other than rectangular Cartesian systems. The Integration module embodies solution algorithms for large-order ordinary differential and algebraic equation systems, either of which is produced by application of the finite element algorithm to the parent partial differential equation system. For discretized-equivalent initial value problems, the basic operation is evaluation of the derivative vector on an element basis and assembly of the global vector using Boolean algebra. For solution of an algebraic system, the diffusion (that is, "stiffness" in elasticity) matrix is formed on an element basis and the equation system inhomogeniety evaluated, if present. Each is then assembled into the global representation through Boolean algebra. The matrix equation system rank is established by evaluating boundary condition constraints, and the effective inverse found by equation solver techniques. The final Output module serves its standard function.

The Navier-Stokes Variant of COMOC has been evaluated for several problems to assess solution accuracy, convergence, versatility, and overall performance of the system. Accuracy studies were performed for developing flow in a duct, and convergence of velocity with discretization is numerically demonstrated. Factors affecting solution accuracy have been evaluated including non-uniform discretizations, the vorticity boundary condition, and the use of a "condensed" mass matrix for solving transient problems. A basic character of full Navier-Stokes solutions is prediction of imbedded regions of recirculation, and the finite element algorithm is assessed to correctly predict such phenomena for a sample problem without resorting to special boundary condition techniques. A stable solution for the rearward step problem has been obtained for the largest flow Reynolds number reported in the literature. Variations on this problem have illustrated stable solutions for time-dependent solution domain closure configurations and solutions in multiply-connected domains. Evaluation of the accuracy of pressure computations for these problems is presented as well as extension to flow fields with variable density. The computed results have yielded a favorable assessment of the viability of the solution algorithm and its computational embodiment.

NOMENCLATURE

a	boundary condition coefficient; unit vector
b	body force unit vector
B	body force
c	expansion coefficient; specific heat
D	diffusion coefficient
e	general alternating tensor
E	symmetric velocity gradient
Ec	Eckert Number

f	function of known argument
Fr	Froude Number
g	mass flow; function of known argument
h	metric coefficient
H	stagnation enthalpy
$\hat{i},\hat{j},\hat{k}$	rectangular Cartesian unit vectors
J	determinant of Cartesian space metric
k	function of known argument; thermal conductivity
K	generalized diffusion coefficient
L	characteristic length; natural coordinate function; arc length
Le	Lewis Number
M	Mach Number; number of finite elements
n	unit normal vector; summation limit
N	differential operator
p	pressure
Pr	Prandtl Number
Q,q	generalized dependent variable; energy source term
$\{r, \phi, \theta\}$	spherical Cartesian coordinate system
r	position vector; radius
R	domain of space variables; gas constant
Re	Reynolds Number
s	displacement
S	mass source term
t	time
T	temperature; total stress tensor; tensor
u, U	velocity
v	vector
W	weighting function
$\{x, y, z\}$	rectangular Cartesian coordinate system
x	independent space variables
y	rectangular Cartesian scalar components
Y	mass fraction
$\{z, r, \theta\}$	cylindrical Cartesian coordinate system
α	coefficient for spherical coordinates; mass fraction; direction cosine
γ	ratio of specific heats

Γ	finite element coefficient matrix
δ	Kronecker delta
∂R	closure of solution domain
ϵ	alternating tensor; strain; vector
η	differential operator
θ	angle
κ	coefficient
λ	Lagrange multiplier
μ	viscosity
ν	unit normal vector
ρ	density
σ	surface integral kernel
τ	stress tensor; domain integral kernel
ϕ	angle; function
ψ	x_3 scalar component of streamfunction
Ψ	vector potential
ω	x_3 scalar component of vorticity; wryness coefficient
Ω	vorticity vector
$\{\ \}$	column matrix
$[\ ]$	square matrix
$\lceil\ \rfloor$	diagonal matrix

Superscripts and Subscripts

*	approximate solution
'	temporal derivative
T	matrix transpose
$\wedge$	unit vector
$\rightarrow$	vector
$-$	average; constrained to domain closure
i, j, k, ℓ	tensor indices
m	pertaining to m^{th} subdomain (finite element)
∞	reference condition

THE NAVIER-STOKES EQUATIONS FOR A MULTICOMPONENT VISCOUS FLUID

The complete description of a fluid dynamical state is contained within the solution of the system of coupled, nonlinear, second order partial differential equations describing the local conservation of species, mass, linear (or angular) momentum, and energy, in conjunction with an appropriate specification of constitutive behavior and applicable initial and boundary conditions. In Cartesian tensor notation (see Appendix A) the conservation form of these differential equations is respectively

$$(\rho Y^a)_{,t} = -[\rho u_i Y^a - \rho D Y^a{}_{,i}]_{;i} + S^a \tag{1}$$

$$\rho_{,t} = -[\rho u_i]_{;i} \tag{2}$$

$$(\rho u_i)_{,t} = -[\rho u_i u_j + p\delta_{ij} - \tau_{ij}]_{;j} + \rho B_i \tag{3}$$

$$(\rho H - p)_{,t} = -[\rho u_i H - \tau_{ij} u_j - kT_{,i}]_{;i} + \rho \dot{Q} \tag{4}$$

The dependent variables have their usual fluid dynamic interpretation, with ρ the mass density, Y^a the mass fraction of the a^{th} species, u_i the local velocity vector, S^a the generation term of the a^{th} species, B_i the applicable body force, τ_{ij} the viscous stress tensor, H the stagnation enthalpy, p the pressure, T the temperature, and $\dot{Q}$ the local heat generation rate. In equations (1) - (4) the comma denotes partial differentiation of a scalar, while the semicolon indicates the vector derivative of a Cartesian tensor, the Cartesian equivalent of covariant differentiation of the contravarient components of a general tensor. The comma by t indicates the partial derivative with respect to time.

The solution of the equation system (1) - (4) requires specification of constitutive relationships between the dependent variables and the diffusion coefficient D, the stress tensor τ_{ij}, the viscosity μ and thermal conductivity k. A specification of an equation of state relating the thermodynamic variables is also required. For the laminar flow of a Newtonian fluid, the dynamic relations are contained within Stokes' viscosity law

$$\tau_{ij} \equiv 2\mu \left[E_{ij} - \frac{1}{3} E_{kk}\delta_{ij}\right] \tag{5}$$

$$E_{ij} \equiv \frac{1}{2}(u_{i;j} + u_{j;i}) \tag{6}$$

The thermodynamic properties are typically

$$p = p(\rho, Y^a, T) \tag{7}$$

$$H = H(\rho, T, u_i) = \int_0^T c_p \, dT \tag{8}$$

$$D^{a} = D(Y^{a}, u_i) \qquad (9)$$

$$S^{a} = S(Y^{a}) \qquad (10)$$

$$k = k(T) \qquad (11)$$

$$\mu = \mu(T) \qquad (12)$$

$$Q = Q(Y^{a}, T) \qquad (13)$$

The functional dependence indicated in equations (7) - (13) can be determined experimentally. Equations (1) - (13) form a deterministic system for the dependent variables Y^{a}, ρ, u_i, and T, and represent a well posed, initial-boundary value problem in mathematical physics for proper specification of these constraints.

Before transforming equations (1) - (13) into the desired form, it is convenient to nondimensionalize all variables to extract the useful non-dimensional groupings, the magnitudes of which characterize various flow regimes. Denoting non-dimensional variables by an asterisk, let

$$x_i = L x_i^{*} \qquad (14)$$

$$u_i = U_\infty u_i^{*} \qquad (15)$$

$$t = \frac{L}{U_\infty} t^{*} \qquad (16)$$

$$\rho = \rho_\infty \rho^{*} \qquad (17)$$

$$p = \rho_\infty U^2{}_\infty p^{*} \qquad (18)$$

$$\mu = \mu_\infty \mu^{*} \qquad (19)$$

$$T = T_\infty T^{*} \qquad (20)$$

$$c_p = c_{p_\infty} c_p^{*} \qquad (21)$$

$$k = \frac{c_p \mu}{Pr} \qquad (22)$$

$$Q = \frac{k_\infty T_\infty}{\rho_\infty L^2} Q^{*} \qquad (23)$$

$$D = \frac{Le}{Pr} \frac{\mu}{\rho} \qquad (24)$$

where the subscript (∞) variables are suitably selected reference values for the dynamic and thermodynamic variables, L is the characteristic length dimension, and the Lewis and Prandtl numbers are to be defined. (Note: in problems corresponding to very slow viscous flow, the pressure, equation (18), must be non-dimensionalized by a viscous rather than dynamical reference state.)

Substituting equations (14) - (24) for the dimensional variables in equations (1) - (4), and deleting the asterisk notation, yields the governing differential equations in non-dimensional form.

$$(\rho Y^{a})_{,t} = -\left[\rho u_i Y^{a} - \frac{Le}{Pr} \mu Y^{a}{}_{,i}\right]_{;i} + S^{a} \qquad (25)$$

$$\rho_{,t} = -[\rho u_i]_{;i} \qquad (26)$$

$$(\rho u_i)_{,t} = -\left[\rho u_i u_j + p\delta_{ij} - \frac{1}{Re} \tau_{ij}\right]_{;j} + \frac{1}{Fr} \rho b_i \qquad (27)$$

$$(\rho H - (Ec)\, p)_{,t} = -\left[\rho u_i H - \frac{Ec}{Re} \tau_{ij} u_j - \frac{1}{Re\, Pr} \mu H_{,i}\right]_{;i} + \frac{1}{Re\, Pr_\infty} \rho \dot{Q} \qquad (28)$$

Equations (25) - (28) introduce the important non-dimensional parameters for fluid dynamics as

$$\text{Reynolds Number:} \quad Re \equiv \frac{\rho_\infty U_\infty L}{\mu_\infty} \tag{29}$$

$$\text{Prandtl Number:} \quad Pr \equiv \frac{c_p \mu}{k} \tag{30}$$

$$\text{Eckert Number:} \quad Ec \equiv \frac{U_\infty^2}{c_{p_\infty} T_\infty} \tag{31}$$

$$\text{Froude Number:} \quad Fr \equiv \frac{U_\infty^2}{Lg} \tag{32}$$

$$\text{Lewis Number:} \quad Le \equiv \frac{\rho D}{\mu} Pr \tag{33}$$

In equation (27) the assumption that the applicable body force is gravity is evidenced in the term containing b_i, the unit vector parallel to the gravity vector. In equation (28) Pr_∞ is equation (30) evaluated at the reference conditions. For a thermodynamically perfect fluid,

$$Ec = (\gamma - 1) M^2_\infty \tag{34}$$

where γ is the ratio of specific heats and M_∞ is the reference Mach Number, defined as

$$M_\infty = \frac{U_\infty}{\sqrt{\gamma RT_\infty}} \tag{35}$$

DIFFERENTIAL EQUATION DEVELOPMENT FOR THE DESIRED PROBLEM CLASS IN FLUID MECHANICS

The solution of equations (25) - (28) represents a formidable task. It is desired to restrict the generality of the description to the degree that the concomitant mathematical advantages are applicable to non-trivial problems. The essence of the development is restriction to two independent space dimensions, but in which three-dimensional flows may exist.

Continuity Equation

From mathematical physics it is known that a vector field is completely defined when its divergence and curl are known. The vector field of fluid mechanics is velocity, and equation (26) defines the divergence of velocity in terms of the density. Identifying the mass flow vector g_i as ρu_i, the divergence of g_i vanishes for either incompressible or steady compressible flows. Henceforth, restrict consideration to these two distinct problem classes.

The vanishing divergence of g_i allows specification of g_i as the curl of some vector potential Ψ_i. No analytical benefit accrues from this specification (as does occur, for example in Maxwell's equations) in fluid mechanics, due primarily to the nonlinearity of equation (27). But a significant numerical benefit can occur if the mass flow vector g_i is planar, or if the three scalar components

of g_i are independent of one independent variable, as occurs in problems possessing axisymmetry. In either case, equation (26), for incompressible or steady compressible flow, is identically satisfied by the x_3 scalar component of the vector potential Ψ_i, in the form

$$g_i \equiv \rho u_i = \frac{1}{J} \epsilon_{3ij} \Psi_{3\,;j} + \rho u_3 \delta_{i3} \tag{36}$$

In equation (36), ϵ_{3ij} is the Cartesian alternating tensor, and J is the determinant of the space metric.

Since all problems of physical interest can be spanned by rectangular, cylindrical and/or spherical orthogonal coordinates, equation (36) can be written in terms of a scalar function ψ, and the gradient operator, as

$$\rho u_i \equiv \frac{1}{r \sin^a \phi} \epsilon_{3ij} \psi_{,j} + \rho u_3 \delta_{i_3} \tag{37}$$

In equation (37), a is non-zero only for spherical coordinates when it is unity, r is set equal to unity (and $u_3 \equiv 0$) for rectangular coordinates, and x_3 corresponds to the azimuthal angle (θ) in both cylindrical and spherical coordinates with domain $0 \leqslant x_3 \leqslant 2\pi$.

Equation (37) identically satisfies equation (26), in the three Cartesian coordinate systems, for both incompressible and steady compressible flow. For example, in spherical coordinates,

$$(\rho u_i)_{;i} = \left[\frac{1}{r \sin\phi} \epsilon_{3ij} \psi_{,j} + \rho u_3 \delta_{i3} \right]_{;i}$$

$$= \frac{1}{r^2 \sin\phi} \left[\left(\frac{1}{r \sin\phi} \psi_{,2} \right)_{;1} - \left(\frac{1}{r \sin\phi} \psi_{,1} \right)_{;2} + (\rho u_3)_{;3} \right]$$

Identifying x_i as $\{ r, \phi, \theta \}$ and transforming the vector derivative to partial differentiation in spherical coordinates, yields

$$(\rho u_i)_{;i} = \frac{1}{r^2 \sin\phi} \left[\left(\frac{1}{r \sin\phi} r^2 \sin\phi \frac{1}{r} \frac{\partial \psi}{\partial \phi} \right)_{,r} - \left(\frac{1}{r \sin\phi} r \sin\phi \frac{\partial \psi}{\partial r} \right)_{,\phi} + (\rho u_3)_{,\theta} \right]$$

$$= \frac{1}{r^2 \sin\phi} \left[\frac{\partial^2 \psi}{\partial \phi \, \partial r} - \frac{\partial^2 \psi}{\partial r \, \partial \phi} + 0 \right]$$

$$= 0$$

since ρu_3 is independent of x_3, i.e., θ. The proof in cylindrical and rectangular coordinates is similarly direct.

Compatibility Equation

With the zero divergence of the mass flow vector g_i ensured by identification of the streamfunction, it remains to obtain its curl. It is useful to identify the vorticity vector Ω_i

$$\Omega_i \equiv \frac{1}{J} \epsilon_{ijk} u_{k;j} \tag{38}$$

The x_3 scalar component (ω) of Ω_i, in the three orthogonal coordinate systems, is,

$$\omega = \frac{1}{r^a} \epsilon_{3ij} u_{j;i} \tag{39}$$

with a interpreted as before.

The vorticity scalar component ω will be employed as an auxiliary dependent variable; therefore, it is necessary that it be related to ψ, the primary dependent flow variable. Substituting for u_i from equation (37), the desired relation is

$$\omega = -\frac{1}{r^a} \left(\frac{1}{\rho r \sin^a \phi} \psi_{,k} \right)_{;k} \tag{40}$$

where use has been made of the skew-symmetric properties of the alternating tensor contraction

$$\epsilon_{3ij} \epsilon_{3jk} = -\delta_{ik} \tag{41}$$

In rectangular coordinates, equation (40) reduces to the familar Poisson equation involving the Laplacian operator. In the other two coordinate systems, equation (40) lacks certain metric coefficients of being the Laplacian operator.

The Curl of the Navier-Stokes Equation

Since the problem class is restricted from full-dimensional generality, a specification of the x_3 scalar component of the curl of g_i yields the desired differential equation. Using equation (27), the curl equation is

$$\epsilon_{3ki} \left\{ \rho u_{i,t} + \left[\rho u_i u_j + p \delta_{ij} - \frac{1}{Re} \tau_{ij} \right]_{;j} - \frac{1}{Fr} \rho b_i \right\}_{;k} = 0 \tag{42}$$

Since the pressure and (gravity) body force fields are conservative, their respective curls vanish identically. (The elimination of pressure as a coupled dependent variable is a prime computational feature of the transformation to vorticity - streamfunction variables.) Hence, equation (42) can be simplified to

$$\epsilon_{3ki} \left(\rho u_{i,t} \right)_{;k} = -\epsilon_{3ki} \left[\rho u_i u_j - \frac{1}{Re} \tau_{ij} \right]_{;jk} \tag{43}$$

It is required to transform the velocity vector in equation (43) to terms in the x_3 scalar components of velocity, vorticity and streamfunction. Considering first the convection term, from equation (26), for incompressible and compressible steady flow, obtain

$$\epsilon_{3ki}\left(\rho u_i u_j\right)_{;jk} = \epsilon_{3ki}\left(\rho u_j u_{i;j}\right)_{;k} \tag{44}$$

Substitute equation (37) for ρu_j and u_j. Perform the indicated vector differentiation, and using the skew-symmetric properties of the alternating tensor contraction

$$\epsilon_{3ki}\,\epsilon_{3j\ell} = \delta_{kj}\,\delta_{i\ell} - \delta_{k\ell}\,\delta_{ij} \tag{45}$$

the convection term becomes

$$\epsilon_{3ki}\,(\rho u_i u_j)_{;jk} = \epsilon_{3ki}\left[\left(\frac{r^a\,\omega\psi_{,i}}{r\sin^a\phi}\right)_{;k} - \frac{1}{2}\left(\frac{\psi_{,\ell}}{r\sin^a\phi}\right)^2_{;i}\left(\frac{1}{\rho}\right)_{,k} + \rho u_3\;\epsilon_{3i\ell}\left(\frac{\psi_{,\ell}}{\rho r\sin^a\phi}\right)_{;3}\right] \tag{46}$$

which involves only the dependent flow variables ω, ψ and u_3. Since the vector differentiation has been performed where appropriate, the remaining alternating tensors merely restrict the range of subscripts and provide for correct signs.

Consider next the term in equation (43) involving the stress tensor τ_{ij}. At this juncture, assume that either, (1) the fluid is Newtonian, or, (2) that turbulent flow is adequately characterized by the laminar flow equations with the molecular viscosity replaced by a scalar turbulent "eddy viscosity." In both cases, equation (5) defines the stress tensor constitutive relationship to velocity gradient and viscosity. (Note, that since these equation developments begin with the stress tensor explicitly, other stress-strain laws could be invoked, as might occur for turbulent flows where the eddy viscosity is not adequately represented by a non-directional scalar quantity.) Substituting equation (5) into (43) yields

$$\epsilon_{3ki}\;\tau_{ij;jk} = \epsilon_{3ki}\left[\mu\,(u_{i;j} + u_{j;i}) - \frac{2}{3}\mu\,u_{\ell;\ell}\,\delta_{ij}\right]_{;jk} \tag{47}$$

The last term in equation (47) vanishes identically from symmetry considerations. Expanding the remaining terms, and noting that the $u_{j;ik}$ term vanishes identically in Euclidean space, the stress tensor expression reduces to

$$\epsilon_{3ki}\;\tau_{ij;jk} = \epsilon_{3ki}\left[\mu_{,k}\,(u_{i;j} + u_{j;i}) + \mu\,u_{i;jk}\right]_{;j} \tag{48}$$

Considering equation (48) in detail, the last term can be written as

$$\left[\mu\ (\epsilon_3 ki\ u_{i;k})_{;j}\right]_{;j}$$

Using equation (39), obtain equivalently

$$\epsilon_3 ki\ (\mu u_{i;jk})_{;j} = (\mu\ (r^a\omega)_{,j})_{;j} \tag{49}$$

In the remaining terms in equation (48), substitute from equation (37) for the velocities u_i and u_j. Performing the indicated vector differentiations, and using the symmetry properties for alternating tensor contractions, obtain

$$\epsilon_3 ki\left[\mu,k\ (u_{i;j} + u_{j;i})\right]_{;j} = -(\mu,_k r^a\omega)_{;k} - 2\left[\mu,k\ \left(\frac{\psi,k}{\rho r\sin^a\phi}\right)_{;j}\right]_{;j} \tag{50}$$

Combining equation (49) with equation (50), and expanding the last term for clarity, the stress tensor term in equation (43) becomes, in terms of vorticity and streamfunction,

$$\epsilon_3 ki\ \tau_{ij;jk} = \left[\mu(r^a\omega)_{,j} - \mu_{,j}r^a\omega - \mu,k\left(\frac{2\psi,k}{\rho r\sin^a\phi}\right)_{;j} + \mu,k\,\epsilon_3 ki\,\delta_{j3}\,u_{3;i}\right]_{;j} \tag{51}$$

There remains the left-hand side of equation (43) which is non-vanishing, within the assumptions regarding the validity of ψ, only for incompressible flow. For this case,

$$\rho\epsilon_3 ki\ u_{i;kt} = \rho r^a\omega_{,t} \tag{52}$$

Combining equations (46), (51) and (52), the x_3 scalar component of the curl of the Navier-Stokes equation (27), written entirely in terms of the vorticity, streamfunction and x_3 component of velocity u_3, becomes

$$(\rho r^a\omega)_{,t} = -\epsilon_3 ki\left[\left(\frac{r^a\omega\psi,i}{r\sin^a\phi}\right)_{;k} - \frac{1}{2}\left(\frac{\psi,\ell}{r\sin^a\phi}\right)^2_{;i}\left(\frac{1}{\rho}\right)_{,k} + \left(\rho u_3\,\epsilon_{3i\ell}\left(\frac{\psi,\ell}{\rho r\sin^a\phi}\right)_{;3}\right)_{;k}\right]$$

$$+\frac{1}{Re}\left[\mu(r^a\omega)_{,j} - \mu_{,j}r^a\omega - \mu',k\left(\frac{2\psi,k}{\rho r\sin^a\phi}\right)_{;j} + \mu,k\,\epsilon_3 ki\,\delta_{j3}\,u_{3;i}\right]_{;j} \tag{53}$$

The form of equation (53) is desired for computational purposes, since the velocity vector and pressure have been explicitly eliminated. However, conceptual clarity results from transformation of the terms containing ψ,k into velocities. Contracting equation (37) with ϵ_{3jk} and using equation (41) yields

$$\frac{\psi,k}{\rho r\sin^a\phi} = \epsilon_3 jk u_j \tag{54}$$

Removing the $\psi_{,k}$ the terms in equation (53), the equivalent form with velocities is

$$\rho r^{a}\omega_{,t} = -\left[(\rho u_k r^{a}\omega)_{;k} + \frac{1}{2}\,\epsilon_{3ki}(u_\ell u_\ell)_{;i}\,\rho_{,k} + \epsilon_{3ki}\left(\rho u_3 \delta_{j3}\,(u_i - u_3\delta_{i3})_{;j}\right)_{;k}\right]$$

$$+ \frac{1}{Re}\left[\mu(r^{a}\omega)_{,k} - \mu_{,k}\,(r^{a}\omega) - 2\mu_{,j}\,\epsilon_{3\ell j}\,u_{\ell;k}\right]_{;k} \qquad (55)$$

The convention on x_3 in each coordinate system allows simplification of terms involving ρu_3. For rectangular, cylindrical, and spherical coordinates, respectively, define

$$\begin{aligned} x_i &\equiv \{x,y,0\} \\ &= \{z,r,\theta\} \\ &= \{r,\phi,\theta\} \end{aligned} \qquad (56)$$

Then, for example, in cylindrical and spherical coordinates, respectively obtain

$$\epsilon_{3ki}\,(\rho u_3 \delta_{j3}(u_i - u_3\delta_{i3})_{;j})_{;k} = \begin{cases} -\frac{1}{2\rho r}\,(\rho u_3)^2_{,z} \\ \frac{1}{r}\left(\frac{\rho u_3{}^2}{r}\right)_{,\phi} - \left(\frac{\cot\phi}{r}\,\rho u_3{}^2\right)_{,r} \end{cases} \qquad (57)$$

The x_3 Component of the Navier-Stokes Equation

The determination of u_3, in terms of ω and ψ, is obtained from solution of the x_3 component of the Navier-Stokes equation, which is

$$(\rho u_3)_{,t} = -(\rho u_i u_3)_{;i} - p_{,3} + \tau_{3j;j} \qquad (58)$$

assuming the body force distribution has no x_3 component. The x_3 derivative of pressure is included in equation (58) to account for flow processes through "corkscrew" devices.

Using equation (37) to replace ρu_i and proceeding through the details of the vector derivative of u_3, equation (58) becomes

$$(\rho u_3)_{,t} = -\epsilon_{3ij}\left(\frac{\psi_{,j}}{r\sin^{a}\phi}\,u_3\right)_{;i} - \rho u_3 u_{3;3} - p_{,3}$$

$$+ \frac{1}{Re}\left[(\mu\, u_{3;k})_{;k} + \frac{1}{3}\,\mu\, u_{j;j3} + \mu_{,k}\,u_{k;3}\right] \qquad (59)$$

Note that $u_{j;3}$ does not vanish identically. For example, in cylindrical coordinates

$$u_{3;3} = \frac{1}{r}\,u_2 \qquad (60) \qquad\qquad u_{3;33} = -\frac{1}{r^2}\,u_3 \qquad (61)$$

For incompressible flow, the transient term may be retained; otherwise, only the steady state solution is correctly specified.

The Species Continuity Equation

For multi-component flow, equation (25) describes each species mass fraction with respect to mutual convective, diffusive and reactive processes. Transformation to the desired computational form simply involves replacement of ρu_i by the streamfunction definition, equation (37). Since the divergence of equation (37) vanishes, and Y^a is not a function of x_3, the desired equation becomes

$$(\rho Y^a)_{,t} = -\epsilon_{3ij}\left(\frac{\psi_{,j}}{r\sin^a\phi}\,Y^a\right)_{;i} - \left(\rho u_3\,Y^a\right)_{;3} + \left(\frac{\mu Le}{Pr}\,Y^a{}_{,i}\right)_{;i} + S^a \qquad (62)$$

The number of equations (62) equals the total number of species present, and the transient solution is correctly specified only for species of identical molecular weight.

The Energy Equation

The form selected to express energy conservation, equation (28), is particularly well suited for numerical computation in the problem class being considered. The explicit pressure influence is contained solely within the temporal dependence. Since the pressure, as an explicitly coupled dependent variable, has been eliminated from the momentum equations as well, solutions to steady-state problems for either incompressible or compressible flow are possible, without solution for the pressure field, provided that the implicit influence of pressure as a thermodynamic variable can be suitably approximated. This advantage is particularly noteworthy, since most numerical algorithms for fluid mechanics, which contain pressure as an explicitly coupled dependent variable, are specially designed to "half-step" iterate between the flow field and the pressure distribution. Inefficiency or numerical instability characterizes the attempt to march both variable types simultaneously.

To cast equation (28) into the desired computational form, replace the velocity vector by the streamfunction definition, equation (37). The convection term becomes

$$\rho u_i H = \left(\frac{\epsilon_{3ij}\,\psi_{,j}}{r\sin^a\phi} + \rho u_3\,\delta_{i3}\right) H \qquad (63)$$

Using equations (5) and (6), the irreversible work term is

$$\tau_{ij}\,u_j = \mu\left[\frac{1}{2}(u_j u_j)_{;i} + u_j u_{i;j} - \frac{2}{3}u_i u_{k;k}\right] \qquad (64)$$

Using equations (37) and (41), the first right hand term becomes

$$(u_j u_j)_{;i} = \left[\left(\frac{\psi_{,k}}{\rho r\sin^a\phi}\right)^2 + u_3{}^2\right]_{;i} \qquad (65)$$

Using equation (45) also, the second term becomes

$$u_j u_{i;j} = \frac{1}{2}\left[\left(\frac{\psi_{,k}}{\rho r\sin^a\phi}\right)^2_{;i} - \frac{\psi_{,i}}{\rho r\sin^a\phi}\left(\frac{\psi_{,j}}{\rho r\sin^a\phi}\right)_{;j}\right]$$

$$+\left[\frac{1}{2}(u_3)^2_{;3} + u_{3;j}\frac{\epsilon_{3jk}\psi_{,k}}{\rho r\sin^a\phi}\right]\delta_{i3} \qquad (66)$$

The final term in equation (64) can be transformed using equation (26), to

$$u_i u_{k;k} = -u_i u_k \ell n\rho_{,k} \qquad (67)$$

Its desired computational equivalent is

$$u_i u_{k;k} = \frac{1}{2}\left(\frac{\psi,\ell}{r\sin^a\phi}\right)^2\left(\frac{1}{\rho}\right)^2_{,i} - \frac{1}{2}\left(\frac{\psi_{,k}\psi_{,i}}{(r\sin^a\phi)^2}\right)\left(\frac{1}{\rho}\right)^2_{,k} + u_3\frac{\epsilon_{3k\ell}\psi_{,\ell}}{r\sin^a\phi}\left(\frac{1}{\rho}\right)_{,k}\delta_{i3} \qquad (68)$$

Combining equations (64) - (67), the irreversible work contribution to the energy equation becomes

$$\tau_{ij}u_j = \mu\left[\left(\frac{\psi_{,k}}{\rho r\sin^a\phi}\right)^2_{;i} - \frac{\psi_{,i}}{\rho r\sin^a\phi}\left(\frac{\psi_{,j}}{\rho r\sin^a\phi}\right)_{;j}\right]$$

$$+\frac{\mu}{2}\left[u_{3;i}^2 + \left(u_3^2{}_{;3} + 2u_{3;j}\frac{\epsilon_{3jk}\psi_{,k}}{\rho r\sin^a\phi}\right)\delta_{i3}\right]$$

$$+\frac{\mu}{3}\left[-\left(\frac{\psi,\ell}{r\sin^a\phi}\right)^2\left(\frac{1}{\rho}\right)^2_{,i} + \frac{\psi_{,k}}{r\sin^a\phi}\frac{\psi_{,i}}{r\sin^a\phi}\left(\frac{1}{\rho}\right)^2_{,k} - 2u_3\,\epsilon_{3k\ell}\frac{\psi_{,\ell}}{r\sin^a\phi}\left(\frac{1}{\rho}\right)_{,k}\delta_{i3}\right] \qquad (69)$$

The computational form for the energy equation thus becomes

$$(\rho H)_{,t} = (Ec)\, p_{,t} - \left\{ \left(\frac{\epsilon_{3kj}\psi_{,j}}{r\sin^{\alpha}\phi} + \rho u_3 \delta_{k3} \right) H - \frac{1}{Re}\frac{\mu}{Pr} H_{,k} \right.$$

$$- \frac{\mu Ec}{Re}\left[\left(\frac{\psi_{,i}}{\rho r\sin^{\alpha}\phi} \right)^2_{;k} - \frac{\psi_{,k}}{\rho r\sin^{\alpha}\phi}\left(\frac{\psi_{,j}}{\rho r\sin^{\alpha}\phi} \right)_{;j} \right]$$

$$- \frac{\mu Ec}{2Re}\left[u_3^2{}_{;k} + \left(u_3^2{}_{;3} + 2u_{3;j} \frac{\epsilon_{3j\ell}\psi_{,\ell}}{\rho r\sin^{\alpha}\phi} \right) \delta_{k3} \right]$$

$$- \frac{\mu Ec}{3Re}\left[-\left(\frac{\psi_{,\ell}}{r\sin^{\alpha}\phi} \right)^2 \left(\frac{1}{\rho} \right)^2_{,k} + \frac{\psi_{,k}}{r\sin^{\alpha}\phi}\frac{\psi_{,i}}{r\sin^{\alpha}\phi}\left(\frac{1}{\rho} \right)^2_{,i} \right.$$

$$\left. \left. - 2u_3 \epsilon_{3j\ell}\frac{\psi_{,\ell}}{r\sin^{\alpha}\phi}\left(\frac{1}{\rho} \right)_{,j} \delta_{k3} \right] \right\}_{;k} + \frac{1}{RePr_{\infty}} \rho\dot{Q} \qquad (70)$$

For compressible flow, the time derivative terms must be set to zero. Equation (70) is valid as written for transient incompressible flow.

Recovery of Pressure

The pressure distribution is recovered from the vorticity-streamfunction characterization of this problem class by enforcing linear momentum conservation. Equation (27) can be transformed to the Laplacian on pressure by an additional differentiation, and solved as boundary value problem. Since this is not a well-posed description for pressure, the preferable approach may be to integrate equation (27) after contraction with the infinitesimal displacement vector, dx_i, yielding

$$\int p_{,j}\delta_{ij}dx_i = -\int \left[\rho u_i u_j - \frac{1}{Re}\tau_{ij} \right]_{;j} dx_i - \frac{\partial}{\partial t}\int \rho u_i dx_i + \frac{1}{Fr}\int \rho b_i dx_i \qquad (71)$$

Note that the left side of equation (71) is the integral of a perfect differential and thus independent of path. Hence, the pressure at any point in the field can be determined, in comparison to some reference value, by integration over an arbitrary (the easiest) path between the two points. Thus, the entire pressure field need not be computed to obtain selected pressures, for example, at an exterior wall. Upon noting that the integrand in the last term of equation (71) is x_i independent, and denoting integrals of perfect differentials as Δ, equation (71) becomes

$$\Delta p = -\int \left(\rho u_i u_j \right)_{;j} dx_i + \frac{1}{Re}\int \tau_{ij;j}\, dx_i - \frac{\partial}{\partial t}\int \rho u_i dx_i + \frac{1}{Fr}\, \rho\Delta x_b \qquad (72)$$

To consider the convection contribution to equation (72), replace $\rho u_i u_j$ by equation (37). Performing the indicated differentiation, using equations (41) and (45), and noting x_3 independence of some integrands, obtain

$$\int \left(\rho u_i u_j\right)_{;j} dx_i = \Delta \left[\frac{1}{\rho}\left(\frac{\psi_{,k}}{r\sin^\alpha\phi}\right)^2\right] - \int \left[\frac{\psi_{,i}\,\psi_{,j}}{\rho(r\sin^\alpha\phi)^2}\right]_{;j} dx_i$$

$$+ \int u_{3\,;3} \frac{\epsilon_{3\,i\ell}\,\psi_{,\ell}}{r\sin^\alpha\phi} dx_i \qquad (73)$$

$$+ \Delta x_3 \left[\rho u^2_{3\,;3} + \left(u_3 \frac{\epsilon_{3\,j\ell}\,\psi_{,\ell}}{r\sin^\alpha\phi}\right)_{;j}\right]$$

Recall that $u_{3\,;3}$ is transformed to equivalent terms in ψ for each particular coordinate system.

The same procedures are used to transform the stress tensor contribution to computational variables. Integrating selected terms by parts, the following form can be obtained.

$$\int \tau_{ij\,;j}\, dx_i = \Delta \left[\left(\mu \frac{\epsilon_{3\,jk}\,\psi_{,k}}{\rho r\sin^\alpha\phi}\right)_{;j} + \frac{2}{3}\mu \frac{\epsilon_{3\,jk}\,\psi_{,k}}{\rho r\sin^\alpha\phi} \ell n\rho_{,j}\right]$$

$$+ \int \left[\left(\mu \frac{\epsilon_{3\,ik}\,\psi_{,k}}{\rho r\sin^\alpha\phi}\right)_{;j} - \mu_{,i} \frac{\epsilon_{3\,jk}\,\psi_{,k}}{\rho r\sin^\alpha\phi} - \mu_{,j} \frac{\epsilon_{3\,ik}\,\psi_{,k}}{\rho r\sin^\alpha\phi}\right]_{;j} dx_i$$

$$+ \Delta x_3 \left(\mu u_{3\,;j}\right)_{;j} + \int \mu u_{3\,;3\,i}\, dx_i \qquad (74)$$

Substituting equation (37) for the integrand of the time dependent contribution to equation (72), and combining terms, the following form results for determination of the pressure at any point in the field.

$$\Delta p = \Delta \left\{ \frac{1}{Re} \left[\left(\frac{\mu \epsilon_{3jk} \psi_{,k}}{\rho r \sin^{\alpha}\phi} \right)_{;j} - \frac{2}{3} \mu \frac{\epsilon_{3jk} \psi_{,k}}{r \sin^{\alpha}\phi} \left(\frac{1}{\rho} \right)_{,j} \right] \right.$$

$$\left. - \frac{1}{\rho} \left(\frac{\psi_{,k}}{r \sin^{\alpha}\phi} \right)^2 + \frac{1}{Fr} \rho x_b \right\}$$

$$+ \int \left\{ \frac{1}{Re} \left(\frac{\mu \epsilon_{3ik} \psi_{,k}}{\rho r \sin^{\alpha}\phi} \right)_{;j} - \mu_{,i} \frac{\epsilon_{3jk} \psi_{,k}}{\rho r \sin^{\alpha}\phi} - \mu_{,j} \frac{\epsilon_{3ik} \psi_{,k}}{\rho r \sin^{\alpha}\phi} \right.$$

$$\left. + \frac{\psi_{,i} \psi_{,j}}{\rho (r \sin^{\alpha}\phi)^2} \right\}_{;j} dx_i$$

$$+ \int \left\{ \frac{1}{Re} \mu u_{3;3i} - u_{3;3} \frac{\epsilon_{3ik} \psi_{,k}}{r \sin^{\alpha}\phi} - \frac{\partial}{\partial t} \left(\frac{\epsilon_{3ik} \psi_{,k}}{r \sin^{\alpha}\phi} \right) \right\} dx_i$$

$$+ \Delta x_3 \left\{ \frac{1}{Re} \left(\mu u_{3;j} \right)_{;j} - \rho u^2_{3;3} \div \left(u_3 \frac{\epsilon_{3jk} \psi_{,k}}{r \sin^{\alpha}\phi} \right)_{;j} \right\} \qquad (75)$$

In equation (75), the first curly bracket contains terms which are point dependent, the result of integrating perfect differentials. The second bracket requires integration, and hence selection of path. The third bracket contains terms which require evaluation dependent upon the selected coordinate system. The last bracket merely requires evaluation, since all variables are x_3 -independent.

FINITE ELEMENT SOLUTION ALGORITHM FOR THE NAVIER-STOKES EQUATIONS

The desired form for the differential equation system governing the mechanics and thermodynamics of a viscous, variable density fluid in two independent space coordinates has been established. The system of elliptic partial differential equations, which may be initial value as well under certain restrictions, requiring solution includes equations (40), (43), (59), (62), and (70) for stream-function (ψ), vorticity (ω), swirl velocity component (u_3), mass fraction (Y^{α}), and stagnation enthalpy (H). Equation (75) is an algebraic equation for determination of pressure (p) in terms of the flow computational variables, and the density (ρ) is established via equation (7). Closure of this complex equation system is obtained by specification of the thermophysical and transportive properties of the fluid, that is, laminar flow molecular viscosity, thermal conductivity, and specific heat. The formulation is equally valid for steady turbulent flows, described by the time-averaged Navier-Stokes equations, by establishing an "eddy viscosity" model based upon the kinematics of the flow field. The solution algorithm to be established assumes a generalized viscosity description that may be an explicitly prescribed function of dependent as well as independent variables.

The uniformity of the derived differential equation description for the computational dependent variables is evident as specific variants of the nonlinear elliptic partial differential equation of mathematical physics. Identifying q as a generalized dependent variable, the uniform description belonging to each of the equations (40), (43), (59), (62) and (70) is

$$N(q) \equiv \kappa[Kq_{,k}]_{;k} - [\epsilon_{3ki} \frac{\psi_{,i}}{r\sin^{a}\phi} q]_{;k} + f(q,q_{,k},x_i) - g(\rho,q,t) = 0 \qquad (76)$$

In equation (76), N(q) is the specified differential operator for q, the first right side term is the elliptic operator, the second term is the convection operator, and f and g are specified functions of their arguments, see Table 1, corresponding to q identified with each dependent variable. Since equation (76) is elliptic, unique solutions are obtained only after specification of boundary conditions, the most useful and general form of which relates the function and its normal derivative everywhere on the closure, ∂R, of the solution domain, R, as

$$\eta(q) \equiv a^{(1)}(\bar{x}_i,t)\, q(\bar{x}_i,t) + a^{(2)}(\bar{x}_i,t)\, q(\bar{x}_i,t)_{,k} n_k - a^{(3)}(\bar{x}_i,t) = 0 \qquad (77)$$

In equation (77), the $a^{(i)}(\bar{x}_i,t)$ are user-specified coefficients enforcing the boundary conditions which may be time dependent, the superscript bar notation constrains x_i to ∂R, and n_k is the local outward pointing unit normal vector. For g nonvanishing in equation (76), or for use as an estimated distribution to start an iteration to steady state, an initial distribution is also required; hence, assume given throughout R

$$q(x_i,0) = Q_o(x_i) \qquad (78)$$

Formation of the finite element solution for the two-dimensional Navier-Stokes equations is thus obtained by establishing the algorithm for the equation system (76) - (78) identified for each dependent variable requiring solution. The theoretical foundation is the method of weighted residuals (MWR) (Reference 1) applied on a local basis. Discussion on the formulational aspects of this algorithm are reported for a considerably restricted problem class within the Navier-Stokes equations (References 6, 8) as well as for three-dimensional boundary-layer-type flow fields (References 7, 10). Since equation (76) is valid throughout R, it is valid in disjoint interior subdomains R_m, described by $(x_i,t) \epsilon R_m \times [0,\infty)$ called "finite elements," wherein $UR_m = R$. Form an approximate solution to equation (76) within $R_m \times [0,\infty)$, called $q_m^*(x_i,t)$, by expansion into a series solution of the form

$$q_m^*(x_i,t) \equiv \sum_{k=1}^{n} L_k(x_i)\, Q_k^m(t) \equiv \left\{L(x_i)\right\}^T \left\{Q(t)\right\}_m \qquad (79)$$

wherein the functionals $L_k(x_i)$ are members of a function set that is complete in R_m, and the unknown expansion coefficients, $Q_k(t)$, represent the time-dependent values of $q_m^*(x_i,t)$ at specific points called "nodes" interior to R_m and on the closure, ∂R_m. Equation (79) is a scalar, the second form introduces the column matrix notation and its transpose (superscript T), and the method of selection of the L_k is user specifiable and problem class dependent. To establish the values taken by the expansion coefficients in equation (79), require that the local error in the approximate solution to both the differential equation (77), $N(q_m^*)$, and the boundary condition statement, $\eta(q_m^*)$, if applicable, that is, ∂R_m coincident with ∂R, equation (78), be orthogonal to the functional set in

TABLE 1
COEFFICIENTS IN GENERALIZED ELLIPTIC DIFFERENTIAL EQUATION DESCRIPTION, EQ. (76)

Equation No.	q	κ	K	f	g
(40)	ψ	1	$\frac{1}{\rho r \sin^a\phi}$	$r^a\omega + \left[\psi \frac{\epsilon_{3ki}\,\psi_{,i}}{r\sin^a\phi}\right]_{;k}$	0
(53)	$r^a\omega$	$\frac{1}{Re}$	μ	$-\left[\frac{\mu_{,k}}{Re}(r^a\omega) + \frac{2\mu_{,j}}{Re}\left(\frac{\psi_{,j}}{\rho r\sin^a\phi}\right)_{;k} + \rho u_3\left(\frac{\psi_{,k}}{\rho r\sin^a\phi}\right)_{;3}\right]_{;k}$	$\rho q_{,t}$
				$+\frac{1}{2}\epsilon_{3ki}\left(\frac{1}{\rho}\right)_{,k}\left(\frac{\psi_{,\ell}}{r\sin^a\phi}\right)^2_{;i} + \left[\frac{\mu_{,k}}{Re}\epsilon_{3ki}\,u_{3;i}\right]_{;3}$	
(59)	u_3	$\frac{1}{Re}$	μ	$\left[\frac{\mu}{3Re}u_{k;k3} + \frac{\mu_{,k}}{Re}u_{k;3}\right] - \rho u_3 u_{3;3} - p_{,3}$	$\rho q_{,t}$
(62)	Y^a	$\frac{Le}{Pr}$	μ	S^a	$\rho q_{,t}$
(70)	H	$\frac{1}{RePr}$	μ	$-\left[\rho u_3\,\delta_{k3}\,H - \frac{\mu Ec}{Re}\left\{\left(\frac{\psi_{,i}}{\rho r\sin^a\phi}\right)^2_{;k} - \frac{\psi_{,k}}{\rho r\sin^a\phi}\left(\frac{\psi_{,j}}{\rho r\sin^a\phi}\right)_{;j}\right\}\right.$	$\rho q_{,t}$
				$-\frac{\mu Ec}{2Re}\left\{u^2_{3;k} + \left(u^2_{3;3} + 2u_{3;j}\frac{\epsilon_{3j\ell}\,\psi_{,\ell}}{\rho r\sin^a\phi}\right)\delta_{k3}\right\}$	$-(Ec)p_{,t}$
				$-\frac{\mu Ec}{3Re}\left\{-\left(\frac{\psi_{,\ell}}{r\sin^a\phi}\right)^2\left(\frac{1}{\rho}\right)^2_{,k} + \frac{\psi_{,k}}{r\sin^a\phi}\frac{\psi_{,i}}{r\sin^a\phi}\left(\frac{1}{\rho}\right)^2_{,i}\right.$	
				$\left.\left.-2u_3\epsilon_{3j\ell}\frac{\psi_{,\ell}}{r\sin^a\phi}\left(\frac{1}{\rho}\right)_{,j}\delta_{i3}\right\}\right]_{;k} + \frac{1}{RePr_\infty}\rho\dot{Q}$	

equation (79). This is accomplished by enforcing the local variant of the Galerkin criterion of classical MWR, that is, premultiplication of equations (77) and (78) by the approximation functionals, $L_k(x_i)$, and integration over the respective domains. Employing a Lagrange multiplier, λ, these equation sets can be combined to yield

$$\int_{R_m} \left\{ L(x_i) \right\} N(q_m^*) d\tau \; - \; \lambda \oint_{\partial R_m} \left\{ L(x_i) \right\} \eta(q_m^*) d\sigma \; \equiv \; 0 \tag{80}$$

The number of equations (80) is identical to the number of node points associated with the finite element, R_m, that is, the number of elements in the column matrix $\left\{ Q(t) \right\}_m$.

Equation (80) forms the basic operation of the finite element solution procedure. Establishment of the global solution algorithm, and determination of λ, is accomplished by evaluating equation (80) in each of the m finite elements of the discretized solution domain, R, and assembly of these Mxn equations into a global matrix system by Boolean algebra. The rank of the global system is less than Mxn by connectivity of the finite element domains as well as by enforcement of those boundary condition statements on ∂R where $a^{(2)}$, equation (77), vanishes identically. Determination of λ is accomplished by observing that the lead term in equation (76), when incorporated into equation (80), can be integrated by parts; alternatively, using the generalized divergence theorem (Appendix A), obtain

$$\int_{R_m} \left\{ L(x_i) \right\} \kappa [K q_{m,k}^*]_{;k} \, d\tau \; = \; \kappa \oint_{\partial R_m} \left\{ L(x_i) \right\} K q_{m,k}^* n_k d\sigma \; - \; \kappa \int_{R_m} \left\{ L(x_i) \right\}_{,k} K q_{m,k}^* d\tau \tag{81}$$

On those portions of the closure ∂R coincident with ∂R_m, equation (81), the corresponding segment of the closed surface integral will cancel the boundary condition contribution, equation (80), by identifying λ with κ of equation (76) and $a^{(2)}$ with the generalized diffusion coefficient, K. From Table 1, for the Navier-Stokes equations, κ typically involves the Reynolds number and $a^{(2)}$ is the viscosity, μ, except for the vorticity-streamfunction compatibility equation (40), where they are unity and inverse density. The contributions to the closed surface integral, equation (81), where ∂R_m is not coincident with ∂R remain for evaluation. Hence, combining equations (77) - (81), the globally assembled finite element solution algorithm for the representative elliptic partial differential equation system description for the Navier-Stokes equations becomes

$$\sum_{m=1}^{M} \left[-\kappa \int_{R_m} \left\{ L \right\}_{,k} K q_{m,k}^* \, d\tau \; - \int_{R_m} \left\{ L \right\} \epsilon_{3ki} \left(\frac{\psi^*_{,i}}{r \sin^{\alpha_\phi}} q_m^* \right)_{;k} d\tau \; + \int_{R_m} \left\{ L \right\} (f_m^* - g_m^*) \, d\tau \right.$$

$$\left. - \kappa \int_{\partial R} \left\{ L \right\} \left(K q_{m,k}^* n_k \; + \; a_m^{(1)} q_m^* \; - \; a_m^{(3)} \right) d\sigma + \kappa \oint_{\partial R_m} \left\{ L \right\} K q_{m,k}^* n_k d\sigma \right] \; = \; \left\{ 0 \right\} \tag{82}$$

Using Boolean algebra as the assembly (summation) operator, the rank of the global matrix equation system (82) is identical to the total number of node points within the solution domain R, and on the closure ∂R, at which the dependent variable requires solution. Equation (82) is either a first-order ordinary differential, or algebraic equation system dependent upon whether g, equation (76),vanishes identically. In either event, the equation system is large order and the matrix structure

is sparse and banded about the main diagonal, with bandwidth a function of both selected discretization and the order of the employed approximation function, equation (79). Solution of the algebraic system can be obtained by many procedures including direct inverse, Gauss elimination, and equation solver techniques, for example, banded Cholesky. If the equation description is ordinary differential, solution is obtained using either an explicit or implicit numerical integration algorithm for an initial value problem.

FINITE ELEMENT MATRIX GENERATION

Implementation of the finite element theory into a computer code involves assembly of Eq. (82) for the required dependent variables, hence evaluation within each element of the discretized solution domain. The vast experience in structural mechanics has proven the viability of truncated power series as approximation functions. Highly tailored finite elements have been established for specific problem classes in elasticity. But for now, the use of finer discretizations using linear (simplex) approximation functionals, Eq. (79), appears useful for the broader problem class. The intrinsic finite element shapes for one-, two, and three-dimensional spaces, spanned by simplex functionals, are the line, triangle, and tetrahedron. The preferred orientations for these elements in a local coordinate system are shown in Figure 1.

Accurate determination of the element matrices of Eq. (82) is mandatory, and involves evaluation of various-order moment distributions over the domain of the finite element. A straightforward approach involving numerical matrix multiplications, after definition of a transformation matrix (Reference 8), is generally adequate for linear equations; however, it has proven highly susceptible to accumulated round-off for the explicitly nonlinear matrices common to the Navier-Stokes equations. An alternate approach has been developed which expands upon the natural coordinate function description for finite element solution of the energy conservation equation (Reference 11). These functionals, which are an adaptation of the area coordinates of structural mechanics (Reference 12) are a linearly dependent set of normalized functions that are orthogonal to the respective closure segments of the finite element domain. For an n-dimensional space, there are n+1 simplex natural coordinate functions. Table 2 contains the implicit definition of these functions in their respective spaces. (The three-dimensional descriptions, while inappropriate for the particular Navier-Stokes equation system being studied, are included to complete the finite element theoretical foundation for future reference.) As the direct consequence of the definition, the natural coordinate functions vanish at all node points of the finite element except one where the value is unity. Hence, these functions are the elements of the approximation function column matrix, $\{ L \}$, Eq. (79). Of particular impact for solution of the Navier-Stokes equations is that integration of arbitrary-order products of scalar components of the $\{ L \}$, over the domain of the finite element, are analytically evaluable in terms of the exponent distribution, Table 3, the determinant of the equation system defining the L_i, Table 2, and the dimensionality of the space of the problem.

It remains to evaluate the solution algorithm, Eq. (82), for the Navier-Stokes equations using the natural coordinate function description, which involves matrix formation over one- and two-dimensional finite elements. (The one-dimensional element is needed to evaluate the domain closure integrals of the solution algorithm.) The evaluations are presented for the two-dimensional flow of a fluid with arbitrary density and viscosity distribution, and the axisymmetric flow of a constant property fluid. Additional integrations by parts have proven useful for the functions f(q), Eq. (76), and the mathematical consequences of these operations are established in Appendix B.

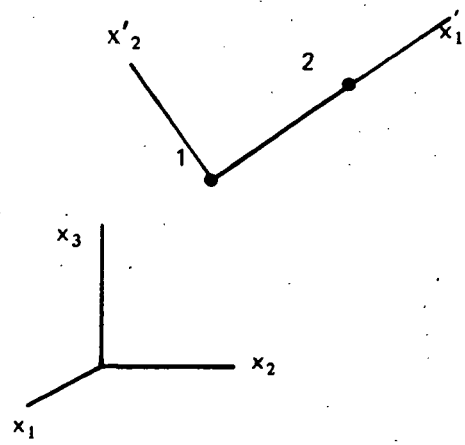

Figure 1a. One Dimensional Space

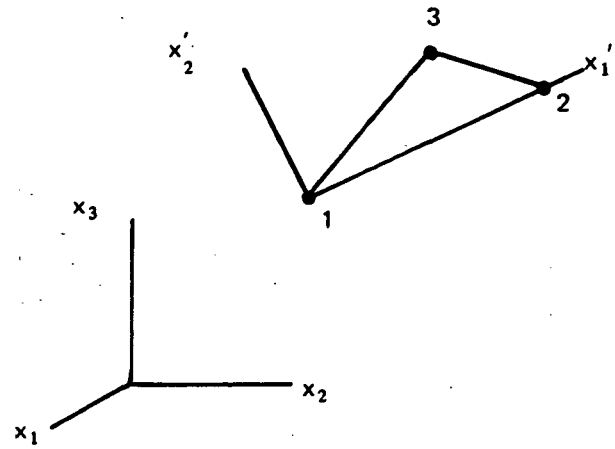

Figure 1b. Two-Dimensional Space

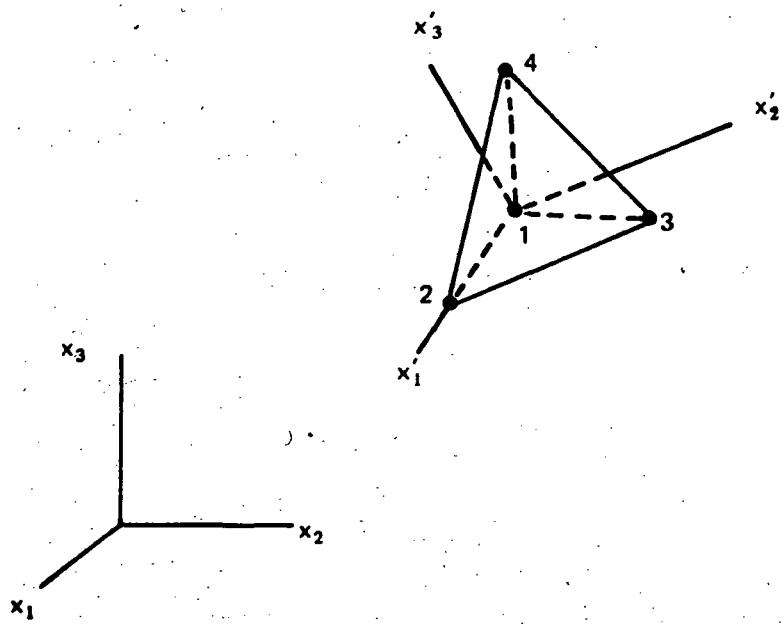

Figure 1c. Three-Dimensional Space

Figure 1. Intrinsic Finite Element Domains for Simplex Approximation Functions

TABLE 2
IMPLICIT DEFINITION OF SIMPLEX NATURAL COORDINATE FUNCTIONS

Dimensions	Element	Nodes	Natural Coordinate Definition
1	Line	2	$\begin{bmatrix} 1 & 1 \\ x_1 & x_2 \end{bmatrix} \begin{Bmatrix} L_1 \\ L_2 \end{Bmatrix} = \begin{Bmatrix} 1 \\ x \end{Bmatrix}$
2	Triangle	3	$\begin{bmatrix} 1 & 1 & 1 \\ x_1 & x_2 & x_3 \\ y_1 & y_2 & y_3 \end{bmatrix} \begin{Bmatrix} L_1 \\ L_2 \\ L_3 \end{Bmatrix} = \begin{Bmatrix} 1 \\ x \\ y \end{Bmatrix}$
3	Tetrahedron	4	$\begin{bmatrix} 1 & 1 & 1 & 1 \\ x_1 & x_2 & x_3 & x_4 \\ y_1 & y_2 & y_3 & y_4 \\ z_1 & z_2 & z_3 & z_4 \end{bmatrix} \begin{Bmatrix} L_1 \\ L_2 \\ L_3 \\ L_4 \end{Bmatrix} = \begin{Bmatrix} 1 \\ x \\ y \\ z \end{Bmatrix}$

TABLE 3
INTEGRALS OF NATURAL COORDINATE FUNCTION PRODUCTS OVER FINITE ELEMENT DOMAINS

Dimensions	Integrals*
1	$\int_R L_1^{n_1} L_2^{n_2} dx = D \frac{n_1! n_2!}{(n+n_1+n_2)!}$
2	$\int_R L_1^{n_1} L_2^{n_2} L_3^{n_3} dxdy = D \frac{n_1! n_2! n_3!}{(n+n_1+n_2+n_3)!}$
3	$\int_R L_1^{n_1} L_2^{n_2} L_3^{n_3} L_4^{n_4} dxdydz = D \frac{n_1! n_2! n_3! n_4!}{(n+n_1+n_2+n_3+n_4)!}$

* D = Determinant of coefficient matrix defining the natural coordinate system, see Table 2.

n = Dimensionality of the finite element space

With the advent of the natural coordinate function description for the finite element approximation functions, matrix evaluation is straightforward. Moment generation is invariant under both coordinate translation and rotation in Euclidean space spanned by a rectangular Cartesian basis, (Appendix C). All computations are formed in the local (primed) coordinate system, Figure 1, defined by the tensor transformation law

$$x'_i = a_{ij}x_j + r_i \tag{83}$$

where r_i is the position vector to the origin of the primed coordinate system, and the a_{ij} are the direction cosines of the coordinate transformation. The integration kernels for two-dimensional space, Eq. (82), are

$$d\tau = t^m dx'_1\, dx'_2 \tag{84a}$$

$$d\sigma = t^m dx'_1 \tag{84b}$$

where t^m is the thickness of the m^{th} finite element. (Variable element thickness allows solution of predominantly two-dimensional flows in irregular depth channels, for example, rivers.) Since no difference exists between differentiation of scalars and vectors, the semi-colon operator reduces to the comma. Furthermore, no u_3 velocity component can exist in rectangular Cartesian space.

All expressions but the third, Eq. (82), are standard for all dependent variables. For the generalized diffusion term, using Eq. (79) for both q^*_m and the generalized diffusion term, K^m, and transposing scalar quantities, obtain

$$\kappa \int_R \{L\}_{,k} K^m q^*_{m,k}\, d\tau = \kappa \int \{K\}^T_m \{L\} \{L\}_{,k} \{L\}^T_{,k} \{Q\}_m d\tau$$

$$= \kappa \{K\}^T_m \{B10\}\ [B211S]\ \{Q\}_m \tag{85}$$

The standard matrices, as used in Eq. (85) and the following, are defined in Table 4. If $\{Q\}$ in Eq. (85) is identified, for example, with vorticity, then κ^{-1} equals the Reynolds number, Re, and the elements of $\{K\}_m$ are the element node point values of viscosity, μ. The second term of Eq. (82), which accounts for convection processes, becomes

$$\int_{R_m} \{L\}\, \epsilon_{3ki} \frac{\psi^*_{,i}}{r \sin^a \phi}\, q^*_{m,k}\, d\tau = \int_{R_m} \{L\}\ \{\psi\}^T_m \{L\}_{,i} \epsilon_{3ki} \{L\}^T_{,k} \{Q\}_m d\tau$$

$$= \{B10\}\ \{\psi\}^T_m\ [B211A]\ \{Q\}_m \tag{86}$$

Equation (86) is eligible for integration by parts; however, no arbitrariness exists for its evaluation, Appendix B, so no benefit accrues from that operation. In contra-distinction to this, the contributions to Eq. (82) stemming from the final term, involving a closed integration on ∂R_m, are non-vanishing for all R_m, but can be made to cancel in pairs upon Boolean assembly of the global algorithm, see Appendix B. Hence, the sole surface integrals requiring evaluation occur when ∂R_m and ∂R are coincident, and $a_m^{(1)}$ and/or $a_m^{(3)}$ are non-vanishing. Therefore, the only contribution to Eq. (82), from all surface integrals, reduces to two terms,

TABLE 4

STANDARD FINITE ELEMENT MATRIX FORMS FOR SIMPLEX FUNCTIONALS IN TWO-DIMENSIONAL SPACE

MATRIX NAME(1)	MATRIX FUNCTION	MATRIX EVALUATION(2)
[B200S]	$\int_{R_m} \{L\}\{L\}^T d\tau$	$\frac{A^m t^m}{12}\begin{bmatrix}2 & 1 & 1\\ & 2 & 1\\ & & 2\end{bmatrix}$ (3)
[B211S]	$\{L\}_{,k}\{L\}_{,k}^T$	$\left(\frac{1}{X1P2}\right)^2\begin{bmatrix}1 & -1 & 0\\ & 1 & 0\\ & & 0\end{bmatrix}$
		$+\left(\frac{1}{X2P3}\right)^2\begin{bmatrix}\left(\frac{X2P3}{X1P2}-1\right)^2 & -\frac{X2P3}{X1P2}\left(\frac{X2P3}{X1P2}-1\right) & \left(\frac{X2P3}{X1P2}-1\right)\\ & \left(\frac{X2P3}{X1P2}\right)^2 & -\left(\frac{X2P3}{X1P2}\right)\\ & & 1\end{bmatrix}$
[B211A]	$\epsilon_{3ki}\{L\}_{,i}\{L\}_{,k}^T$	$\frac{1}{2A^m}\begin{bmatrix}0 & -1 & 1\\ 1 & 0 & -1\\ -1 & 1 & 0\end{bmatrix}$
{B10}	$\int_{R_m}\{L\}\,d\tau$	$\frac{A^m t^m}{3}\begin{Bmatrix}1\\1\\1\end{Bmatrix}$
[A200S]	$\int_{\partial R_m}\{L\}\{L\}^T d\sigma$	$\frac{t^m \ell^m}{6}\begin{bmatrix}2 & 1 & 0\\ & 2 & 0\\ & & 0\end{bmatrix}$
{A10}	$\int_{\partial R_m}\{L\}\,d\sigma$	$\frac{t^m \ell^m}{2}\begin{Bmatrix}1\\1\\0\end{Bmatrix}$

(1) Matrix names are a 6 digit code covering dimensionality, nonlinearity, degree of differentiation and special matrix properties, as [a, b, c, d, e, f] where:

a = A, B, C for spaces of one-, two-, and three-dimensions,

b = number of natural coordinate functions appearing in integral or matrix,

c, d, e = (0, 1) Boolean counters indicating (no, yes) differentiation of each function,

e or f = S, A, Δ for matrix symmetric, antisymmetric or general.

(2) A^m = ½ (X1P2) (X2P3), the plane area of the (triangular) finite element, where the four digit codes signify node point coordinates in the primed system, for example,

X1P2 = the x_1 prime coordinate of node 2,

X2P3 = the x_2 prime coordinate of node 3,

t^m = average thickness of the finite element,

ℓ^m = length of side along which the boundary condition is applied (=X1P2)

(3) Symmetric matrices are written in upper triangular form.

$$\kappa \int_{\partial R} \{L\}\, a_m^{(1)}\, q_m^* d\sigma = \kappa a_m^{(1)}\, [A200S]\, \{Q\}_m \tag{87}$$

$$\kappa \int_{\partial R} \{L\}\, a_m^{(3)}\, d\sigma = \kappa a_m^{(3)}\, \{A10\} \tag{88}$$

where the $a_m^{(i)}$ are user-supplied boundary condition constraints.

One more standard matrix exists should the analysis be performed for the transient motion of an incompressible fluid, that is, hydrodynamics. The function g_m^*, Eq. (82), is non-vanishing for all dependent variables excepting streamfunction. The numerical evaluation for vorticity and mass fraction takes the form:

$$\int_{R_m} \{L\}\, g_m^* d\tau = \int_{R_m} \{L\}\, \bar{\rho}_m \{L\}^T \frac{d}{dt} \{Q(t)\}_m d\tau = \bar{\rho}_m\, [B200S]\, \{Q(t)\}'_m \tag{89}$$

In Eq. (89), the superscript bar signifies an element-averaged value for density, while the prime denotes that the dependent variable matrix contains the time derivatives of the node point values of the respective functions. Hence, in this case, Eq. (82) is a system of ordinary differential equations. For the energy equation, a more convenient form exists in terms of temperature as the time dependent variable. Hence, obtain

$$\int_{R_m} \{L\}\, g_m^*(H) d\tau = \int_{R_m} \{L\} \frac{d}{dt} \left(\bar{\rho}_m c_p^m T_m^* + \frac{Ec}{2\bar{\rho}_m} (\psi^*_{m,k})^2 \right) d\tau$$

$$= \bar{\rho}_m c_p^m\, [B200S]\, \{T(t)\}'_m + \frac{Ec}{\bar{\rho}_m} \{B10\}\, \{\psi\}_m^T\, [B211S]\, \{\psi\}'_m \tag{90}$$

Since the mechanics and thermodynamics of incompressible flow are separable, $\{\psi\}'_m$ can be independently evaluated using a finite difference formula for the derivative of a tabulated function. Thus, the second term in Eq. (90) is at most a source term, usually of negligible magnitude, since the Eckert number is typically small for the more common incompressible flow configurations.

Several additional matrix evaluations are required for f_m^* to complete the description of Eq. (82) for specific dependent variables. Taking them in the order of occurrence in Table 1 (f_m^* is the approximation to f in R_m), for streamfunction, the second term simply cancels the convection operator of the standard equation form, Eq. (82). For the remaining term, obtain

$$\int_{R_m} \{L\}\, \omega_m^* d\tau = [B200S]\, \{\Omega\}_m \tag{91}$$

For solution of vorticity, the terms involving u_3 are discarded, and the remaining terms can be effectively integrated by parts to render the forms more tractable. Considering the density term, contributions stemming from the resultant surface integral can be made to vanish in pairs on all ∂R_m interior to ∂R upon assembly of the global algorithm, as discussed in Appendix B. For locations where

∂R_m coincides with ∂R, no arbitrariness exists for evaluation of the surface integral. However, ∂R coincides with ψ equal to a constant everywhere except at mass flow injection points. At these locations, the density may usually be assumed constant, and either condition is sufficient to render the matrix identically zero. So, the sole term requiring evaluation is

$$\int_{R_m} \{L\}_{,i}\left(\frac{1}{\rho^*}\right)_{,k}\epsilon_{3ki}\frac{1}{2}(\psi^*_{,\ell})^2 d\tau = \frac{A^m t^m}{2}\{\psi\}^T_m [B211S]\{\psi\}_m [B211A]\left\{\frac{1}{\rho}\right\}_m \quad (92)$$

where ρ^{-1} is selected as the preferred primative computational variable due to its universal appearance. Thus, the elements of $\left\{\frac{1}{\rho}\right\}_m$ are the inverse of the node point densities of R_m.

After integration by parts of the viscosity gradient terms, no surface integral evaluations on interior ∂R_m are required, based on the analysis used for density. For those segments of ∂R_m, coincident with ∂R and for no mass injection, the flow is laminar, hence viscosity is only weakly temperature dependent. At injection points, the density may be assumed constant, and either condition renders the surface integral terms identically zero. So, for variable viscosity, the sole contributing terms from f^*_m for vorticity become

$$\frac{1}{Re}\int_{R_m}\{L\}_{,k}\left(\mu^*_{,k}\omega^*_m + 2\mu^*_{,j}\psi^*_{m,_j}\left(\frac{1}{\rho}\right)_{,k}\right)d\tau = \frac{1}{Re}\{\Omega\}^T_m [B10][B211S]\{\mu\}_m + \frac{2A^m t^m}{Re}[B211S]\left\{\frac{1}{\rho}\right\}_m \{\mu\}^T_m [B211S]\{\psi\}_m \quad (93)$$

where the elements of the column matrix $\{\mu\}$ are the node point values of viscosity.

The sole term in f^*_m for the species continuity equation is that due to sources of mass. This term could be conveniently expressed as either element or node point dependent. The respective matrix forms are,

$$\int_{R_m}\{L\}S^a d\tau = S^a_m\{B10\} \quad (94a)$$

$$= [B200S]\{S^a\}_m \quad (94b)$$

For energy conservation, Eq. (70), the entire viscous dissipation term may be integrated by parts, and the resultant surface integrals on interior ∂R_m vanish in pairs upon assembly and rendered zero on exterior surfaces. The various terms are combined to yield the following form

$$\int_{R_m}\{L\}_{,k}\frac{\mu Ec}{3Re}\left(4\psi_{,i}\psi_{,i}\left(\frac{1}{\rho}\right)\left(\frac{1}{\rho}\right)_{,k} - \psi_{,k}\psi_{,j}\left(\frac{1}{\rho}\right)\left(\frac{1}{\rho}\right)_{,j}\right)d\tau$$

$$= \frac{Ec}{3Re}\left(4\{\psi\}^T_m [B211S]\{\psi\}_m [B211S]\left\{\frac{1}{\rho}\right\}_m \{\mu\}^T_m [B200S]\left\{\frac{1}{\rho}\right\}_m - \{\psi\}^T_m [B211S]\left\{\frac{1}{\rho}\right\}_m [B211S]\{\psi\}_m \{\mu\}^T_m [B200S]\left\{\frac{1}{\rho}\right\}_m\right) \quad (95)$$

Finally, the source term, $\rho\dot{Q}$, in the energy equation would typically be node point dependent; hence

$$\int_{R_m} \{L\}\rho\dot{Q}_m d\tau = [B200S]\{\rho\dot{Q}\}_m \tag{96}$$

It remains to establish the boundary condition specifications, $a^{(i)}$, Eq. (77), for the derived dependent variables, streamfunction and vorticity, in terms of known velocity and density distributions. The practical engineering specification is velocity scalar components perpendicular and parallel to the domain closure ∂R, and mass flux across appropriate closure segments. The closure specifically need not be, and oftentimes is not, parallel to coordinate surfaces of the global reference frame. Establishment is straightforward; contracting Eq. (37) with an alternator, and using Eq. (41), obtain

$$\frac{1}{\rho}\psi_{,k} = \epsilon_{3ik}u_i \tag{97}$$

Referring to Figure 1b, identify the surface between nodes 1 and 2 of R_m as coinciding with a segment, ∂R_m, of ∂R whereupon a specified velocity and mass flux distribution exists. Assume the velocity scalar components perpendicular ($u_\perp$) and parallel ($u_\parallel$) to the line are assigned at each node point. Contract Eq. (97) with an infinitesimal displacement vector tangent to ∂R_m and integrate to obtain

$$\int_0^{x_1^{(2)}} \frac{1}{\rho}\psi_{,1}dx_1' = \int_0^{x_1^{(2)}} \epsilon_{3il}u_i dx_1' = \int_0^{x_1^{(2)}} u_\perp dx_1' \tag{98}$$

Using Eq. (79) for all variables, the integrals are directly evaluable, Table 3; hence for a specified normal velocity on ∂R_m, the equivalent streamfunction constraint is

$$\psi_m^{(2)} = \psi_m^{(1)} + \frac{\ell^m t^m \left(u_\perp^{(1)} + u_\perp^{(2)}\right)_m}{\left(\frac{1}{\rho}\right)^{(1)} + \left(\frac{1}{\rho}\right)^{(2)}} \tag{99}$$

Equation (99), in combination with the normal mass flux specification, determines both ψ and $\frac{1}{\rho}$ on ∂R_m. In Eq. (99), $u_\perp$ is defined positive for mass efflux from R_m, and ℓ^m is the length of the closure segment between nodes 1 and 2.

The counterpart evaluation of Eq. (97), contracted with the outward pointing unit normal vector, n_k, becomes

$$\frac{1}{\rho}\psi_{,k}{}^{I}n_k = \epsilon_{3ik}u_i{}^{I}n_k = -u_\parallel \tag{100}$$

where $u_{||}$ is defined positive for alignment parallel to the x'_1 axis, Figure 1b. Using Eq. (77), the equivalent streamfunction boundary condition constraint becomes

$$a_m^{(3)} = -u_{||}$$
$$a_m^{(1)} = 0 \qquad (101)$$

The vorticity equivalent of the no-slip, wall boundary condition requires establishment. Referring to Figure 2, finite element discretization of R using linear functionals involves approximation of arbitrarily curved surfaces by piecewise continuous chords. These surface approximations, by definition, are lines of constant streamfunction, even at mass injection points, see Figure 2. At each node point on ∂R, an approximation to the local normal to the surface can be constructed by bisecting the included angle, as shown. Along each of these lines the streamfunction-vorticity compatability equation, Eq. (40), locally approximates an ordinary differential equation in the direction normal to the surface. After integration by parts, the equation takes the form

$$\int_0^{\ell} ds \int_0^{\eta} \omega(\eta) d\eta = \int_0^{\ell} ds \int_0^{\eta} \left[d\left(\frac{1}{\rho}\psi\right)_{,\eta} - d\left(\psi \frac{1}{\rho}_{,\eta}\right) \right] \qquad (102)$$

Using Eq. (79) to represent the functional dependence for all dependent variables, the values of vorticity, Ω_w, at node points lying on the solution domain closure where no-slip is enforced, is expressible in terms of wall and next-interior node point values of the variables as

$$\Omega_w = -\left[\frac{3\left[\left(\frac{\psi}{\rho}\right) - \left(\frac{\psi}{\rho}\right)_w\right] - \frac{3}{2}[\psi - \psi_w]\left[\frac{1}{\rho} - \frac{1}{\rho_w}\right]}{\ell^2} + \frac{\Omega}{2} \right] \qquad (103)$$

where ℓ is the normal displacement of the interior node from ∂R. The vorticity vanishes identically on portions of the solution domain closure that are planes of symmetry. For closure segments where unknown (outflow) velocity profiles exist, use of the vanishing normal gradient of vorticity is appropriate.

Equations (83) - (103) complete the finite element solution algorithm specification for numerical solution of the steady-state, two-dimensional, Navier-Stokes equations for a fluid with variable density and viscosity. For flows where the density is time invariant, the transient solution is additionally specified. Should violation of the stated assumptions regarding density and/or viscosity variations on ∂R occur for a specific problem, the discarded surface integrals can be readily evaluated and their contribution to the solution inserted appropriately.

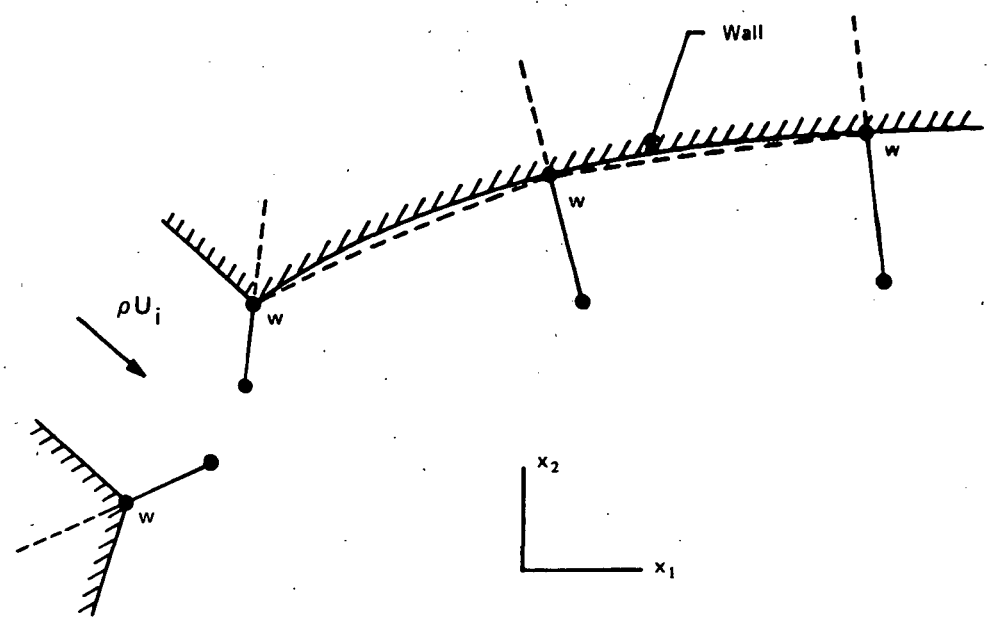

Figure 2. Establishment of Vorticity Boundary Condition Statement

Planar Ring Finite Elements for the Axisymmetric Incompressible Navier-Stokes Equations

In axisymmetric space, moment generation is invariant only under coordinate rotation, see Appendix C. The preferred element orientation remains in the primed coordinate systems, Figure 1, as defined by Eq. (83). The integration kernels become, respectively,

$$d\tau = 2\pi x_2 dx_1' dx_2' \tag{104a}$$

$$d\sigma = 2\pi x_2 dx_1' \tag{104b}$$

where x_2 is the radial coordinate in the global reference frame of a point in R_m. Before integrations can be performed, it is necessary to express x_2 in the primed system; using Table 2 obtain

$$x_2 = x_2^{(1)} + x_i' L_i \tag{105}$$

where $x_2^{(1)}$ is the radial coordinate of node point 1 in the global reference frame.

The finite element counterpart of the generalized diffusion term, Eq. (82), now requires additional consideration for streamfunction. Since the diffusion coefficient contains a metric coefficient, Table 1, the resultant differential operator is not the Laplacian in cylindrical coordinates. The explicit appearance of a Laplacian can be extracted by definition of a new variable, $\phi \equiv \psi/x_2$, whereupon the compatibility equation, Eq. (40) takes the form

$$-\omega = \left[\frac{1}{\rho}\phi, _k\right]_{;k} + \phi \left(\frac{1}{\rho x_2}\right)_{,2} \tag{106}$$

For the function ϕ, as well as the remainder of the dependent variables, the generalized diffusion term for constant density and viscosity takes the form

$$\kappa \int_{R_m} \{L\}_{,k} K^m q^*_{m;k} d\tau = \kappa \int \{L\}_{,k} K^m \{L\}^T_{,k} \{Q\}_m d\tau$$

$$= \kappa K^m \{R\}^T_m \{B10\} [B211S] \{Q\}_m \qquad (107)$$

where K^m is an element scalar stemming from the assumed constant properties, the elements of $\{R\}_m$ are the node radial coordinates in the global reference frame, and in axisymmetric space, the element thickness t^m defined in $\{B10\}$, Table 4, is replaced by 2π.

The convection matrix becomes

$$\int_{R_m} \{L\} \epsilon_{3ki} \frac{\psi^*_i}{x_2} q^*_{m;k} d\tau = \int_{R_m} \{L\} \{\psi\}^T_m \{L\}_{,i} \epsilon_{3ki} \{L\}^T_{,k} \{Q\}_m dx'_1 dx'_2$$

$$= \{B10\} \{\psi\}^T_m [B211A] \{Q\}_m \qquad (108)$$

which is identical to the two-dimensional form with t^m replaced by 2π. The boundary condition matrices for the dependent variables are

$$\kappa \int_{\partial R_m} \{L\} a_m^{(1)} q^*_m d\sigma = \kappa a_m^{(1)} [A200SA] \{Q\}_m \qquad (109)$$

$$\kappa \int_{\partial R_m} \{L\} a_m^{(3)} d\sigma = \kappa a_m^{(3)} \{A10A\} \qquad (110)$$

In Eqs. (109) - (110), the suffix A in the matrix name refers to the axisymmetric counterpart of the standard form, see Table 5. In each case, the first term is identical to the two-dimensional form with t^m replaced by 2π.

The transient algorithm is correctly specified for constant density flows. The axisymmetric finite element evaluation for g^*_m, Eq. (82), becomes

$$\int_{R_m} \{L\} g^*_m d\tau = \int_{R_m} \{L\} \bar{\rho}_m \{L\}^T \frac{d}{dt} \{Q\}_m d\tau$$

$$= \bar{\rho}_m [B200SA] \{Q(t)\}'_m \qquad (111)$$

The added complexity of the [B200SA] standard matrix, Table 5, stems from lack of translational invariance.

The sole source terms requiring evaluation for constant property axisymmetric flows are in the modified streamfunction equation, Eq. (106). For the vorticity term, obtain

$$\int_{R_m} \{L\} \omega^*_m d\tau = [B200SA] \{\Omega\}_m \qquad (112)$$

TABLE 5
ADDITIONAL STANDARD MATRIX FORMS FOR SIMPLEX FUNCTIONALS IN AXISYMMETRIC SPACE

MATRIX NAME	MATRIX FUNCTION	MATRIX EVALUATION(1), (2)
[A200SA]	$\int_{\partial R_m} \{L\}\{L\}^T d\sigma$	$\frac{2\pi \ell^m}{6}\left(r_1 \begin{bmatrix} 2 & 1 & 0 \\ & 2 & 0 \\ & & 0 \end{bmatrix} + \frac{r_2 - r_1}{2} \begin{bmatrix} 1 & 1 & 0 \\ & 3 & 0 \\ & & 0 \end{bmatrix}\right)$
{A10A}	$\int_{\partial R_m} \{L\}\, d\sigma$	$\frac{2\pi \ell^m}{2}\left(r_1 \begin{Bmatrix} 1 \\ 1 \\ 0 \end{Bmatrix} + \frac{r_2 - r_1}{3} \begin{Bmatrix} 1 \\ 2 \\ 0 \end{Bmatrix}\right)$
[B200SA]	$\int_{R_m} \{L\}\{L\}^T d\tau$	$\frac{2\pi A_m}{12}\left(r_1 \begin{bmatrix} 2 & 1 & 1 \\ & 2 & 1 \\ & & 2 \end{bmatrix} + \frac{r_2 - r_1}{5} \begin{bmatrix} 2 & 2 & 1 \\ & 6 & 2 \\ & & 2 \end{bmatrix} + \frac{r_3 - r_1}{5} \begin{bmatrix} 2 & 1 & 2 \\ & 2 & 2 \\ & & 6 \end{bmatrix}\right)$
[B200SC]	$\int_{R_m} \{L\}\{L\}_C^T d\tau$ (3)	$\frac{2\pi A_m}{12} \begin{bmatrix} 2r_1 + r_2 + r_3 & & \\ r_1 + 2r_2 + r_3 & & \\ r_1 + r_2 + 2r_3 & & \end{bmatrix}$

(1) The lower case r refers to node radial coordinates in the global reference frame.

(2) Symmetric matrices are written in upper triangular form.

(3) [B200SC] is a diagonal matrix.

For constant density, the form for the remaining term is

$$\int_{R_m} \{L\}\{L\}^T \{\phi\}_m \frac{1}{\rho x_2^2} d\tau = \frac{3}{\bar{\rho}_m \{1, 1, 1\}\{R\}_m} [B200S]\{\phi\}_m \qquad (113)$$

where [B200S] is the rectangular Cartesian matrix defined in Table 4 with t^m replaced by 2π. The boundary condition statements for both streamfunction and vorticity are identical to the two dimensional specifications, with the addition of respective inverse node radii to the denominator of Eq. (99) and the numerator of Eq. (103).

COMOC COMPUTER PROGRAM

The COMOC (Computational Continuum Mechanics) general-purpose computer program system embodies the derived finite element solution algorithm for the general initial value, elliptic boundary value equation system, and is coded entirely in terms of generalized non-dimensional independent and dependent variables. In addition to producing the results to be discussed, it has been exercised for problems in transient heat conduction (Reference 11) and the three-dimensional boundary layer equations (References 7 and 9). The program consists of four basic Modules. In the INPUT Module, the desired discretization is formed by specification of the plane coordinates of the triad of vertex nodes for each finite element. The non-vanishing boundary condition coefficients $a_m^{(i)}$, Equation (82), are included as element information for each dependent variable to be solved, since in general the different Q's have individual specifications. The next two Modules are basically DO loops on the finite elements of the discretization. In the GEOMETRY Module, the element standard matrices are formed and stored. The INTEGRATION Module embodies the integration algorithm for the system of ordinary differential equations as well as access to an algebraic equation system solver. For either case, the basic element operation is formation of Eq. (82), and assembly of the element matrices into the global representation. The integration algorithm presently used by COMOC is an explicit, single-step, multi-stage finite difference procedure with a large region of absolute stability (Reference 11). A banded Cholesky equation solver is used for the algebraic systems. At user-selected points, the OUTPUT Module is called to record the arrays within the dependent variable vectors $\{Q\}$ and other desired parameters.

NUMERICAL RESULTS

Numerical evaluation of the finite-element solution algorithm for the two-dimensional Navier-Stokes equations, as embodied in the COMOC computer program, has been performed to assess solution accuracy, convergence, and versatility of the finite-element concept. A problem of particular value for accuracy studies is developing flow in a rectangular duct of an isothermal, constant-density fluid. This problem retains the full nonlinear character of the Navier-Stokes equations, and the outflow boundary conditions of vanishing normal gradient for both streamfunction and vorticity are analytically exact for sufficient duct length. Figure 3 illustrates the basic 144 finite element discretization of the duct flow problem; for Re = 200, based on duct width, the fully developed velocity flow field should be attained within the duct (Reference 13). Additional discretizations studied have doubled and halved the number of node rows, and doubled the number of node columns; these are referred to, respectively, as the 264, 54 and 276 finite element discretizations. Figure 4 shows the COMOC computed velocity distributions at the terminal node column of the solution domain for the four studied discretizations. Since velocity is a constant within an element for linear streamfunction approximations, Equation (37), the velocity contours are correspondingly constructed. For all discretizations, the analytic solution approximately bisects the computed constant velocity within each element, and convergence with discretization is illustrated. Within the constraint of element constant velocity, solution accuracy is generally good for all discretizations, although refinement of the grid certainly improves the solution for points not coincident with an approximate element centroid. Poorest improvement in accuracy occurs near the duct centerline where the 2.5% inaccuracy of the 264 element solution is modestly poorer than either the 144 or 276 element solutions. It is recalled that the 264 element solution doubles the node rows only, which yields element aspect (length/width) ratios of about 50 in this region. Propagation of vorticity to the duct centerline is consequential only for $x/L > 8.0$, and its underprediction in the far downstream region is reflected in the lack of computed velocity improvement. This is illustrated further in Figure 5 which presents computed streamfunc-

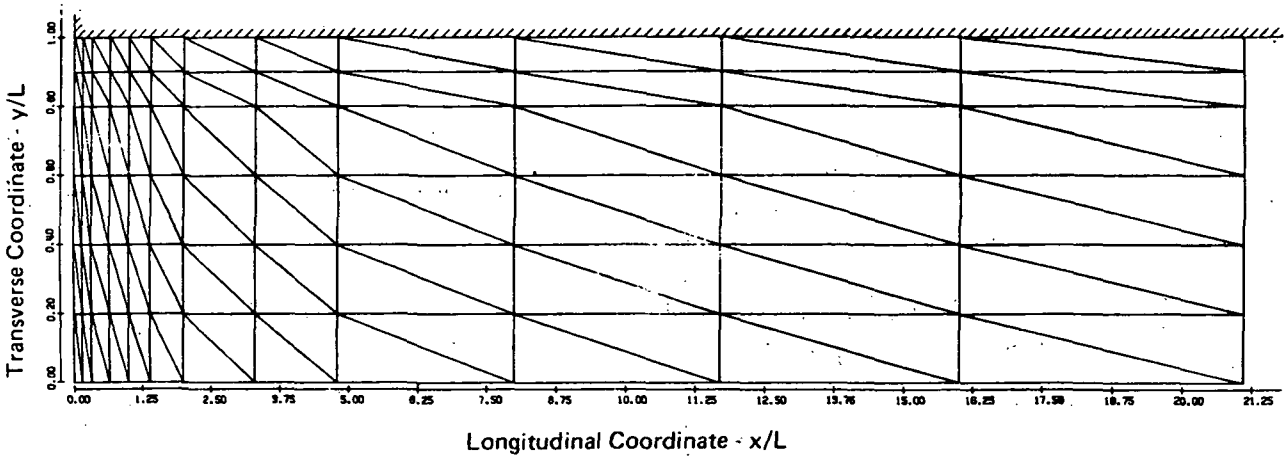

Figure 3. Discretization of Rectangular Duct into 144 Triangular Finite Elements

tion and vorticity in comparison to the analytic values. The improvement in computed vorticity with discretization is also illustrated, and the nodal accuracy of the 54 element streamfunction solution is remarkable and reflects the well-posedness of streamfunction cast as a boundary value problem. Figure 6 illustrates computed longitudinal velocity contours at various stations downstream of the duct inlet for the 264 element discretization. Velocity overshoot is predicted to occur over the first 4.8% of the duct length and is maximum at the 1.5% length station. The magnitude and location of velocity overshoot is in agreement with other solutions of the same problem (References 12, 14).

Solution accuracy, as well as computational speed for a transient problem, depends not only upon discretization but also upon the manner selected for assembly of the finite-element equivalent of the function, g, Equation (82). Initial value integration algorithms are typically derived for ordinary differential equation systems that are explicitly uncoupled in the derivatives; that is, the standard form is

$$\{Q\}' = f(\{Q\}, t) \tag{114}$$

Global assembly of the finite element solution algorithm, Equation (82), produces a transient equation description wherein the derivatives are explicitly coupled by the [B200S] or [B200SA] finite-element matrices. Hence, Boolean assembly of the transient term yields a global description that contains a sparse symmetric matrix banded about the main diagonal modifying the $\{Q\}'$ matrix. The bandwidth is a function of discretization, and premultiplication of the entire equation system by its inverse (or equation solver equivalent) is needed to achieve the required form, Eq. (114). The inverse is symmetric and a full matrix. Thus, this operation couples the time varying behavior of node point dependent variables to all nodes of the discretization. The inversion process can be made trivial, and nearest-neighbor transient behavior maintained, by "condensing" the elements of the [B200S] and [B200SA] matrices, on rows, which renders the global matrix diagonal. In two-dimensional space, this operation is a simple averaging, see Table 4. In axisymmetry, the geometry of the discretization and lack of translational invariance produces the condensed matrix form listed as [B200SC] in Table 5.

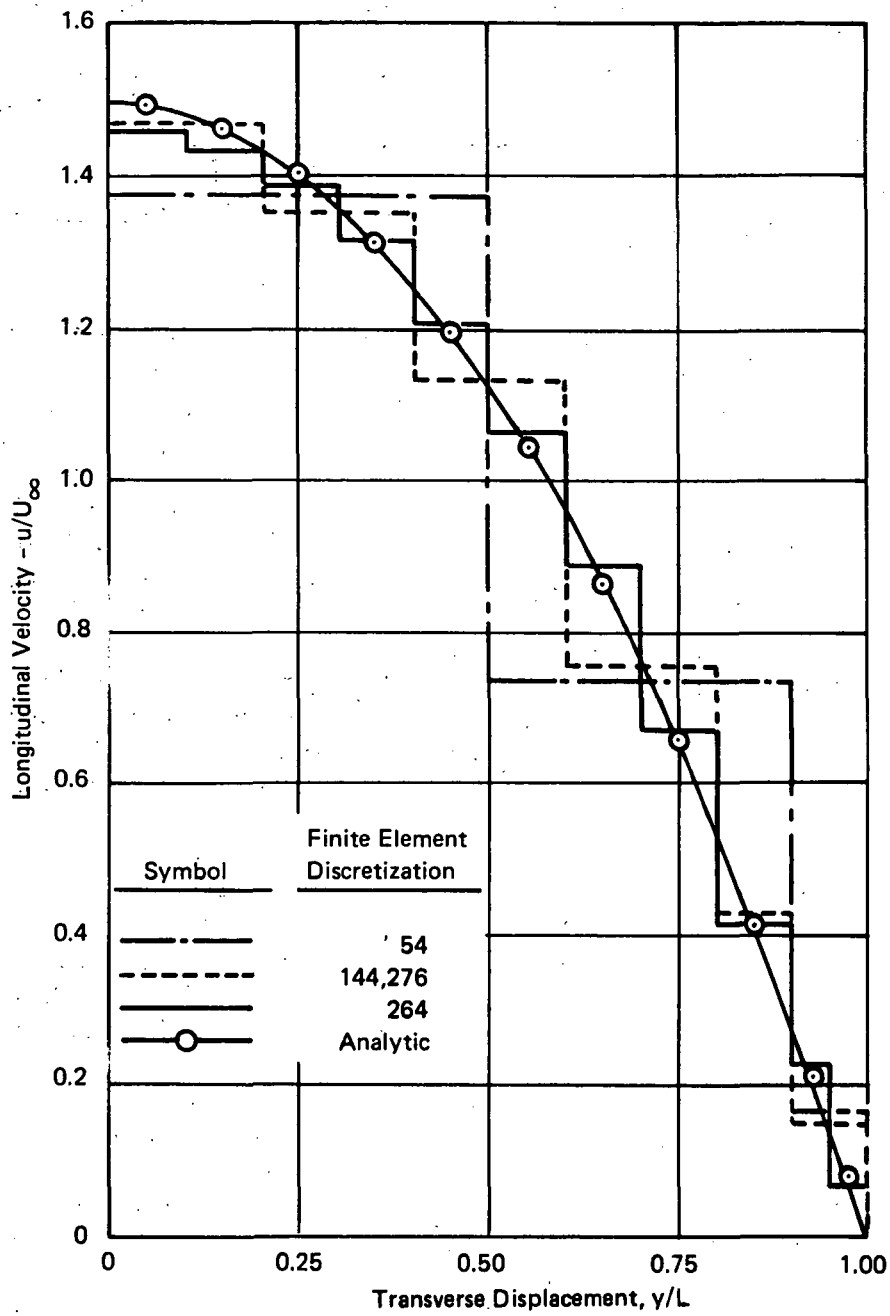

Figure 4. Computed Fully Developed Longitudinal Velocity Distributions, Re = 200

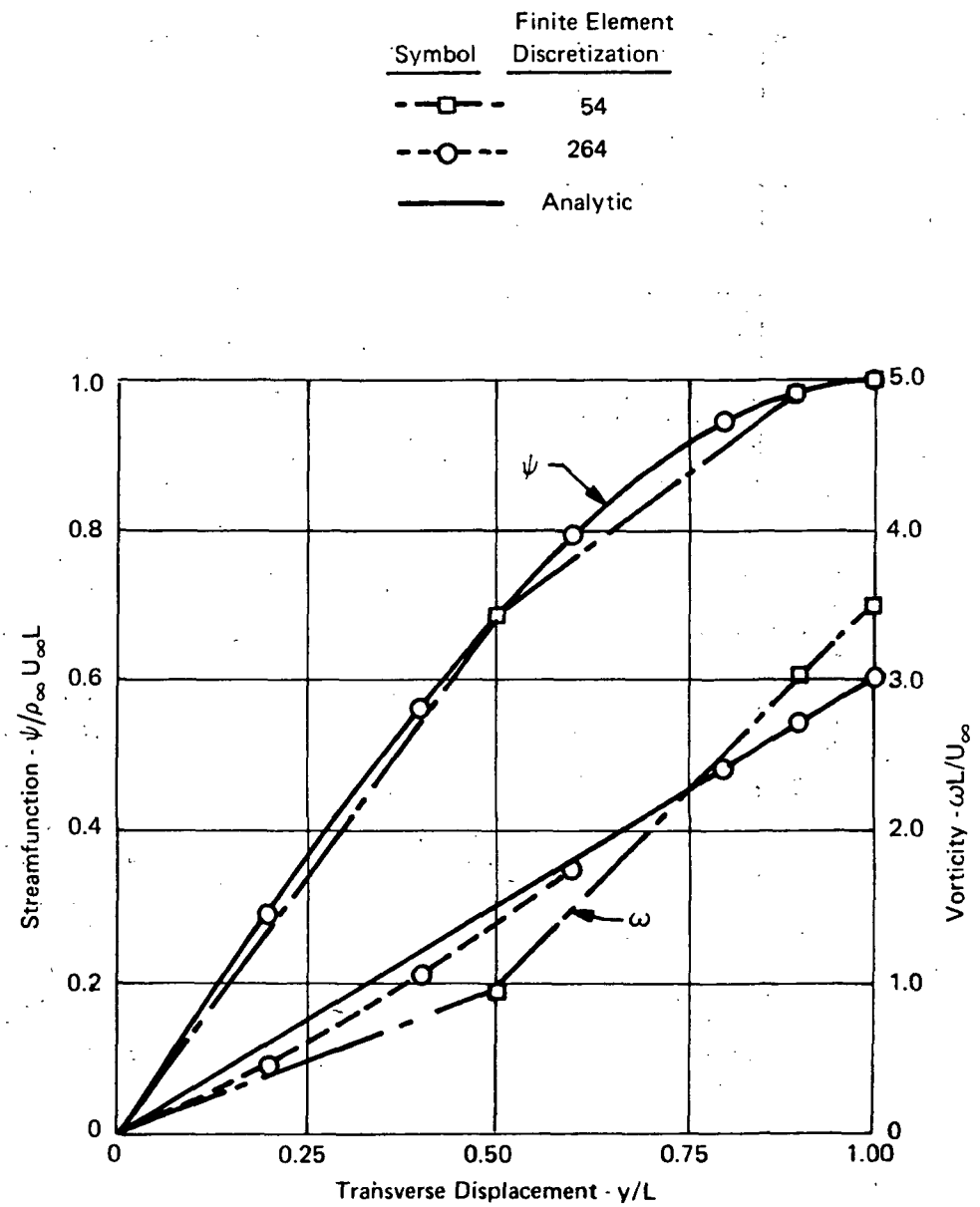

Figure 5. Computed Fully Developed Streamfunction and Vorticity for Duct Flow, Re = 200

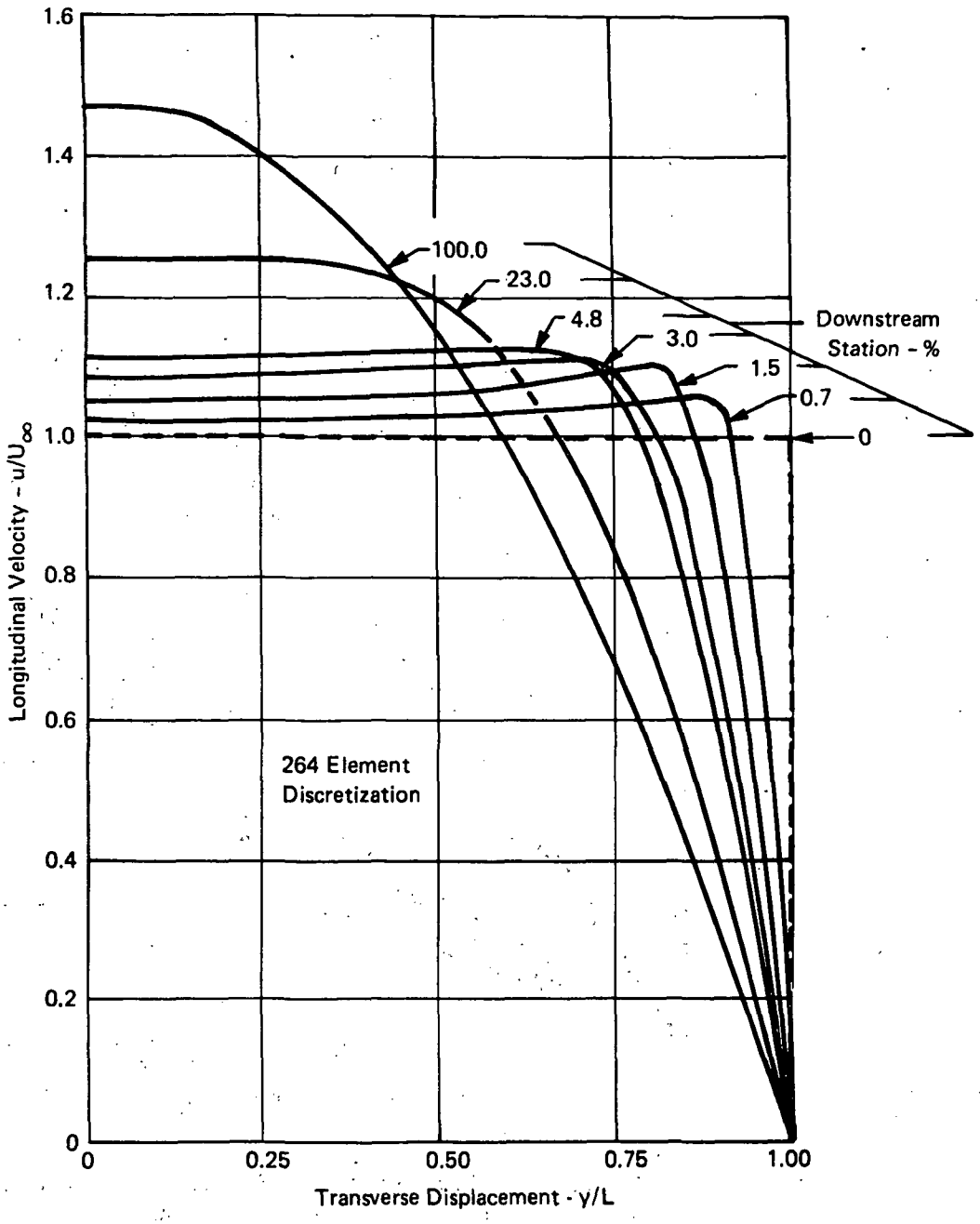

Figure 6. Longitudinal Velocity Distributions for Incompressible Duct Flow, Re = 200

Both the consistent and condensed forms for the initial value matrix have been evaluated for transient problems by COMOC. Employing the consistent form produces a significantly "stiffer" ordinary differential equation system as manifested by the small integration step-size accepted by COMOC. Solution accuracy appears generally acceptable except for spurious behavior during impulsive starts in regions of initially uniform variable distributions. For uniformly positive fluxes into these domains, wave-like depression of selective node point values below their initial values is observed. Evaluation of this phenomenon, and absolute assessment of solution accuracy was made by studying the heating of a quiescent fluid in an axisymmetric duct subject to external uniform heating from the wall. For this problem, the flow equations are identically satisfied, and only the energy equation (70) requires solution after deletion of both the nonlinear source term, Equation (90), and the convection term. Figure 7 shows a comparison between COMOC computed radial temperature distributions in the fluid, for two discretizations and both assembly options for the initial value matrix, and an analytic solution (Reference 15). At the outer wall, $\frac{r}{r_o} = 1$, solution accuracy for the coarse discretization and consistent matrix assembly is excellent. The depression below the initial uniform temperature at the interior radii nodes is illustrated to propagate into the interior region. The solution accuracy for the same discretization using the condensed matrix form is noticeably poorer at the wall, and although devoid of the depressions is only a local improvement elsewhere. However, doubling the discretization and employing the condensed form produces a comparable or uniformly more accurate solution everywhere.

For small-scale problems involving less than about 50 finite elements, experimentation indicates that computer CPU execution time for double discretization and condensed form solutions is about equal to the corresponding consistent form solution. Even though the consistent form inverse can be stored, for larger problems, the lengthy multiplication process coupled with lower stability produces execution times uniformly in excess of the corresponding condensed, double-discretization solution. Hence, until integration algorithms for equation systems that are explicitly coupled in the derivatives are developed (for example, see Reference 16), it appears uniformly preferable to employ finer discretizations and the condensed matrix form for solution of transient problems by finite element techniques.

Abrupt non-uniformities in discretization near a no-slip surface of the domain closure have been observed to adversely affected solution accuracy, primarily through the vorticity boundary condition statement, Equation (103). Evaluation of solution deviations was accomplished using variations of the duct flow discretization, Figure 3 after removal of the row of nodes at y/L = 0.95. The analytic steady-state vorticity distribution was uniformly applied across the entire duct length as the initial condition. The affect on computed streamfunction accuracy, of sequentially replacing nodes along the line y/L = 0.95, starting from the left, is illustrated in Figure 8a. At each abrupt change in discretization, the streamfunction alternately over- and under - predicts the correct value by less than about ± 0.5%. This variation in streamfunction accuracy is probably acceptable for most practical flow field predictions. However, near a no-slip wall, these minor errors in streamfunction can produce an extremely large error in wall vorticity, as computed through Equation (103) and illustrated in Figure 8b. In all cases, continuing the transient solution from these initial computations produced convergence to the correct solution for both streamfunction and vorticity. The direction of the diagonals of elements near a wall did not materially affect solution accuracy as long as they were all of the same slope, that is, positive or negative. However, Figure 9 shows that alternating the slopes has a detrimental effect on computed streamfunction accuracy. As also illustrated, finer discretization improved solution accuracy. This evidence indicates that regular and uniform discretizations near a no-slip wall are preferable.

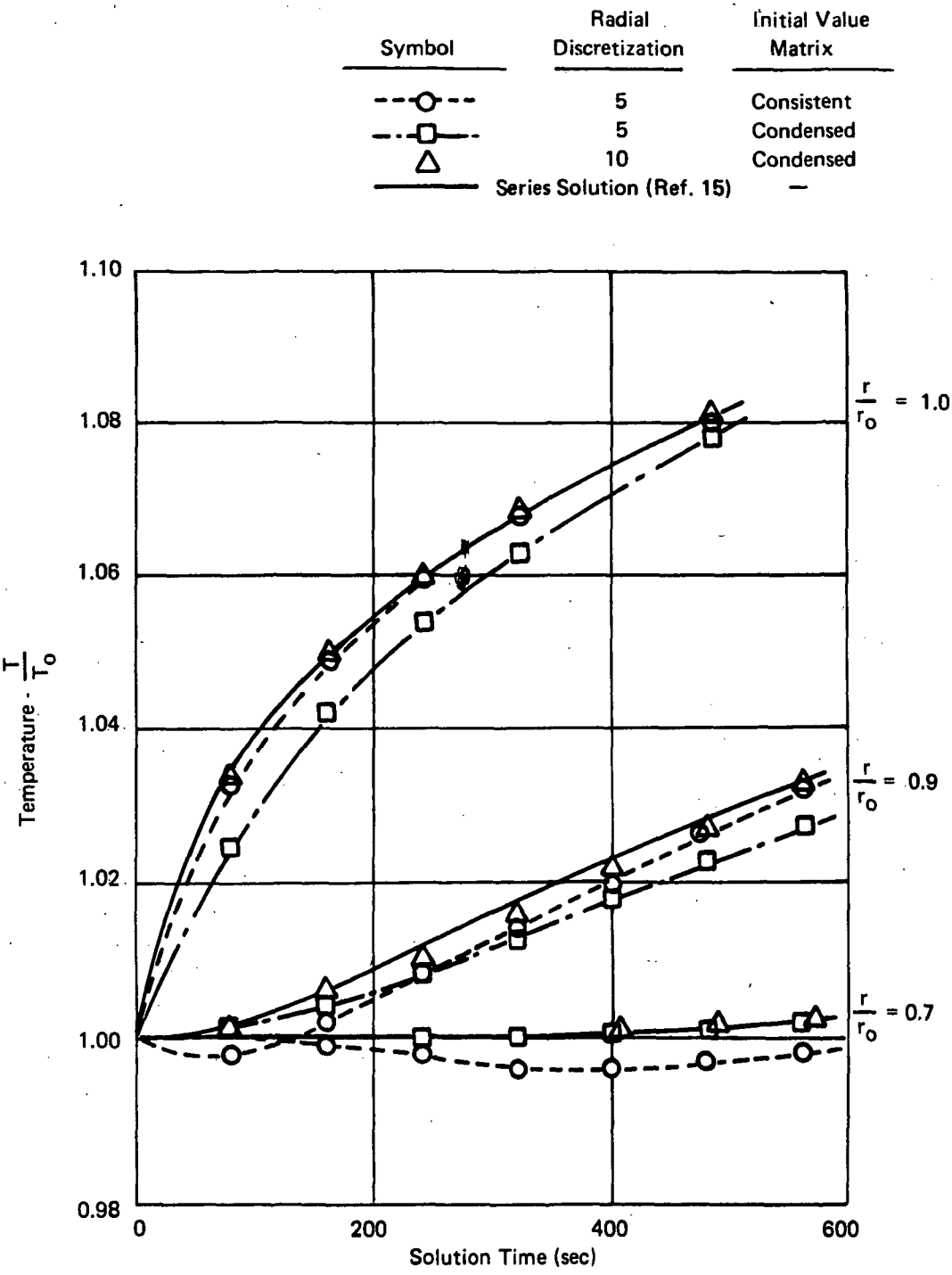

Figure 7. Computed Transient Temperature Distribution in Axisymmetric Quiescent Duct

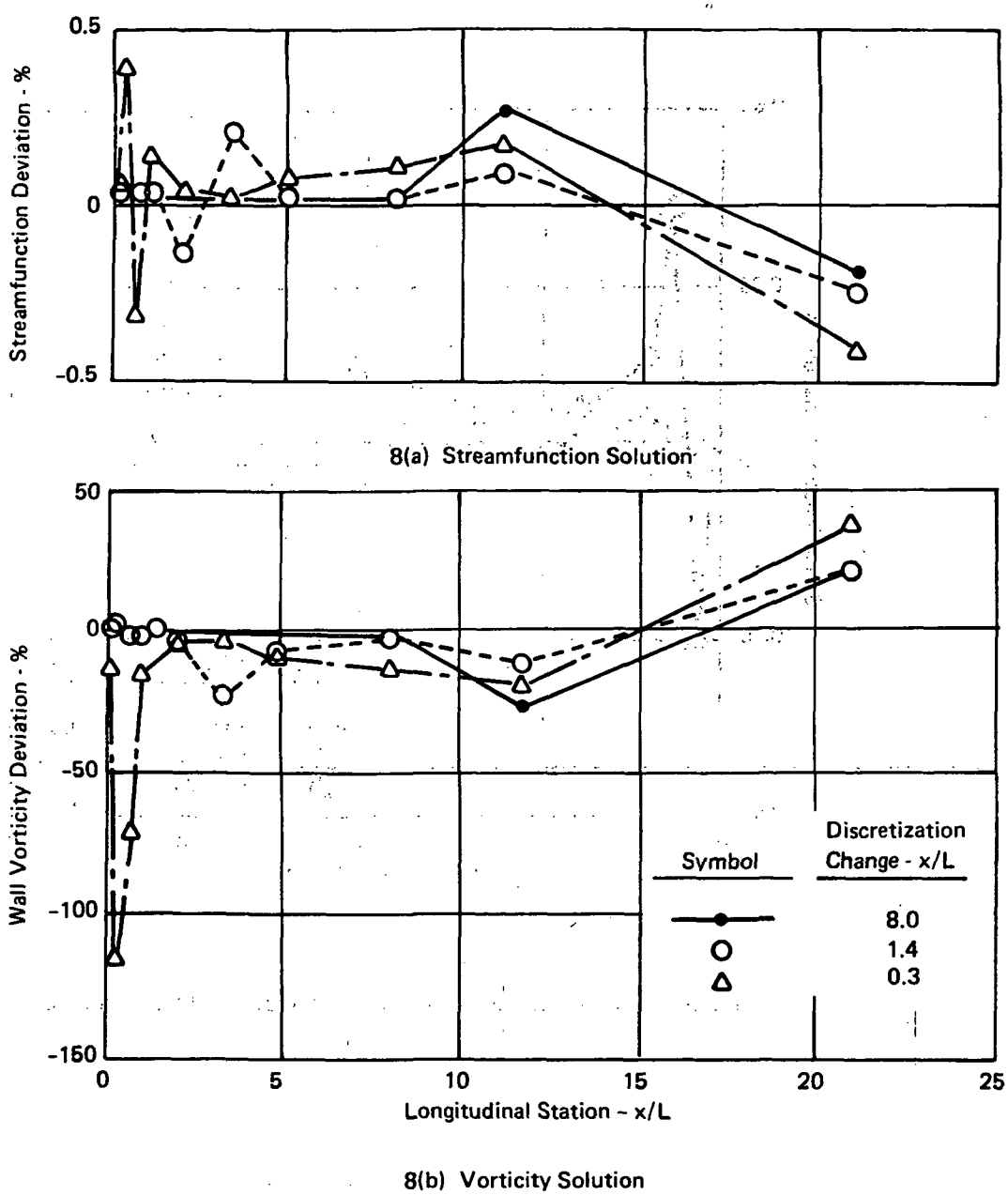

Figure 8. Discretization Influence on Vorticity and Streamfunction Near a Wall

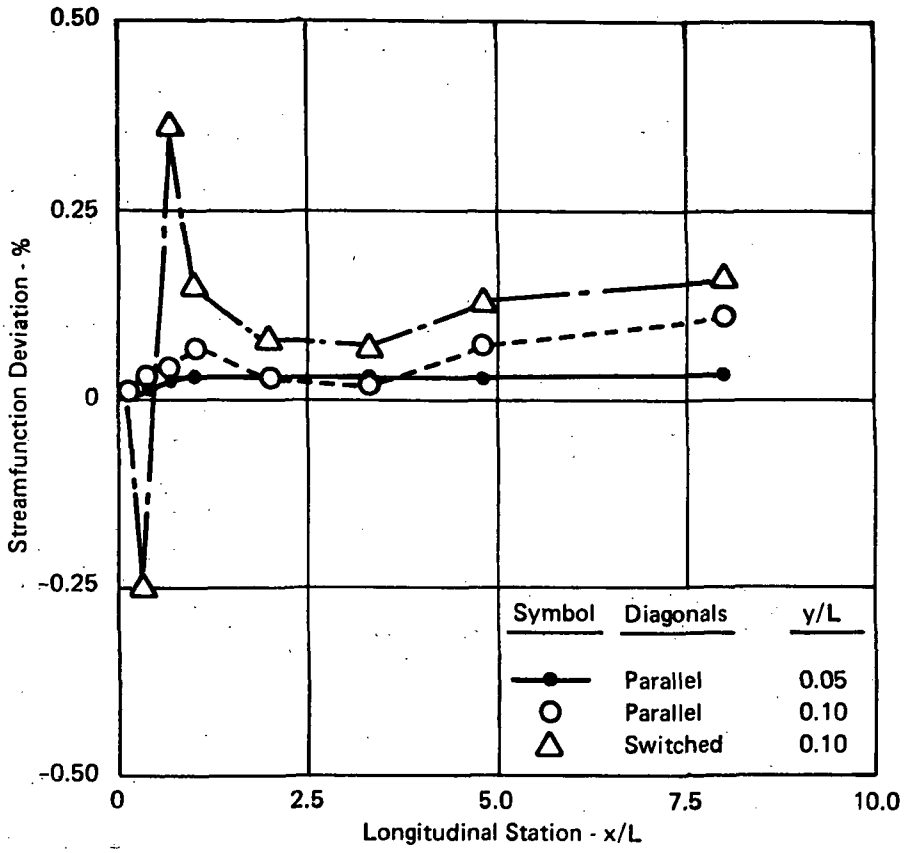

Figure 9. Discretization Influence on Computed Streamfunction

A crucial analysis for the class of flows governed by the full Navier-Stokes equations is prediction of regions of recirculation imbedded within an arbitrary flow field. For example, it is precisely this phenomenon that prevents use of boundary layer theory in regions of separation in otherwise predominantly boundary layer flows. A great deal of laboratory and numerical experimentation has been conducted for the sample geometry illustrated in Figure 10, which is flow in a duct with a considerable enlargement in cross-sectional area. The fluid will not turn the corner, but instead provides a smooth area transition by self-generation of a recirculation region. Finite difference numerical solution procedures for this problem typically require special handling of the corner region to promote generation of the recirculation zone (References 14, 17). There is no such requirement for the finite element algorithm and all wall-node vorticities are computed in a uniform fashion. Of critical importance for accurate computational representation of this problem is prediction of the points of attachment of the streamline dividing the recirculation region from the main flow, both at the step and at the downstream reattachment point, points A and B, Figure 10. For flow Reynolds numbers based upon step height larger than 20 (Reference 17) the attachment at the step occurs just below the corner on the vertical face. The downstream attachment point is approximately linear with Reynolds number in the range $20 < Re < 200$ (Reference 18). The points of attachment are identified by a vorticity sign change, and the streamfunction solution must numerically bifurcate to predict recirculation.

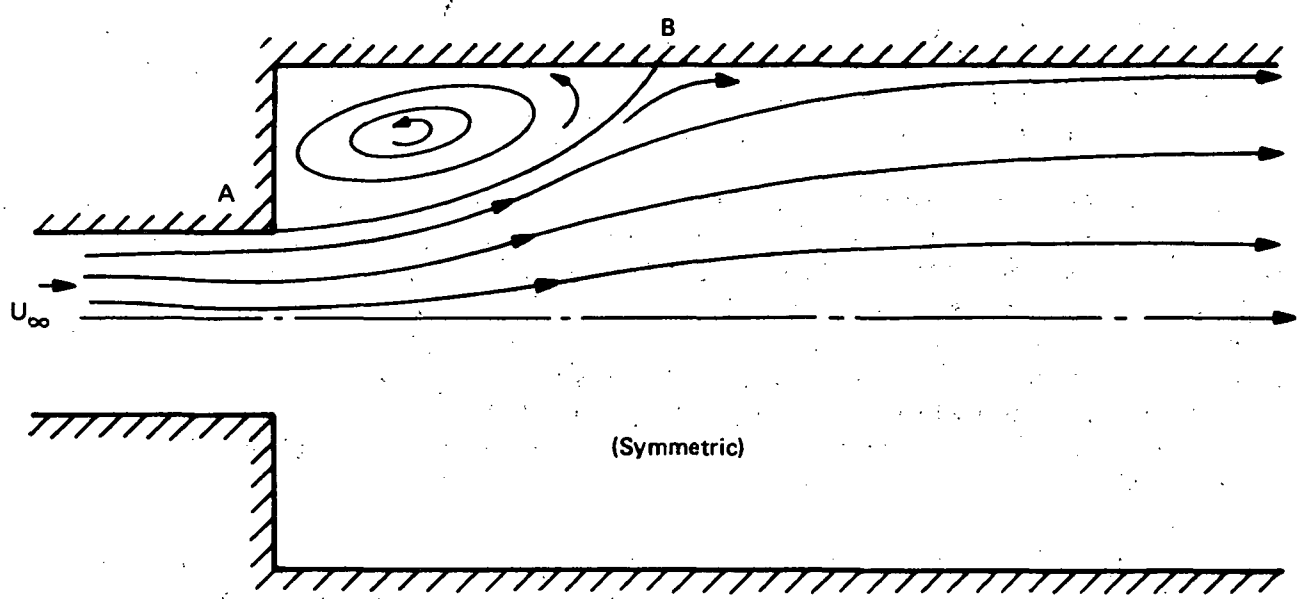

Figure 10. Flow Over a Rearward Facing Step

The finite element solution algorithm, as embodied in COMOC, has been assessed to accurately predict the rearward step steady-state flow field for Re = 200, treating the problem as transient. Shown in Figure 11, is the finite element discretization employed for the problem. The description employs 211 finite elements and is non-uniform to gain definition in the corner region. Figure 12 shows computer-generated plots of computed streamfunction and vorticity distributions (upper and lower half planes) at various time stations in the transient solution. Figure 12a presents the essentially inviscid starting solution corresponding to impulsive application of a pressure gradient to a quiescent, fluid-filled duct. In Figure 12b, the streamfunction contours have drawn away from the step base and the resultant separation bubble is detected. This bubble rapidly proceeds up the step face, Figure 12c, and then proceeds to grow in strength and size, Figure 12d. Figures 12e - 12h pre-

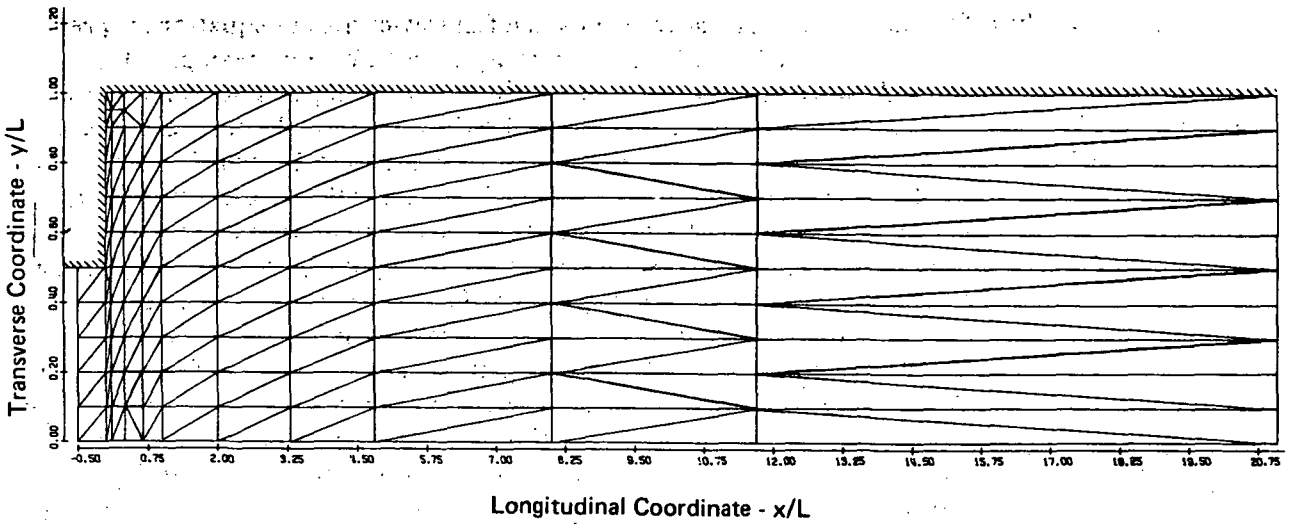

Figure 11. Discretization of Rearward Facing Step in a Rectangular Duct into 211 Triangular Finite Elements

sent growth of the recirculation region to an essential steady-state solution. Note in each figure the predicted occurrence of a second recirculation region at the base of the step. Within this region, the flow field corresponds to flow into a forward facing step, and the fluid again shields itself from abrupt changes in cross-sectional area by self-generation of smooth transitions.

The point of reattachment of the dividing streamline for essential steady state, Figure 12h is about 21 step-heights downstream. This prediction agrees within 10% of an extrapolation of data presented in Reference 18 for two-dimensional flows and with the computations of Reference 19 for axisymmetric flow. No other numerical solution to the two-dimensional rearward step problem at this Reynolds number is published; further, Dorodnitsyn (Reference 18) observed that several independent solution techniques for the finite difference equivalent equations become unstable at Reynolds numbers approaching 200. The overall shape of the predicted recirculation zone, Figure 12h, is in general agreement with the experimental data of Reference 17 obtained for Re = 130.

Several additional experiments have been performed with the rearward step problem to evaluate performance of the versatility of COMOC. Time dependent and non-coordinate surface boundary conditions are explicitly acceptable subject to a present limitation in COMOC that rezoning is not an automatic feature. Figure 13a shows a close-up of the steady-state rearward step solution, which served as the initial condition for the experiments. In the first case, a portion of the duct wall was allowed to move outwards in a specified fashion somewhat similar to what might occur for pulsatile flow in an elastic vessel. Figure 13b shows the steady-state computed solution after the indentation had been stopped and held stationary at 0.4 step heights relative displacement. Computed solution behavior

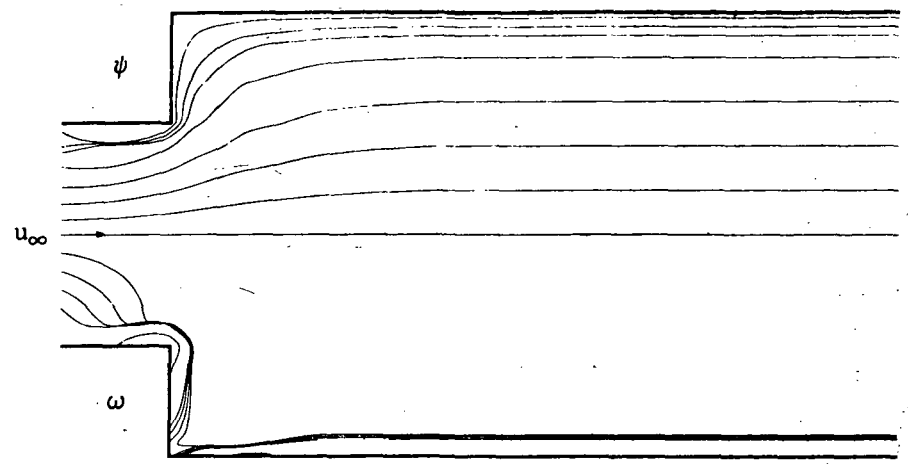

Figure 12a. COMOC Computed Streamfunction and Vorticity Distribution for Transient Flow Over a Rearward Facing Step, Re = 200, t = 0.000 sec

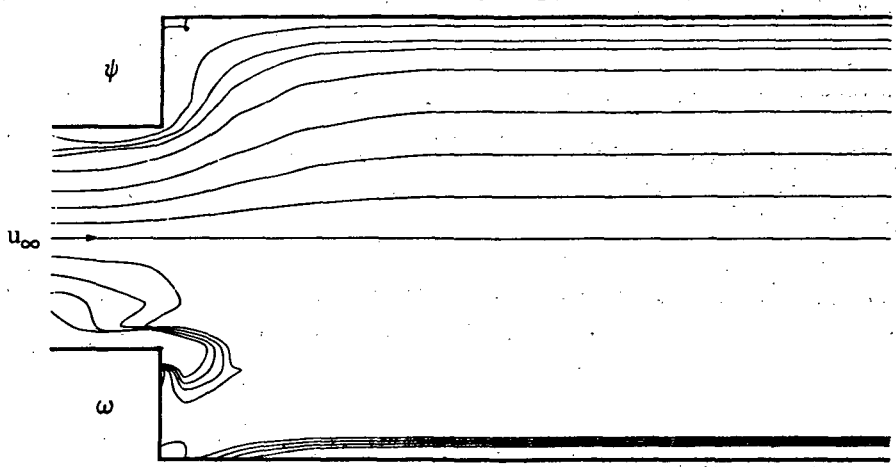

Figure 12b. COMOC Computed Streamfunction and Vorticity Distribution for Transient Flow Over a Rearward Facing Step, Re = 200, t = 0.200 sec

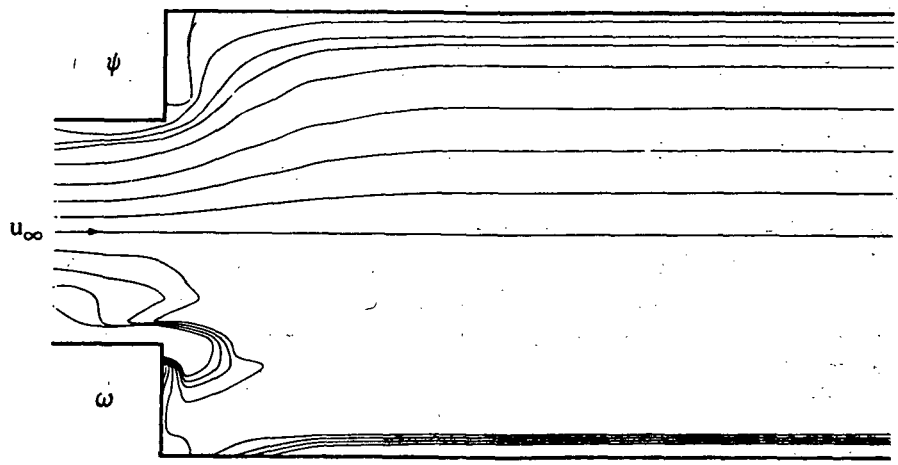

Figure 12c. COMOC Computed Streamfunction and Vorticity Distribution for Transient Flow Over a Rearward Facing Step, Re = 200, t = 0.250 sec

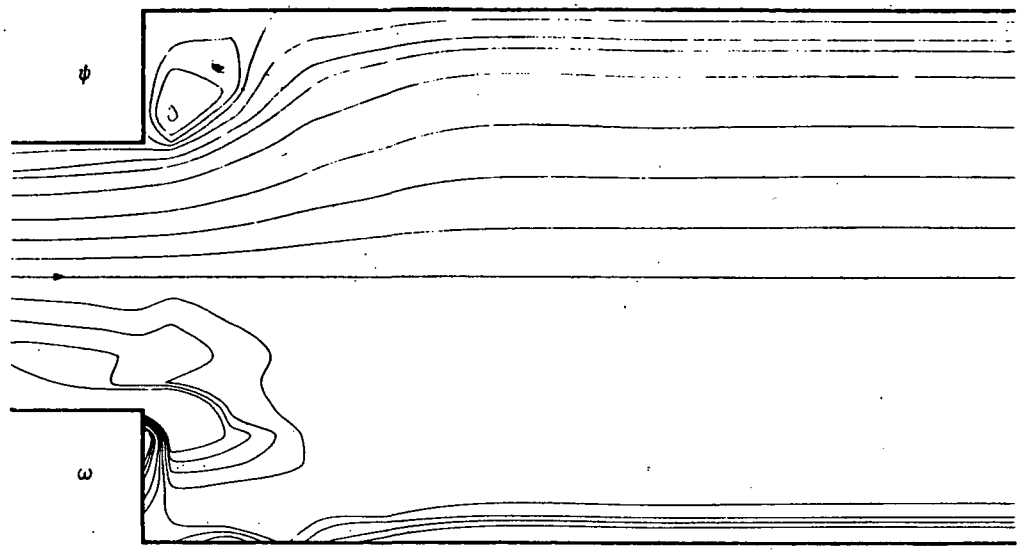

Figure 12d. COMOC Computed Streamfunction and Vorticity Distribution for Transient Flow Over a Rearward Facing Step, Re = 200, t = 0.500 sec

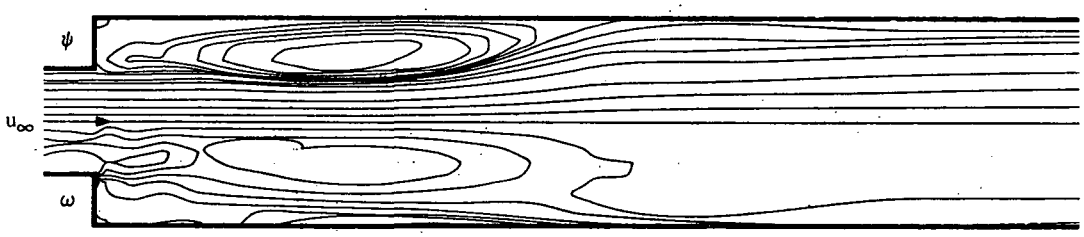

Figure 12e. COMOC Computed Streamfunction and Vorticity Distribution for Transient Flow Over a Rearward Facing Step, Re = 200, t = 5.008 sec

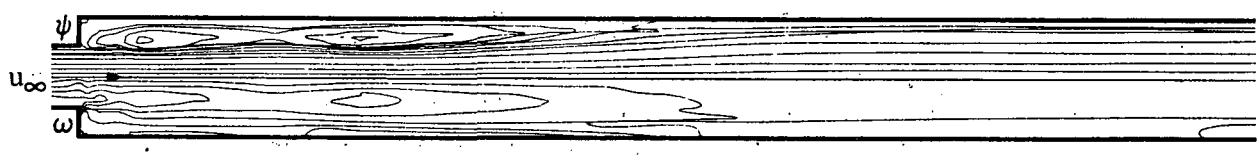

Figure 12f. COMOC Computed Streamfunction and Vorticity Distribution for Transient Flow Over a Rearward Facing Step, Re = 200, t = 9.998 sec

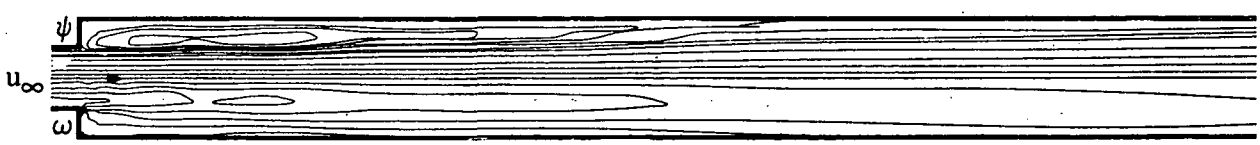

Figure 12g. COMOC Computed Streamfunction and Vorticity Distribution for Transient Flow Over a Rearward Facing Step, Re = 200, t = 22.365 sec

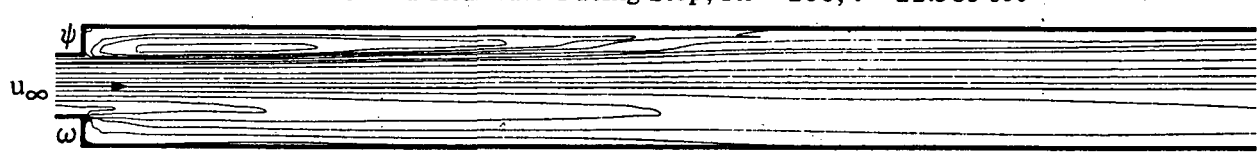

Figure 12h. COMOC Computed Streamfunction and Vorticity Distribution for Transient Flow Over a Rearward Facing Step, Re = 200, t = 29.209 sec

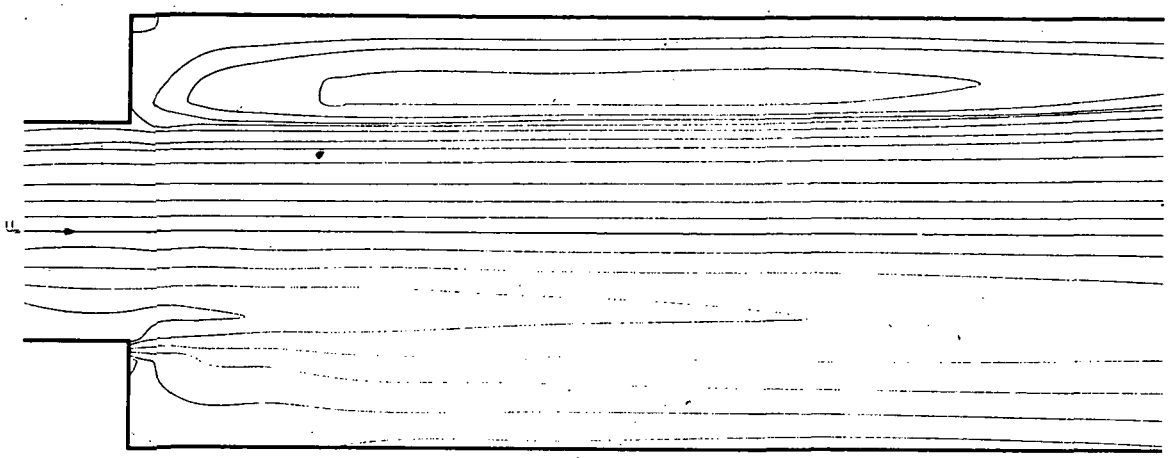

Figure 13a. COMOC Computed Steady-State Streamfunction and Vorticity for Flow over a Rearward Step, Re = 200

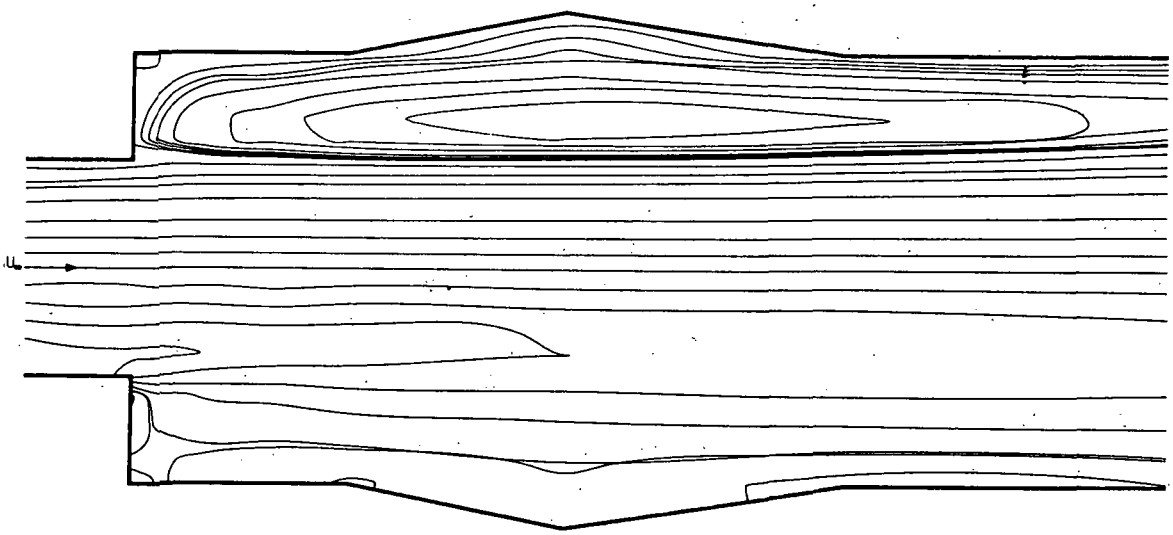

Figure 13b. COMOC Computed Steady-State Streamfunction and Vorticity for Flow over a Rearward Step in Irregular Shaped Duct, Re = 200

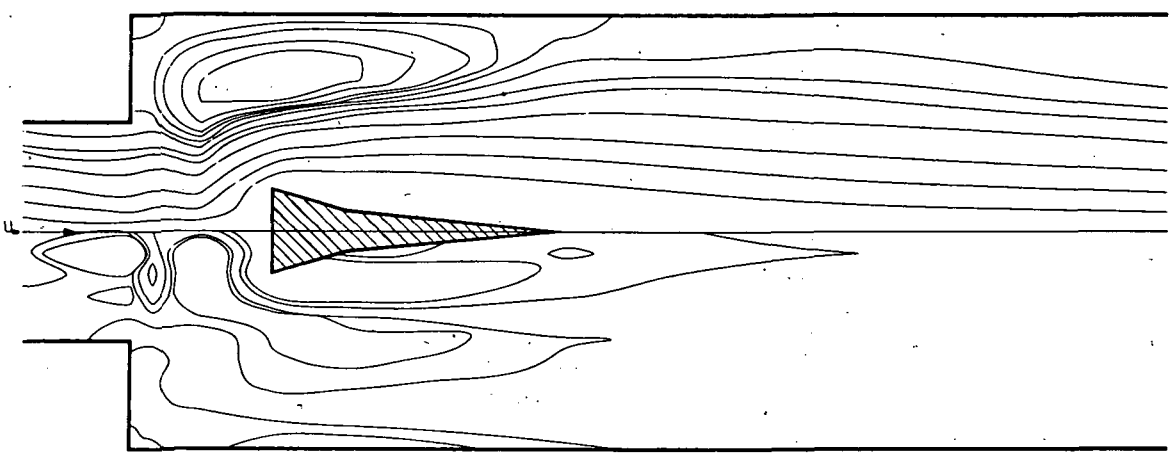

Figure 13c. COMOC Computed Steady-State Streamfunction and Vorticity for Flow over a Rearward Step with Internal Obstacle, Re = 200

was stable and the recirculation region has simply readjusted to fill the new interior domain. (The indicated appearance of vorticity lines crossing is strictly a function of the high order curve fitting operations in the automatic plot package.) The downstream point-of-attachment of the dividing streamline was essentially unaffected by the changed wall shape. However, as shown in Figure 13c, the insertion of a blunt body into the solution domain drastically alters the predicted recirculation region. The inserted obstacle was tapered downstream to preclude the shedding of vortices, hence allow attainment of the illustrated steady-state, time-independent solution. The computed vorticity solution is markedly altered from Figure 13a, and the dividing streamline reattachment has moved to within about four step-heights downstream. The second recirculation region at the step base is retained in both sample solutions; its apparent unstreamlined shape could be improved with added discretization, and resolution could be improved if required. No independent measures are available to assess the accuracy of either of these solutions, but the computed solutions do appear acceptable on a physical basis. They amply illustrate the boundary shape variability that is automatically acceptable to COMOC.

Equation (75) has been evaluated for computation of static pressure distributions along the centerplane of the duct flow problems. For two-dimensional steady flow with constant density and viscosity, Eq. (75) evaluated on the centerplane becomes

$$\Delta p = -\Delta\left(\frac{1}{\rho}\,\psi_{,2}\right)^2 - \frac{\mu}{Re}\int \omega_{,2}\,dx_1 + \frac{\mu}{\rho Re}\int \psi_{,12}\,\psi_{,2}\,dx_1 \qquad (115)$$

In Eq. (115), the first term represents the purely dynamic pressure change due to streamline convergence. The second accounts for viscous dissipation, and the generic third derivative in streamfunction has been replaced in terms of vorticity through Eq. (40). The last term contains the viscous contribution stemming from non-parallel flow. Evaluation of Eq. (115) between any two points provides the corresponding pressure difference. For fully developed, parallel flow, only the middle term in Eq. (115) is non-vanishing and the expression is analytically exact. For general flows, evaluation of first and second order derivatives of tabulated functions is required. In keeping with the use of linear finite element approximation functions for computation of the flow field variables, low order difference formulas appear appropriate.

Shown in Figures 14 and 15 are the calculated static pressure distributions along the centerplane of the duct and the rearward step problems, for Re = 200, for the computed steady-state streamfunction and vorticity distributions previously discussed. The total viscous contribution to Eq. (115) is separately noted in each case. For both problems, the dynamic contribution dominates the distribution. For the duct case, the viscous contribution near the centerplane is quite small for about 30% of the duct length. For fully developed parallel flow, the pressure decay is solely due to vorticity, and the analytic pressure gradient for fully developed flow is also shown in Figure 14. The computed solution for viscous contribution to pressure decay and total decay are observed to both be approaching this value. Concerning accuracy, the computed streamfunction distribution predicts fully developed parallel flow to within 0.75% across the entire duct terminus. The maximum computed deviation ($\sim$ 25%) from fully developed vorticity occurs adjacent to the centerplane at the duct terminus. The error in computed vorticity signficantly affects the accuracy of viscous dominated pressure computations which accounts for the slope dispairty at the duct terminus. In most practical flows of interest, viscous effects are strongest near the containing walls. For the duct flow case, the computed terminal vorticity distribution near the wall is accurate to within 2%; a corresponding improvement in accuracy of computed pressure in this region would accrue.

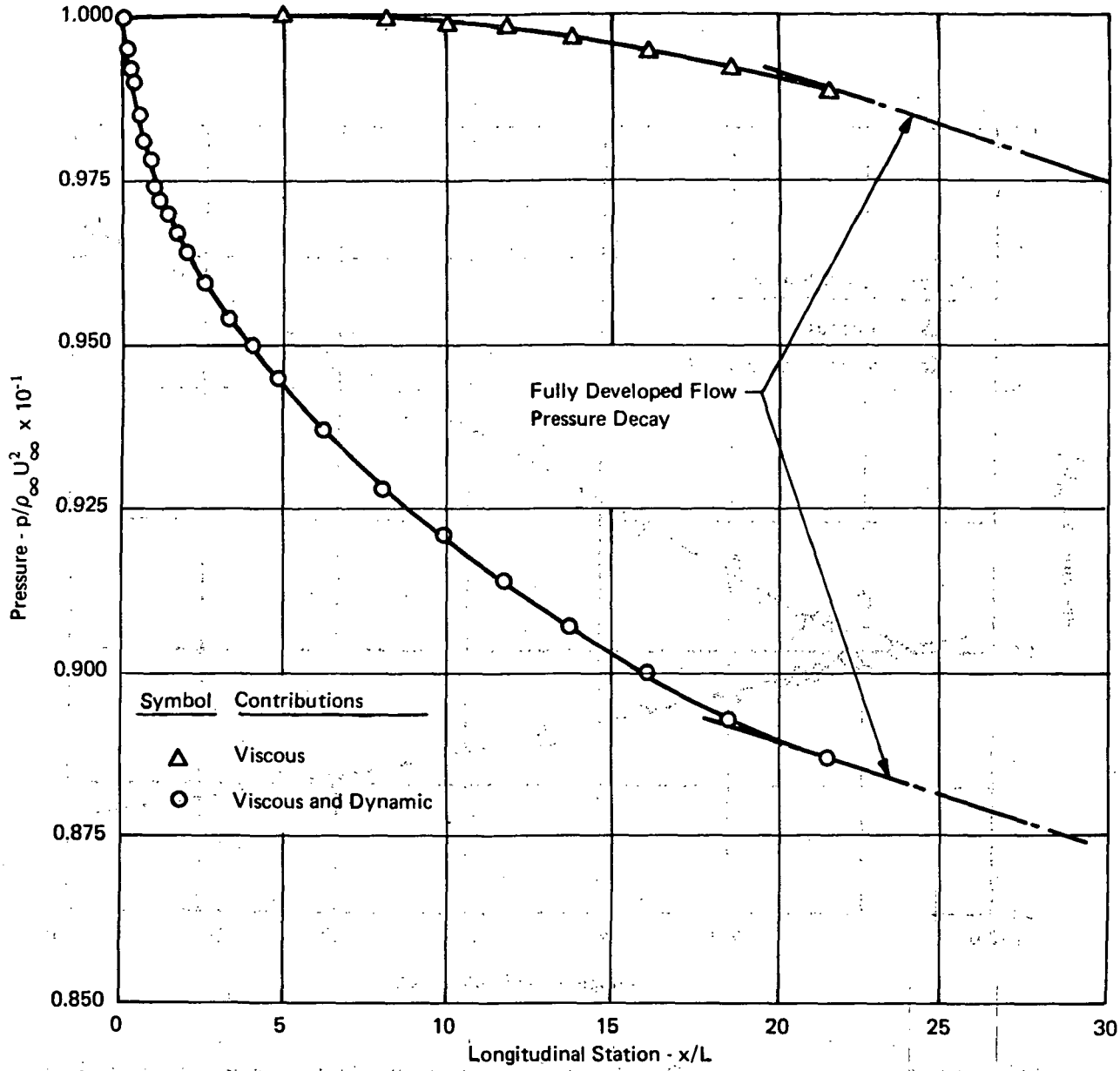

Figure 14. Centerplane Pressure Decay in Steady-State Duct Flow, Re = 200

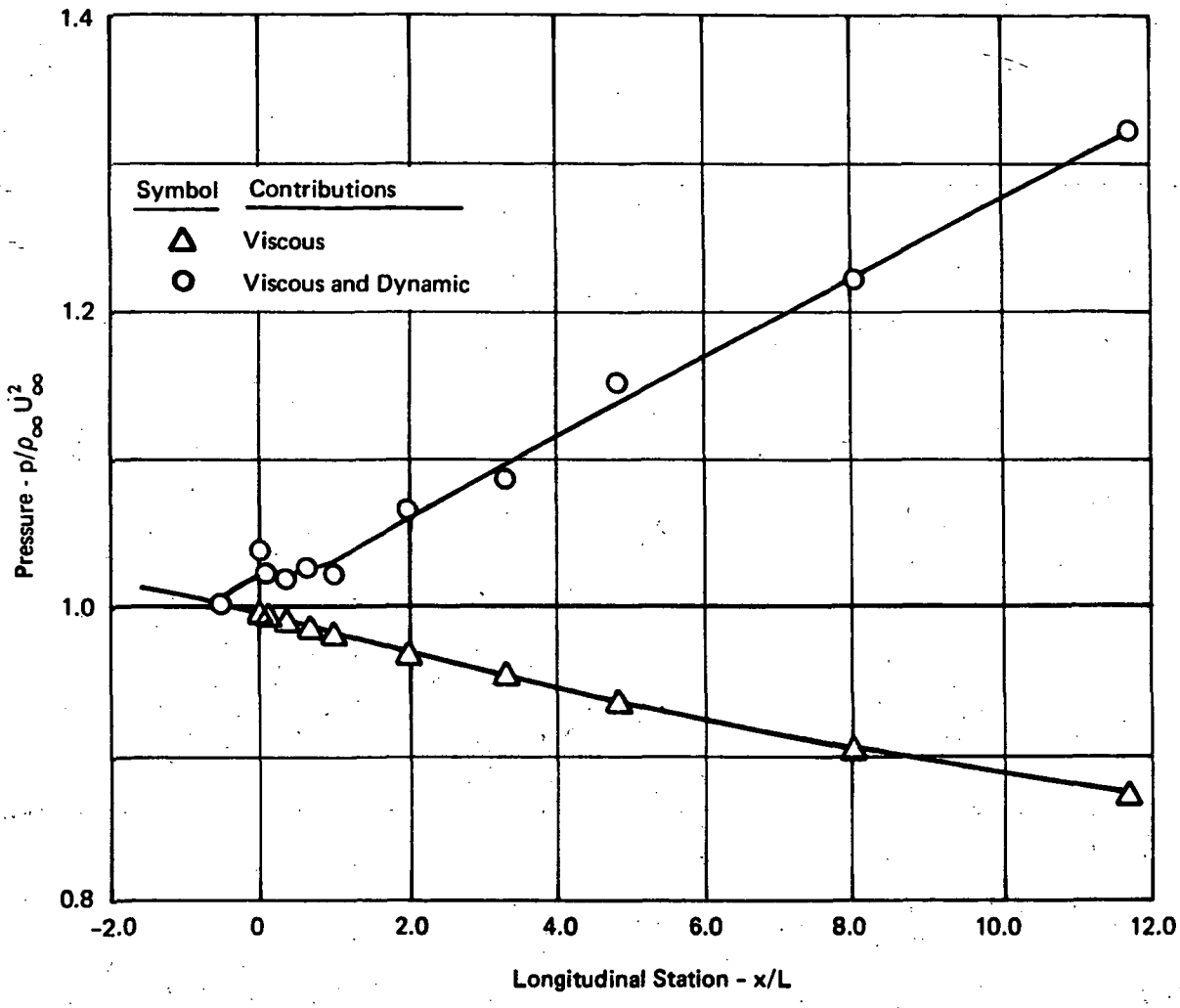

Figure 15. Centerplane Pressure Distribution for Steady Flow Over a Rearward Facing Step, Re = 200

Solution of the Navier-Stokes equations is typically required for internal—that is, confined—flow problems as has been illustrated. A vast number of practical aerospace and aeronautical flow field configurations correspond to external flow problems wherein a significant simplification to the Navier-Stokes system exists as "boundary layer" theory. This equation system is parabolic for steady flows over a wide range of Mach numbers, even for three-dimensional problems, and its solution has been greatly explored, see Blottner (Reference 20). However, with the blown flap systems on todays aircraft, and/or the supersonic and hypersonic cruise speeds of the space shuttle and hypersonic research vehicle, there are numerous opportunities to form local regions of imbedded recirculation within a predominantly boundary-layer-type flow field. Classical examples for supersonic flows are shown in Figures 16 and 17 which illustrate how complex shock wave interaction can induce local separated flow regions. Such occurrences are of critical design importance since aerodynamic control is affected, and local heat transfer rates are significantly increased in these zones. Attempts have been made to use the boundary layer equations for solution of shockwave-boundary layer interaction problems (Reference 21), including the neglect of instability-producing negative convection terms (Reference 22). These methods have generally proven unsuccessful since the numerical mathematics are basically incompatible with the physics of flow. The compression corner problem is somewhat more tractable since the approximate location of the shock, hence recirculation zone, is at least known. Extension of Navier-Stokes incompressible flow finite difference techniques to this problem are reported (Reference 23), and a comprehensive numerical solution of the entire transient, viscid-inviscid interaction region flow field is recently published (Reference 24). The rearward facing cone-step problem is particularly difficult; factors affecting the extent of the recirculation region are reported (Reference 25); and the results of a numerical study of the companion problem of base flow behind a wedge are published (Reference 26).

The developed finite element solution algorithm for the steady Navier-Stokes for a compressible fluid is potentially applicable to this problem class in conjunction with appropriate means for establishing the required boundary conditions. For interaction problems, this typically includes knowledge of shock impingement location, as well as inflow distributions and outflow location and parameters. Inclusion of density as a computed variable is concomitant with addition of an equation of state, Eq. (7). From the definition of stagnation enthalpy, and for a perfect gas, a quadratic expression for density is obtained after substitution of Eq. (37) for velocity. Only the positive root is admissible which yields the following equation for density in terms of static pressure (p_s), stagnation enthalpy (H) and streamfunction derivative.

$$\rho = \frac{1}{2H}\left(c_p p_s \frac{W}{R} + \sqrt{\left(\frac{c_p p_s W}{R}\right)^2 + 2H\left(\psi_{,j}\right)^2} \right) \tag{116}$$

The finite element solution requires establishment of density at node points of the solution domain. No complication arises from either pressure or enthalpy, since their nodal values are directly available. However, for linear approximation functionals, the streamfunction derivative term becomes

$$\left(\psi^*_{m,j}\right)^2 = \{\psi\}^T_m \, [B211S] \, \{\psi\}_m \tag{117}$$

which is strictly element dependent. To establish a unique nodal value of density, Eq. (116) is evaluated within an element loop in COMOC, and nodal values of computed density summed into a global

array. The summation is then divided by the number of entries to establish an averaged value representative of density at a node point. This approach is somewhat similar to certain finite difference techniques that employ nodal values for dynamic variables and cell averaged thermodynamic parameters.

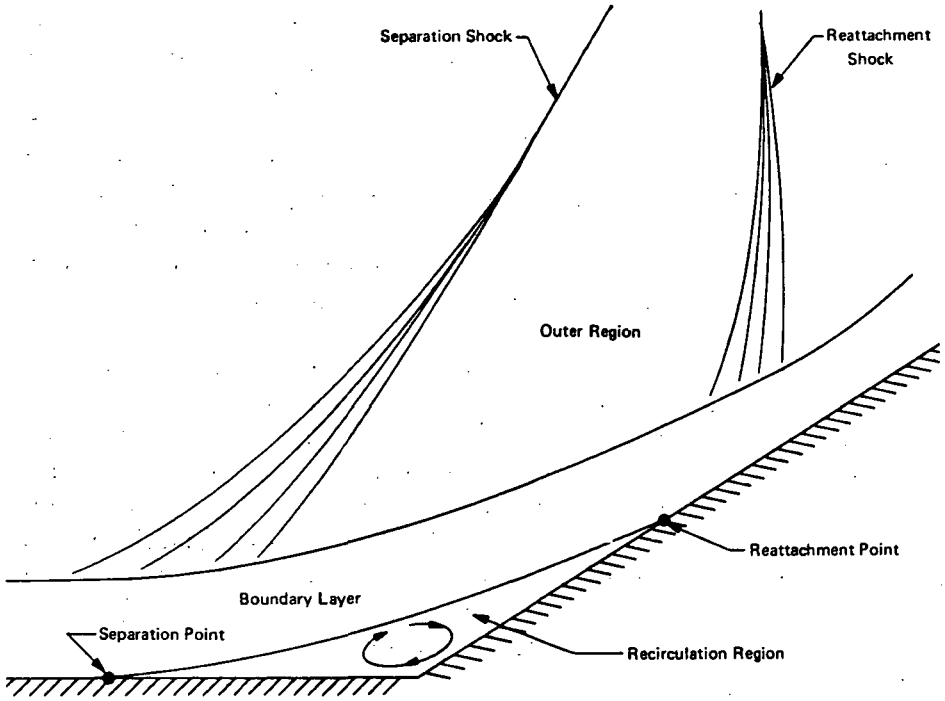

Figure 16. Flow Into a Compression Corner

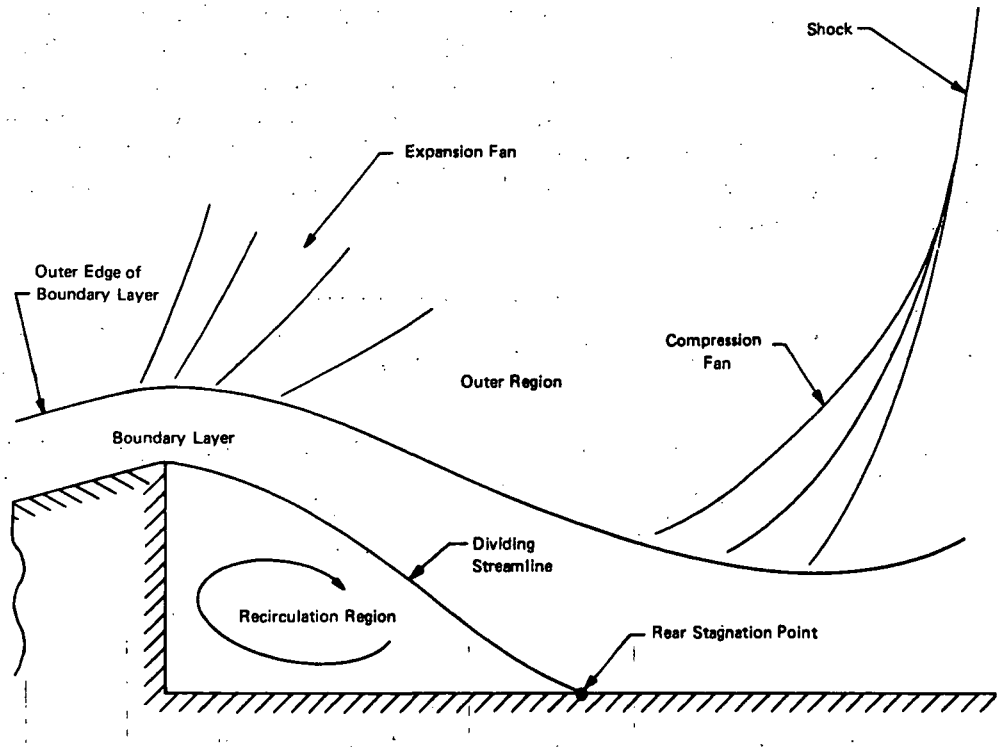

Figure 17. Supersonic Flow Over a Rearward Facing Cone-Step

The utility of the finite element approach for analysis of compressible flows has been evaluated in a cursory manner for two problems. Additional downstream discretization was added for the rearward step configuration, Figure 11, and the solution parameters scaled to simulate isoenergetic flow of air at $M_\infty = 0.6$, based upon a mass-averaged inlet velocity of 122 m/s (400 ft/s), and Re = 200 based upon step height. Under these conditions, compressibility and temperature-dependent viscosity (via Sutherland's Law) should be measurable, but their combined effect should not measurably alter the essential Reynold's number invariance of the flow field. As with previous evaluations, the duct flow was initiated impulsively and the computed recirculation zone allowed to develop during the transient solution. Essential steady-state flow was achieved within 0.15 second; at this time, the downstream duct terminus contained fully developed flow to within 0.125% maximum deviation, employing the vanishing normal gradient boundary condition for both streamfunction and vorticity. As expected, the contours of the computed distributions appeared very similar to those of Figure 12h. The downstream attachment point of the dividing streamline was identically located; the attachment at the step had moved to the corner, although a refined discretization would be required to accurately evaluate its location for this test case. As before, a second recirculation zone was predicted at the base of the step. The null point of the primary recirculation zone occurred on the node column located seven step heights downstream of the step. Shown in Figure 18 are computed steady-state distributions of the dependent variables across the transverse dimension of the duct at this longitudinal station and at the duct terminus. The streamfunction solution illustrates the small flow velocities occurring within the recirculation zone; a null point in vorticity is correspondingly indicated. Freestream density occurs within this region, and the "pinch" effect of the recirculation zone correspondingly increased main flow density by up to 5%. The computed viscosity distributions similarly show largest variations outside the recirculation region.

The finite element solution procedure may be useful for studies of imbedded recirculation zones within boundary layer flows, provided boundary conditions are available and shock locations known. The supersonic compression corner falls into this category, and a computational solution might involve establishing the vorticity-streamfunction equivalent of supersonic boundary layer flow as an initial condition, and then bending the plate surface, and skewing the discretization downstream of the hinge, to the required angle. Illustrations of sample discretizations for such a procedure are shown in Figure 19, for the geometry studied by Carter (Reference 24). The existence of the shock in Figure 19b could be computationally simulated by the (jump) parallel-velocity boundary condition for streamfunction, Eq. (101). As an introductory step to analysis of this problem, the discretization of Figure 19a was employed by COMOC to solve for the vorticity-streamfunction equivalent of supersonic laminar boundary layer flow of air for $M_\infty = 3.0$, and Re = 7750, based upon distance from the plate leading edge to the midpoint of the solution domain. The inflow boundary condition for streamfunction, and slope of the top of the solution domain, were established using Eq. (99) and a similarity solution for boundary layer flow. The vorticity distribution at inflow was established from its definition, Eq. (39), vanished along the top, and was evaluated on the no-slip plate surface using Eq. (103). The vanishing normal gradient, although locally incorrect for boundary layer flows, was employed downstream for both variables. Shown in Figure 20a is the computed essential steady-state vorticity distribution ($|\Omega|' \leq 0.001$) for the domain of Figure 19a. A high plateau of vorticity exists near the plate surface which drops off rapidly as freestream is approached. Figure 20b compares computed streamfunction and density distributions at x/L = 1.0 to corresponding values obtained from the similarity solution. Agreement is good except for density near the freestream, where use of Eq. (116) rounded the distribution. This may result from a poor local speed approximation, using Eq. (117), for regions with large gradients in streamfunction; a finer discretization should

improve results. The accuracy of computed streamfunction at the downstream terminus was noticeably poorer, as a direct consequence of the applied gradient boundary condition. Judging from these results, it appears adequate to extend the solution domain a distance of x/L = 1 downstream of the region of interest for this problem. Furthermore, use of Eq. (116) appears valid for compressible flows when combined with attention to discretization.

CONCLUDING REMARKS

A finite element algorithm for solution of problems in the two-dimensional Navier-Stokes equations has been established. Numerical evaluation within the COMOC computer program system has produced a favorable assessment of solution accuracy and convergence. The versatility of the code has been illustrated for several problem variations. It appears that the finite element approach of computational fluid mechanics exhibits much of the required generality and flexibility to serve as an effective design and communication tool between the engineer and scientist and the present and next generation of digital computer systems.

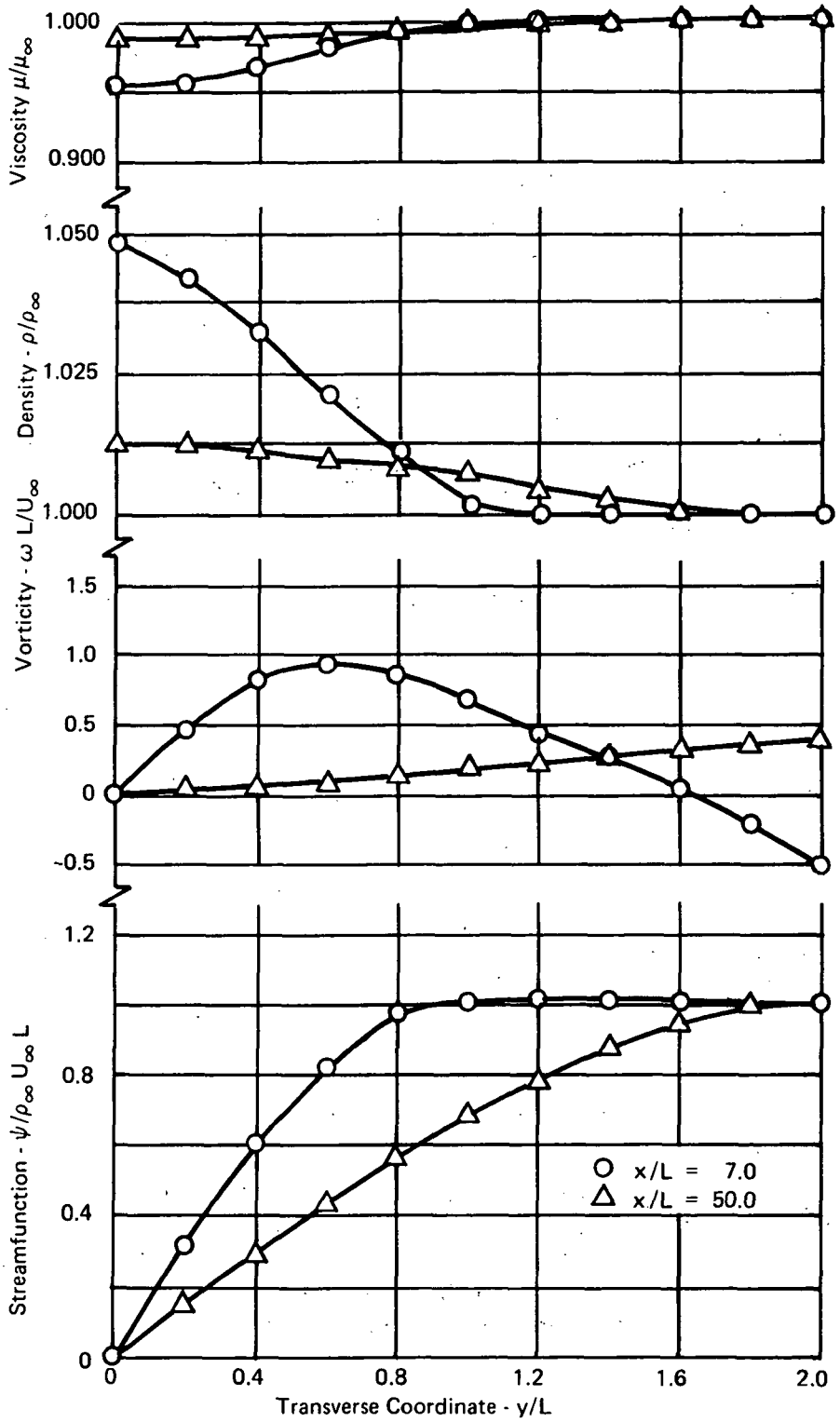

Figure 18. Computed Steady State Distributions for Compressible Flow Over a Rearward Facing Step, Re = 200, M_∞ = 0.6

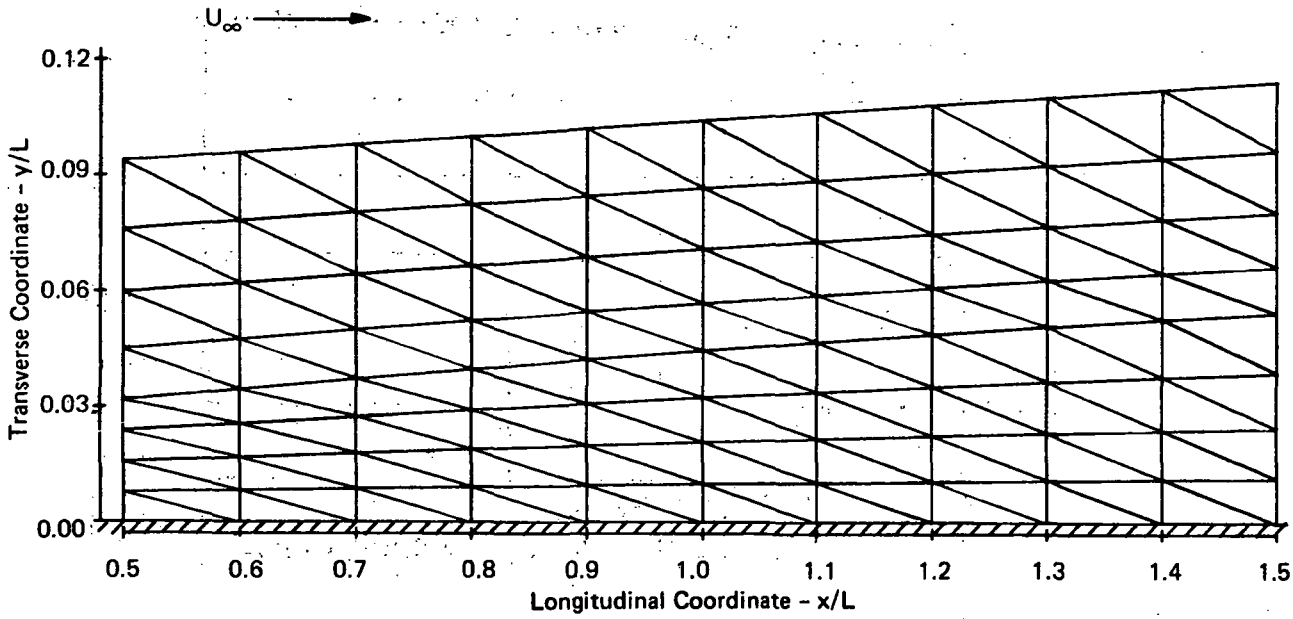

(a) Flat Plate, $M_\infty = 3.0$

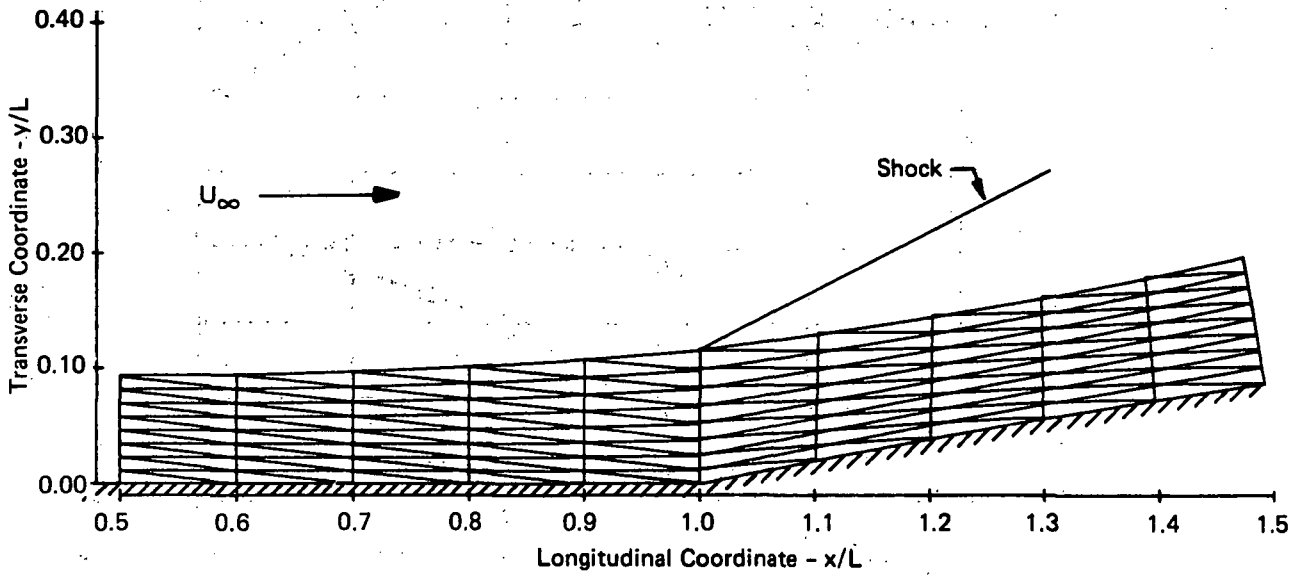

(b) Compression Corner, $M_\infty = 3.0$

Figure 19. Finite Element Discretizations for Supersonic Boundary Flows

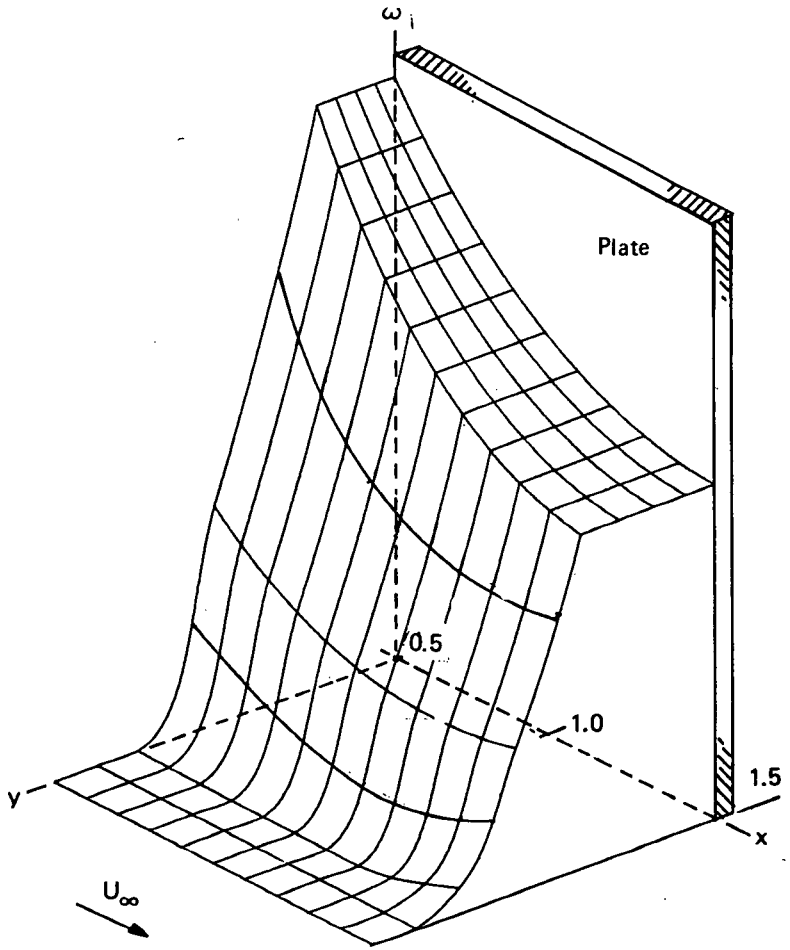

(a) Vorticity Solution

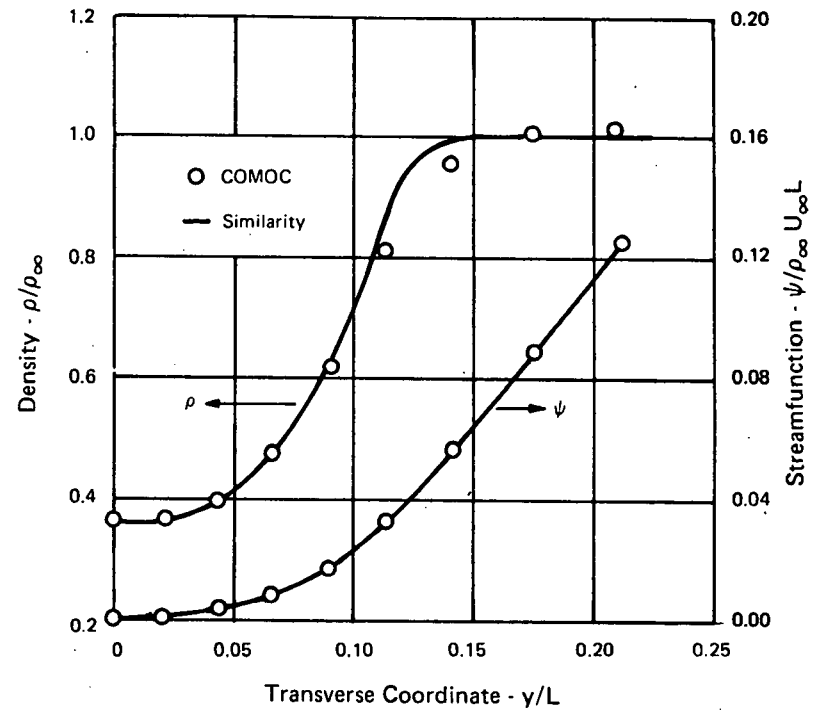

(b) Streamfunction and Density Distributions, x/L = 1.0

Figure 20. Computed Steady-State Distributions for Supersonic Boundary Layer Flow, $M_\infty = 3.0$

APPENDIX A
CARTESIAN TENSORS IN EUCLIDEAN SPACE

In the rectangular Cartesian coordinate description of Euclidean space, $x_i = \{ x, y, z \}$, simple subscript tensor notation and the summation convention are sufficient to describe the calculus of tensor fields. In general curvilinear coordinates, the completely general tensor formalism involving co- and contra-variant scalar components and basis vectors is required, see Reference (27). When dealing with orthogonal curvilinear (i.e., Cartesian) coordinate systems, simple tensor notation is inadequate and the full power of the general tensor is not needed since no distinction exists between the two variant forms.

The appropriate mathematical tool for tensor field calculus operations in Cartesian coordinates is Cartesian tensor analysis in Euclidean space, Reference (28). The basic concept of geometry is the infinitesimal displacement ds. Denoting y_i as the rectangular Cartesian components of an arbitrary position vector $\vec{r}$, and x_i as the scalar components in any other Cartesian basis, an arbitrary vector can be written as

$$\vec{r} = y_i \hat{a}_i = x_i \vec{\epsilon}_i \tag{A-1}$$

where $\hat{a}_i$ are the (constant) unit vectors $(\hat{i}, \hat{j}, \hat{k})$ and $\vec{\epsilon}_i$ are any other orthogonal basis vector set. The infinitesimal displacement (squared) becomes

$$ds^2 = d\vec{r} \cdot d\vec{r} = dy_i \hat{a}_i \cdot dy_j \hat{a}_j = dy_i \, dy_i \tag{A-2}$$

since contraction of unit vectors in the rectangular basis yields the Kronecker delta. A similar form is obtained for any orthogonal basis, with the exception that, since the basis vectors are not in general unit vectors, their contraction will yield scalar coefficients modifying the Kronecker delta. Denoting these as $h_{\underline{i}}^2$, the general form is

$$ds^2 = h_{\underline{i}}^2 \, dx_i \, dx_i \tag{A-3}$$

where the subscript bar denotes the index is not included in the summation convention. The $h_{\underline{i}}$ are called metric coefficients and are functions of the particular coordinate system. For example, in cylindrical coordinates with $x_i = \{z, r, \theta\}$

$$h_{\underline{i}} = \{1, 1, r\} \tag{A-4}$$

In spherical coordinates with $x_i = \{r, \phi, \theta\}$, with ϕ the polar angle with domain $0 \leq x_2 \leq \pi$,

$$h_{\underline{i}} = \{1, r, r\sin\phi\} \tag{A-5}$$

It is desirable to establish an orthonormal basis for the general Cartesian description. Considering a general vector field $\vec{v}$ (as described by the form of equation A-1), with scalar components v_i and basis $\vec{\epsilon}_i$, multiply and divide by $h_{\underline{i}}$ to obtain

$$\vec{v} = h_{\underline{i}} v_i \frac{\vec{\epsilon}_i}{h_{\underline{i}}} \equiv u_i \hat{\epsilon}_i \tag{A-6}$$

In equation A-6, u_i ($\equiv h_i v_i$) are called the physical components of the vector $\vec{v}$, and $\hat{\epsilon}_i$ are unit vectors of the orthonormal basis.

The fundamental calculus operation requiring identification is differentiation. Referring to equation A-6, the derivative of $\vec{v}$ with respect to the x_j variables is, using the chain rule

$$\frac{\partial \vec{v}}{\partial x_j} = \frac{\partial}{\partial x_j}(u_i \hat{\epsilon}_i)$$

$$= \frac{\partial u_i}{\partial x_j} \hat{\epsilon}_i + u_i \frac{\partial \hat{\epsilon}_i}{\partial x_j} \qquad \text{(A-7)}$$

The last term in equation A-7 describes the change in the unit vector $\hat{\epsilon}_i$ with respect to x_j. Since this is also a vector, it can be described by scalar components projected on the $\hat{\epsilon}_i$ basis. The coefficients of proportionality for this description are the physical components of the Christoffel symbols of general tensors, contracted over index pairs. They have been termed "wryness" coefficients, Reference (29); signifying them by ω_{ijk} and expressing $\vec{v}$ in the $\hat{\epsilon}_i$ basis, equation A-7 becomes

$$\frac{\partial \vec{v}}{\partial x_j} \equiv u_{i\,;j} \hat{\epsilon}_i = (u_{i,j} + \omega_{ijk} u_k) \hat{\epsilon}_i \qquad \text{(A-8)}$$

In equation A-8, the spatial (vector) derivative of a vector is signified by the semicolon. The partial derivative of a scalar (component) is denoted by the comma. Since equation A-8 is a vector identity the scalar components are identical. Hence

$$u_{i\,;j} = u_{i,j} + \omega_{ijk} u_k \qquad \text{(A-9)}$$

defines the vector derivative of the scalar components of a vector (first order tensor) in an arbitrary orthonormal basis. Equation A-9 can be readily generalized to the vector derivative of the scalar components of an n^{th} order tensor, see Reference (28).

The properties of the wryness coefficients are readily determined. They are not scalar components of a third order tensor since they do not obey the tensor transformation law. All components vanish for the indices distinct. The coefficients are skew-symmetric in all index pairs. Hence, the only nonvanishing terms are of the form

$$\omega_{\underline{kjk}} = -\omega_{\underline{jkk}} \qquad \text{(A-10)}$$

In particular, the singular nonvanishing coefficient in cylindrical coordinates is

$$\omega_{233} = \frac{1}{r} \qquad \text{(A-11)}$$

In spherical coordinates, obtain

$$\omega_{122} = \omega_{133} = \frac{1}{r} \qquad \text{(A-12)}$$

$$\omega_{233} = \frac{\dot{c}\cot\phi}{r} \tag{A-13}$$

From equation A-9, the vector derivative of a scalar is simply the partial derivative with respect to x_j, commonly referred to as the gradient. From equations A-1, A-3, and A-6, obtain

$$\frac{\partial\phi}{\partial x_i} \equiv \phi,_i \hat{\epsilon}_i = \frac{1}{h_i}\frac{\partial\phi}{\partial x_i}\hat{\epsilon}_i \tag{A-14}$$

Equation A-14 defines the partial derivative, signified by the comma. Equating scalar coefficients, obtain by components

$$(\ ),_i = \frac{1}{h_i}\frac{\partial}{\partial x_i}(\ ) \tag{A-15}$$

The operation of curl is the contraction of equation A-9 with the general alternating tensor e_{ijk}, which is skew symmetric in all index pairs and has positive scalar components for (i, j, k) in the cyclic order (1, 2, 3). Hence,

$$\text{curl}\ \vec{v}\cdot\hat{\epsilon}_i \equiv e_{ijk}\, u_k\,;j \tag{A-16}$$

The general alternating tensor is related to the Cartesian alternating tensor ϵ_{ijk}, with unit magnitude scalar components, by the determinant of the space metric, which for Cartesian tensors is simply the product

$$J_4 = h_1\, h_2\, h_3 \tag{A-17}$$

Equating scalar coefficients in equation A-16, and using equation A-17, obtain for the i^{th} component the curl of the vector $\vec{v}$

$$\text{curl}\,\vec{v}\cdot\hat{\epsilon}_i = \frac{1}{J}\epsilon_{ijk}\, u_k\,;j \tag{A-18}$$

Equations A-3, A-9, A-10, A-15, and A-18 are sufficient to facilitate the calculus of Cartesian tensors in Euclidean space. Integral theorems, developed for rectangular Cartesian tensor fields, transform directly to general Cartesian tensor fields. Of particular interest, the divergence theorem becomes, for an arbitrary order Cartesian tensor field $T_{ijk}\ldots$,

$$\int_R (T_{ijk}\ldots)\,;_\ell\, d\tau = \oint_{\partial R} (T_{ijk}\ldots)\cdot\nu_\ell\, d\sigma \tag{A-19}$$

where ν_ℓ is the unit outward pointing normal vector to the closure ∂R of the domain R. Similarly, for Stokes' theorem obtain

$$\int_{\partial R} (\text{curl}\, T_{ijk}\ldots)\cdot\nu_\ell\, d\sigma = \oint_{\partial L} (T_{ijk}\ldots)\cdot t_\ell\, ds \tag{A-20}$$

where ∂L is the bounding curve of the closure ∂R and t_ℓ is the unit vector everywhere tangent to ∂L.

APPENDIX B

OBSERVATIONS ON THE FINITE ELEMENT SOLUTION ALGORITHM FOR THE NAVIER-STOKES EQUATIONS USING LINEAR NATURAL COORDINATE APPROXIMATION FUNCTIONALS

The Navier-Stokes equations, governing the two-dimensional flow of a compressible viscous fluid in rectangular Cartesian space, contain several nonlinear terms involving both density and viscosity gradients. The finite element solution algorithm retains the vector differential operations within its formal definitions, and options exist to perform integrations by parts as well as employ integral calculus theorems to simplify terms. This appendix presents observations made during the theoretical exploration of the consequence of such operations and their impact upon the numerical implementation of the finite element theory.

General Observation: The finite element solution algorithm applicable to elliptic partial differential equations is of the form:

$$\int_{R_m} W\phi^*_{,kk}\, d\tau = \int_{R_m} Wf_1\,(\phi^*, \phi^*_{,k}, x_i)\, d\tau + \oint_{\partial R_m} Wf_2\,(\phi^*)\, d\sigma \tag{B.1}$$

where ϕ^* is the approximation to the dependent variable, f_i are specified functions of their arguments and contain no second derivatives of ϕ^*, and the weighting functions W are identical to the approximation function for ϕ^*. Within a finite element,

$$\phi^*_m \equiv \{L\}^T \{\phi\}_m \tag{B.2}$$

$$W \equiv |L| \tag{B.3}$$

and in two-dimensional rectangular Cartesian space

$$\{L\} = \begin{Bmatrix} 1 - \dfrac{x}{x_2} + \left(\dfrac{x_3}{x_2} - 1\right)\dfrac{y}{y_3} \\ \dfrac{x}{x_2} - \dfrac{x_3}{x_2}\dfrac{y}{y_3} \\ \dfrac{y}{y_3} \end{Bmatrix} \tag{B.4}$$

and

$$\{L\}_{,k} = \frac{1}{x_2}\begin{Bmatrix} -1 \\ 1 \\ 0 \end{Bmatrix}\hat{\epsilon}_1 + \frac{1}{x_2 y_3}\begin{Bmatrix} x_3 - x_2 \\ -x_3 \\ +x_2 \end{Bmatrix}\hat{\epsilon}_2 \tag{B.5}$$

where $\hat{\epsilon}_i$ are unit vectors in the local reference system, Figure B-1.

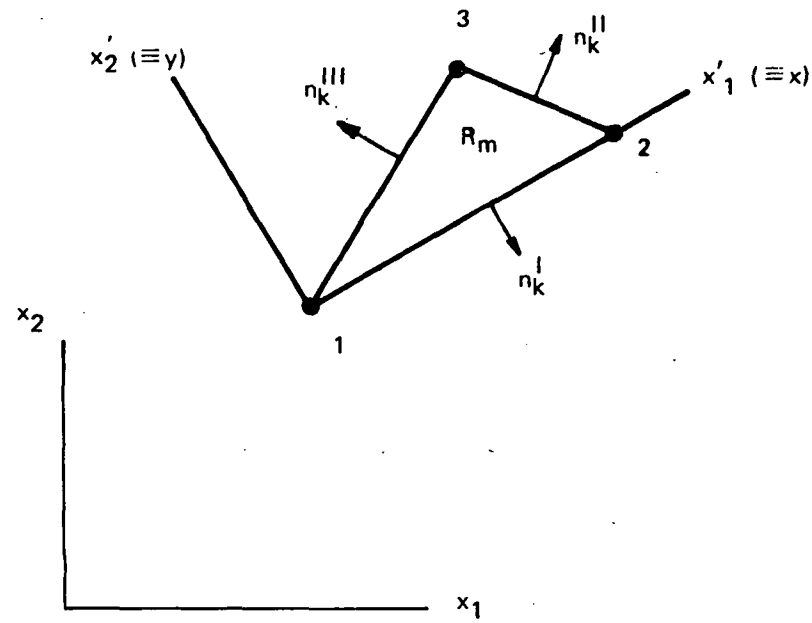

Figure B-1. Two-Dimensional Finite Element

Of particular interest is determining the behavior of Eq. (B.1) when integration by parts is performed on terms of f_1 as well as $\phi^*_{,kk}$. As an introduction, integrate the left side of Eq. (B.1) by parts to obtain:

$$\int_{R_m} W\phi_{,kk}\, d\tau = \oint_{\partial R_m} W\phi_{,k}\, n_k\, d\sigma - \int_{R_m} W_{,k}\, \phi_{,k}\, d\tau \tag{B.6}$$

Theorem 1: If ϕ is a linear function of its arguments, Eq. (B.6) vanishes identically for evaluation within a single finite element,

Proof:

$$\int_{R_m} W\phi_{,kk}\, d\tau = \int_{R_m} \{L\}\, \{L\}^T{}_{,kk}\, d\tau = \int_{R_m} \{L\}\left(\frac{1}{x_2}\begin{Bmatrix}-1\\1\\0\end{Bmatrix}_{,1} + \frac{1}{x_2 y_3}\begin{Bmatrix}x_3-x_2\\-x_3\\x_2\end{Bmatrix}_{,2}\right) d\tau = 0 \tag{B.7}$$

$$\oint_{\partial R_m} W\{L\}_{,k}\, n_k\, d\sigma = \int_{\partial R_I} \{L\}\{L\}^T_{,k}\, n_k^I\, d\sigma^I + \int_{\partial R_{II}} \{L\}\{L\}^T_{,k}\, n_k^{II}\, d\sigma^{II} + \int_{\partial R_{III}} \{L\}\{L\}^T_{,k}\, n_k^{III}\, d\sigma^{III}$$

$$= -\frac{x_2}{2y_3}\begin{Bmatrix}1\\1\\0\end{Bmatrix}\{x_3-x_2,\,-x_3,\,x_2\}\{\phi\}_m$$

$$+\left(\frac{y_3}{2x_2}\begin{Bmatrix}0\\1\\1\end{Bmatrix}\{-1,\,1,\,0\} - \frac{x_3-x_2}{2x_2y_3}\begin{Bmatrix}0\\1\\1\end{Bmatrix}\{x_3-x_2,\,-x_3,\,x_2\}\right)\{\phi\}_m$$

$$+\left(-\frac{y_3}{2x_2}\begin{Bmatrix}1\\0\\1\end{Bmatrix}\{-1,\,1,\,0\} + \frac{x_3}{2x_2y_3}\begin{Bmatrix}1\\0\\1\end{Bmatrix}\{x_3-x_2,\,-x_3,\,x_2\}\right)\{\phi\}_m$$

$$= \frac{x_2y_3}{2}\left(\frac{1}{(x_2)^2}\begin{bmatrix}1 & -1 & 0\\ & 1 & 0\\ \text{sym} & & 0\end{bmatrix}\right.$$

$$\left.+\frac{1}{(x_2y_3)^2}\begin{bmatrix}(x_3-x_2)^2 & -x_3(x_3-x_2) & x_2(x_3-x_2)\\ & x_3^2 & -x_2x_3\\ \text{sym} & & x_2^2\end{bmatrix}\right)\{\phi\}_m$$

$$\equiv \frac{x_2y_3}{2}\,[B211S]_m\{\phi\}_m \tag{B.8}$$

$$\int_{R_m} W_{,k}\,\phi_{,k}\,d\tau = \int_{R_m}\{L\}_{,k}\{L\}^T_{,k}\,d\tau\,\{\phi\}_m$$

$$= \int_{R_m}\left(\frac{1}{(x_2)^2}\begin{Bmatrix}-1\\1\\0\end{Bmatrix}\{-1,\,1,\,0\} + \frac{1}{(x_2y_3)^2}\begin{Bmatrix}x_3-x_2\\-x_3\\x_2\end{Bmatrix}\{x_3-x_2,\,-x_3,\,x_2\}\right)d\tau\,\{\phi\}_m$$

$$= \frac{x_2y_3}{2}\,[B211S]_m\{\phi\}_m \tag{B.9}$$

Combining Eq. (B.8) and Eq. (B.9), the identity in zero is accomplished, Q.E.D.

Theorem 2: If ϕ is a linear function of its arguments, the surface integral contributions resulting from integration by parts, Eq. (B.1), can be made to cancel in pairs upon assembly, by Boolean algebra, of the global solution algorithm.

Proof: Along the line common to the finite elements defined by domains R_I and R_{II}, Figure B-2, specify the local value of the normal gradient of the function ϕ as an algebraic average. The coincident portion of the closed surface integral for each domain becomes

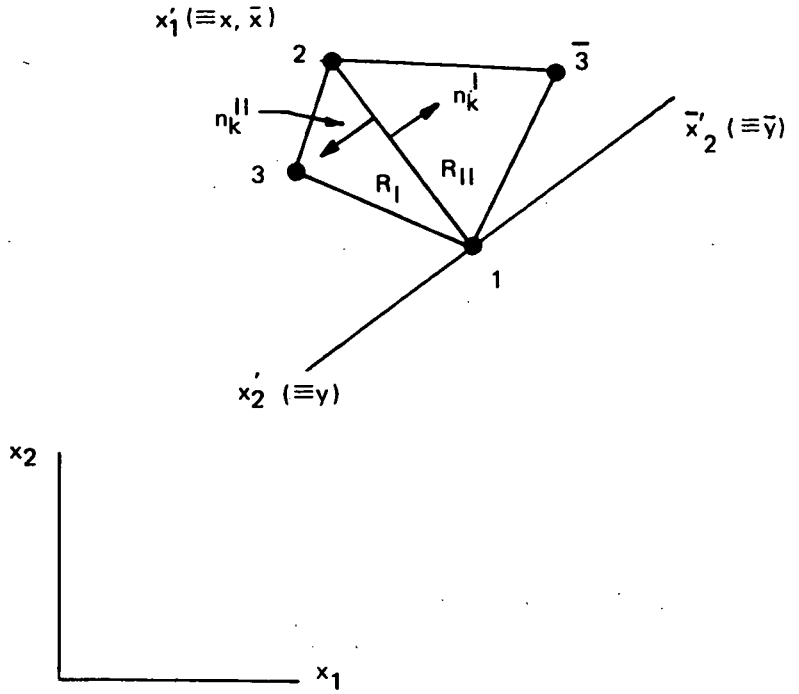

Figure B-2. Adjacent Finite Elements

$$\int_{\partial R_I} W\phi_{,k}\, n_k \, d\sigma = \int_o^{x_2} \{L\}\left(\frac{1}{2}\phi_{,k}^{I}\, n_k^{I} + \frac{1}{2}\,\phi_{,k}^{II}\, n_k^{I}\right) dx \tag{B.10}$$

$$\int_{\partial R_{II}} W\phi_{,k}\, n_k \, d\sigma = \int_o^{x_2} \{L\}\left(\frac{1}{2}\phi_{,k}^{I}\, n_k^{II} + \frac{1}{2}\,\phi_{,k}^{II}\, n_k^{II}\right) dx \tag{B.11}$$

Since $n_k^{I} = -n_k^{II}$, and using Eq. (B.2) - (B.5), along the common line,

$$\int_{\partial R_I} (\;)\, dx = \frac{x_2}{4}\begin{Bmatrix}1\\1\\0\end{Bmatrix}\left(-\frac{1}{x_2 y_3}\left\{x_3 - x_2, -x_3, x_2\right\}\{\phi\}_I + \frac{1}{x_2 \bar{y}_3}\left\{\bar{x}_3 - x_2, -\bar{x}_3, x_2\right\}\{\phi\}_{II}\right) \tag{B.12}$$

$$\int_{\partial R_{II}} (\;)\, dx = \frac{x_2}{4}\begin{Bmatrix}1\\1\\0\end{Bmatrix}\left(+\frac{1}{x_2 y_3}\left\{x_3 - x_2, -x_3, x_2\right\}\{\phi\}_I - \frac{1}{x_2 \bar{y}_3}\left\{\bar{x}_3 - x_2, -\bar{x}_3, x_2\right\}\{\phi\}_{II}\right) \tag{B.13}$$

Upon Boolean assembly of Eq. (B.12) and (B.13), the first of each equation is loaded into the global vector on $\{\phi\}$ at the location ϕ_I. Hence, cancellation by pairs is achieved for the surface integral contributions stemming from Eq. (B.6), Q.E.D..

Theorem 3: If ϕ is a linear function of its arguments, and Eq. (B.1) involves a scalar nonlinearity that is not differentiated, the surface integral contribution stemming from integration by parts can be made to vanish in pairs upon Boolean assembly of the global solution vector.

Proof: The compatibility equation for the two-dimensional Navier-Stokes equation can be integrated by parts, as

$$\int_R W(\frac{1}{\rho}\,\psi_{,k})_{,k}\,d\tau = \oint_{\partial R} W\frac{1}{\rho}\,\psi_{,k}\,n_k\,d\sigma - \int_R W_{,k}\,\frac{1}{\rho}\,\psi_{,k}\,d\tau \tag{B.14}$$

Using the averaging concept developed in the previous proof, obtain from Eq. (B.14) on an element basis:

$$\oint_{\partial R_m} (\;)\,d\sigma = \oint_{\partial R_m} \{L\}\,\{L\}^T \left\{\frac{1}{\rho}\right\}_m \psi^*_{m,k}\,n_k\,d\sigma \tag{B.15}$$

Along the line connecting nodes 1 and 2, Figure B-2, Eq. (B.15) becomes, using Eq. (B.4) and (B.5) within elements R_I and R_{II},

$$\int_{\partial R_I} (\;)\,d\sigma = \frac{x_2}{6}\begin{bmatrix}2 & 1 & 0\\ & 2 & 0\\ \text{sym} & & 0\end{bmatrix}\left\{\frac{1}{\rho}\right\}_I\left(-\frac{1}{2}\psi^{*I}_{,k} + \frac{1}{2}\psi^{*II}_{,k}\right)n^I_k \tag{B.16}$$

$$\int_{\partial R_{II}} (\;)\,d\sigma = \frac{x_2}{6}\begin{bmatrix}2 & 1 & 0\\ & 2 & 0\\ \text{sym} & & 0\end{bmatrix}\left\{\frac{1}{\rho}\right\}_{II}\left(+\frac{1}{2}\psi^{*I}_{,k} - \frac{1}{2}\psi^{*II}_{,k}\right)n^I_k \tag{B.17}$$

The only elements of the finite element matrix $\left\{\frac{1}{\rho}\right\}_m$ involved in non-zero products in Eq. (B.16) and (B.17) are for node locations on the common line. Hence, upon Boolean assembly, the contributions from surface integrals involving a scalar nondifferentiated nonlinearity cancel by pairs, Q.E.D.

Observation: The convection term, involving the curl of the streamfunction (vector potential function), appears in the differential equation and finite element description for each dependent variable except streamfunction. An integration by parts is possible.

Theorem 4: Within the convection operator, and for ϕ a linear function of its arguments, no arbitrariness exists for evaluation of the generated surface integral.

Proof: The typical convection term is, upon integration by parts,

$$\int_{R_m} W\epsilon_{3ki}(\omega\psi_{,i})_{,k}\,d\tau = \oint_{\partial R_m} W\epsilon_{3ki}\,\omega\psi_{,i}\,n_k\,d\sigma - \int_{R_m} W_{,k}\,\epsilon_{3ki}\,\omega\psi_{,i}\,d\tau \qquad (B.18)$$

For the surface integral, using Eq. (B.2) – (B.5), obtain

$$\int_{\partial R_m} W\epsilon_{3ki}\,\omega\psi_{,i}\,n_k\,d\sigma = \oint_{\partial R_m} \{L\}\{L\}^T\{\Omega\}_m\,\epsilon_{3ki}\{L\}^T{}_{,i}\,n_k\,d\sigma\,\{\psi\}_m \qquad (B.19)$$

Note that the gradient operator on $\{L\}$ is orthogonal to the local normal via the alternator. From the natural coordinate function description, Eq. (B.4), such derivatives involve end point nodal values only. Hence, for integration over the three sides of the finite element, Figure B-1, obtain

$$\oint_{\partial R_m} (\;)\,d\sigma = \frac{1}{6}\{\psi\}_m^T\left(\begin{Bmatrix}-1\\1\\0\end{Bmatrix}\begin{bmatrix}2&1&0\\&2&0\\&&0\end{bmatrix} + \begin{Bmatrix}0\\-1\\1\end{Bmatrix}\begin{bmatrix}0&0&0\\&2&1\\&&2\end{bmatrix} + \begin{Bmatrix}1\\0\\1\end{Bmatrix}\begin{bmatrix}2&0&1\\&0&0\\&&2\end{bmatrix}\right)\{\Omega\}_m \qquad (B.20)$$

Evaluating the remaining term on the right side, and subtracting it from Eq. (B.20) produces the identity. Hence, there is no arbitrariness in evaluating the terms stemming from this integration by parts, Q.E.D.

Straightforward evaluation of Eq. (B.18) for linear functionals yields

$$\int_{R_m} W\epsilon_{3ki}(\omega\psi_{,i})_{,k}\,d\tau = \int_{R_m} \{L\}\epsilon_{3ki}\{\psi\}_m^T\{L\}_{,i}\,\epsilon_{3ki}\{L\}^T_{,k}\,d\tau\,\{\Omega\} \qquad (B.21)$$

The alternator contraction produces the skew-symmetric matrix.

$$\epsilon_{3ki}\{L\}_{,i}\{L\}^T_{,k} = \frac{1}{x_2 y_3}\begin{bmatrix}0&-1&1\\1&0&-1\\-1&1&0\end{bmatrix} \qquad (B.22)$$

Equation (B.21) takes the form:

$$\int W\epsilon_{3ki}(\omega\psi_{,i})_{,k}\,d\tau = \frac{1}{6}\begin{Bmatrix}1\\1\\1\end{Bmatrix}\{\psi\}_m^T\begin{bmatrix}0&-1&1\\1&0&-1\\-1&1&0\end{bmatrix}\{\Omega\}_m \qquad (B.23)$$

Observation: The finite element solution algorithm produces several nonlinear matrix forms that are eligible for integration by parts. For example, in the differential equation for vorticity, an additional convection term results for nonuniform density flows of the form:

$$\int_{R_m} W\epsilon_{3ki}\,(\tfrac{1}{\rho})_{,k}\,\tfrac{1}{2}\,(\psi_{,\ell})^2_{,i}\;d\tau$$

This term vanishes identically, for linear functional approximations, unless an integration by parts is performed. Hence,

$$\int_{R_m} (\;)\,d\tau = \oint_{\partial R_m} W\epsilon_{3ki}\,(\tfrac{1}{\rho})_{,k}\,\tfrac{1}{2}\,(\psi_{,\ell})^2\,n_i\,d\sigma - \int_{R_m} W_{,k}\,\epsilon_{3ki}\,(\tfrac{1}{\rho})_{,k}\,\tfrac{1}{2}\,(\psi_{,\ell})^2\,d\tau \tag{B.24}$$

Equation (B.24) vanishes identically for $\psi_{,\ell}$ evaluated solely within R_m. However,

Theorem 5: Using linear functional representations for all dependent variables, the surface integral contribution to Eq. (B.24) can be made to cancel by pairs, upon Boolean assembly of the global solution algorithm, by averaging the available derivative operations over closure segments of the respective finite elements.

Proof: Referring to Figure B-2, along the common closure segment connecting nodes 1 and 2, the surface integral contributions within R_I and R_{II} can be written as

$$\int_{\partial R_I} (\;)\,d\sigma = \tfrac{1}{2}\int_0^{x_2} \{L\}\,\{\psi\}_I^T\,\{L_I\}_{,\ell}\,\{L_{II}\}_{,\ell}^T\,\{\psi\}_{II}\,\epsilon_{3ki}\,\{L\}_{,k}^T\,\{\tfrac{1}{\rho}\}_I\,n_i^I\,dx \tag{B.25}$$

$$\int_{\partial R_{II}} (\;)\,d\sigma = \tfrac{1}{2}\int_0^{x_2} \{L\}\,\{\psi\}_{II}^T\,\{L_{II}\}_{,\ell}\,\{L_I\}_{,\ell}^T\,\{\psi\}_I\,\{L\}_{,k}^T\,\epsilon_{3ki}\,\{\tfrac{1}{\rho}\}_{II}\,n_i^{II}\,dx \tag{B.26}$$

Since the inner product on $\psi_{,\ell}$ is commutative, and since the alternator ϵ_{3ki} removes arbitrariness in the evaluation of $\{L\}_{,k}$, and since n_i are antiparallel, then upon Boolean assembly of Eq. (B.25) and (B.26) into the global vector, cancellation by pairs is achieved, Q.E.D.

Completion of the matrix form of Eq. (B.24) is straightforward.

$$\int_{R_m} (\;)\,d\tau = -\int_{R_m} W_{,i}\,\epsilon_{3ki}\,(\tfrac{1}{\rho})_{,k}\,\tfrac{1}{2}\,(\psi_{,\ell})^2\,d\tau$$

The inner contraction upon $\psi_{,\ell}$ involves the matrix [B211S], Eq. (B.8), while the alternator contraction produces the negative of Eq. (B.22). Hence, the final form becomes:

$$\int_R (\;)\,d\tau = +\tfrac{1}{4}\,\{\psi\}^T\,[B211S]\,\{\psi\}\begin{bmatrix}0 & -1 & 1\\ 1 & 0 & -1\\ -1 & 1 & 0\end{bmatrix}\{\tfrac{1}{\rho}\}_m \tag{B.27}$$

APPENDIX C

SYSTEM INVARIANCE UNDER COORDINATE TRANSFORMATION

Use of a locally defined coordinate system for matrix moment evaluation is desirable from the accuracy standpoint and mandatory for evaluation of the nonlinear terms in the Navier-Stokes equations. The classical Method of Weighted Residuals (MWR) solution to a differential equation, $N(q) = 0$, involves approximation of the dependent variable by a function, q^*, and rendering the error orthogonal to the solution by formation of the residuals

$$\int_R W_j \, N(q^*) d\tau \equiv 0 \tag{C.1}$$

The finite element algorithm transforms formation to a finite element R_m, and there are as many equations (C.1) as unknown expansion coefficients in q^*_m on a local basis. The theoretical complication stemming from gradient boundary conditions can be neglected for this development.

Use of natural coordinate functions in a local Cartesian basis is preferred; hence, it is necessary to transform Eq. (C.1) from the global basis of its derivation. Assuming use of truncated power series, and to within an arbitrary coordinate translation, see Figure C.1, the global reference approximation function can be expressed as

$$q^*_m (x_i) = [x-X]^T [\Gamma]_m \{Q\}_m \tag{C.2}$$

In Eq. (C.2), the elements of the coefficient matrix $[\Gamma]_m$ involve only node point coordinates of R_m and are readily evaluated (reference 12). It is required to establish Eq. (C.2) in the x'_i basis, related to x_i by the tensor transformation law

$$x'_i = \beta_{ij} (x_j - X_j) \tag{C.3}$$

or equivalently, in matrix notation

$$\{x'\} = [\beta] \{x-X\} \tag{C.4}$$

In the primed coordinate system, Eq. (C.2) takes the form

$$q^*_m (x'_i) \equiv \{x'\}^T [\Gamma']_m \{Q\}_m \tag{C.5}$$

Combining Eqs. (C.4) and (C.2), and comparing to Eq. (C.5) provides the definition of $[\Gamma']_m$ as

$$[\Gamma']_m = [\beta]^{-1} [\Gamma]_m \tag{C.6}$$

Identifying the weighting functions for the Galerkin criterion within MWR as

$$W^m_j \equiv [\Gamma]^T_m \{x-X\} \tag{C.7}$$

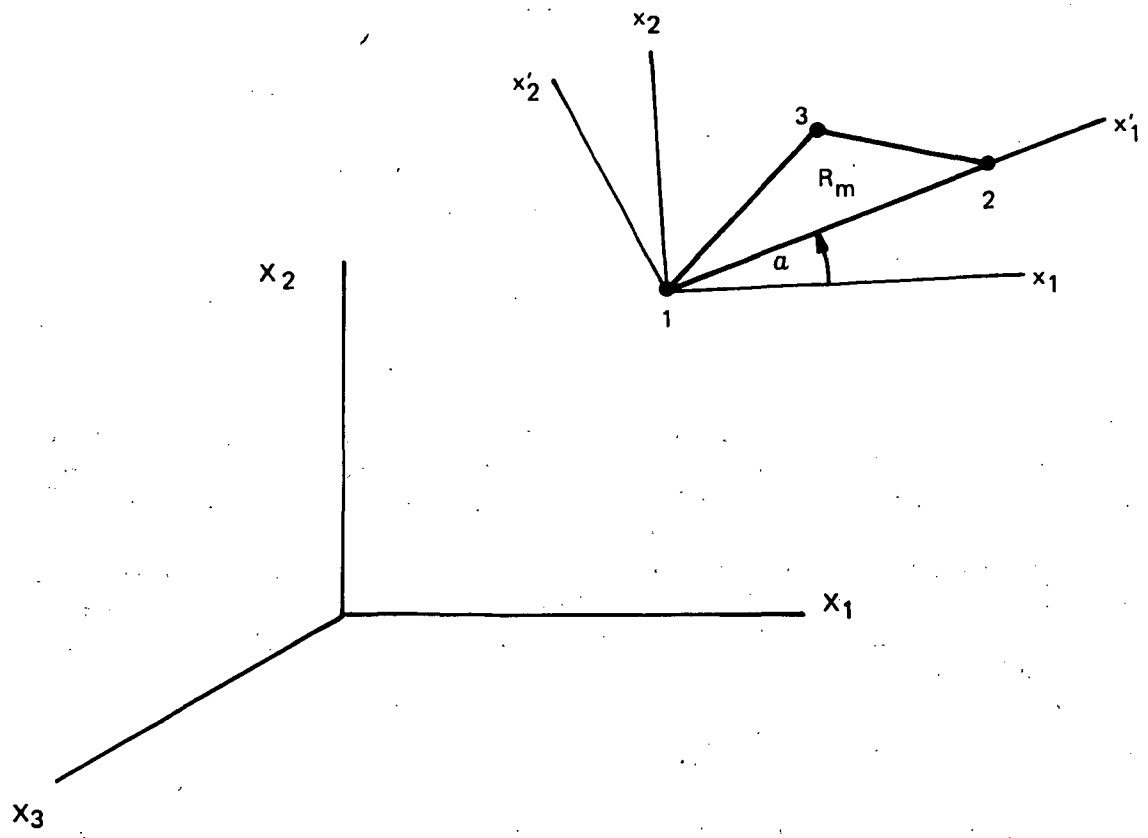

Figure C-1. Coordinate Systems for the Finite Element Solution Algorithm

and substituting Eqs. (C.4) - (C.7) into Eq. (C.1), the finite element residual expression for determination of the matrix elements of $\{Q\}_m$ becomes of the form

$$\int_{R_m} [\Gamma']_m^T \{x'\} N(q_m^*(x_i'))d\tau = 0 \tag{C.8}$$

It remains to cast the integration kernel $d\tau$ into the primed coordinate system to allow evaluation of equation (C.8) entirely in a local basis. From tensor field theory (reference 27), integration kernels in respective spaces spanned by Cartesian coordinate systems are linearly related by the determinant of the Jacobian of the transformation from a rectangular Cartesian basis, y_i, as

$$d\tau' = \frac{1}{|J|} d\tau \tag{C.9}$$

where

$$[J] \equiv \left[\frac{\partial y_i}{\partial x_j'}\right] \tag{C.10}$$

The determinant of the Jacobian for transformation to another rectangular Cartesian basis is unity. However, transformation to either cylindrical or spherical coordinates introduces nonvanishing coefficients. Hence, for the three subject transformations obtain, respectively

$$\begin{aligned} d\tau' &= d\tau \\ &= x_2 d\tau \\ &= x_1 \sin x_2 d\tau \end{aligned} \tag{C.11}$$

For cylindrical coordinates and axisymmetry,

$$x_2 = x_2(1) + x_1' \sin\alpha + x_2' \cos\alpha \tag{C.12}$$

where $x_2(1)$ is the radial coordinate of node 1 for R_m, Figure C.1. The equivalent expression for natural coordinate functions defined by

$$q_m^* \equiv \{L(x_i')\}^T \{Q\}_m \tag{C.13}$$

becomes

$$x_2 = x_2(1) + x_i' L_i \tag{C.14}$$

REFERENCES

1. Finlayson, B. A., and Scriven, L. E., "The Method of Weighted Residuals - A Review," App. Mech. Rev., 19, No. 9, 1966, 735-748.

2. Finlayson, B. A., and Scriven, L. E., "On the Search for Variational Principles," Int. J. Heat Mass Trans., 10, No. 6, 1967, 799-821.

3. Gurtin, M. E., "Variational Principles for Linear Initial-Value Problems," Q. App. Math, 22, 1964, 252.

4. Wilson, E. L., and Nickell, R. E., "Application of the Finite Element Method to Heat Conduction Analysis," Nuc. Engr. Design, 4, 1966, 276-286.

5. Baker, A. J., "A Numerical Solution Technique for Problems in Heat Transfer Employing the Calculus of Variations," Bell Aerospace Technical Note TCTN-1003, 1968.

6. Baker, A. J., "Numerical Solution to the Dynamics of Viscous Fluid Flow by a Finite Element Algorithm; A First Step Towards Computational Continuum Mechanics," Proceedings International Association for Shell Structures Pacific Symposium on Hydromechanically Loaded Shells, 1971.

7. Baker, A. J., "Finite Element Computational Theory for Three-Dimensional Boundary Layer Flow," AIAA Paper 72-108, 1972.

8. Baker, A. J., "Finite Element Solution Algorithm for Viscous Incompressible Fluid Dynamics," Int. J. Num. Mtd. Engr., 6, No. 1, 1973, 89-101.

9. Baker, A. J., and Zelazny, S. W., "A Theoretical Study of Mixing Downstream of Transverse Injection Into a Supersonic Boundary Layer," NASA CR-112254, 1972.

10. Hains, F. D and Baker, A. J., "Binary Diffusion of a Jet Imbedded in a Boundary Layer," AIAA J., 10, No. 7, 1972, 938-940.

11. Baker, A. J., and Manhardt, P. D., "Finite Element Solution for Energy Conservation Using a Highly Stable Explicit Integration Algorithm," NASA CR-130149, 1972.

12. Zienkiewicz, O. C., *The Finite Element Method in Engineering Science*, McGraw Hill, London, 1971.

13. Schlichting, H., *Boundary Layer Theory*, McGraw Hill, New York, 1960.

14. Gosman, A. D., Pun, W. M., Runchal, A. K., Spalding, D. B., and Wolfshtein, M., *Heat and Mass Transfer in Recirculating Flows*, Academic, London, 1969.

15. Carslaw, H. S., and Jaeger, J. C., *Conduction of Heat in Solids*, 1st Ed., Oxford, London, 1948, 275.

16. Gear, C. W., "Simultaneous Numerical Solution of Differential - Algebraic Equations," IEEE Trans., CT-18, 1971, 89-95.

17. Mueller, T. J. and O'Leary, R. A., "Physical and Numerical Experiments in Laminar Incompressible Separating and Reattaching Flows," AIAA Paper 70-763, 1970.

18. Dorodnitsyn, A. A., "Review of Methods for Solving the Navier-Stokes Equations," Proceedings Third Int. Conf. on Num. Mtd. in Fluid Mechanics, 1973, 1-11.

19. Macagno, E. O. and Hung, T. K., "Computational and Experimental Study of a Captive Annular Eddy," J. Flu. Mech. 28, 1, 1967, 43-64.

20. Blottner, F. G., "Finite Difference Methods of Solution of the Boundary Layer Equations," AIAA J., 8, No. 2, 1970, 192-205.

21. Murphy, J. D., "A Critical Evaluation of Analytic Methods for Predicting Laminar Boundary Layer Shock-Wave Interactions," NASA SP-228, 1969.

22. Reyhner, T. and Flugge-Lotz, I., "The Interaction of a Shock Wave with a Laminar Boundary Layer," Int. J. Nonlinear Mech., 3, 1968, 173.

23. Roache, P. J. and Mueller, T. J., "Numerical Solutions of Laminar Separated Flows," AIAA J., 8, No. 3, 1970, 530-538.

24. Carter, J. A., "Numerical Solutions of the Navier-Stokes Equations for The Supersonic Laminar Flow Over a Two-Dimensional Compression Corner," NASA TR R-385, 1972.

25. Ball, K.O.W., "A Summary of Factors Influencing the Extent of Separation of a Laminar Boundary Layer Due to a Compression Corner at Moderately Hypersonic Speeds," ARL 71-0065, 1971.

26. Carpenter, P. W., "A Numerical Investigation into the Effects of Compressibility and Total Enthalpy Difference on the Development of a Laminar Free Shear Layer," J. Flu. Mech., 50, 4, 1971, 785-799.

27. Sedov, L. I., *Foundations of the Nonlinear Mechanics of Continua,* Chap. 1, Pergamon, London, 1966.

28. Jaunzemis, W., *Continuum Mechanics,* Chap. 1, MacMillan, New York 1967.

29. Ericksen, J.L. and Truesdell, C., "Exact Theory of Stress and Strain in Rods and Shells," Arch. for Rat. Mech. and Anal., 1, 1958, 295-323.

★ U.S. GOVERNMENT PRINTING OFFICE: 1974—737-768/87 REGION NO. 3-11

NATIONAL AERONAUTICS AND SPACE ADMINISTRATION
WASHINGTON, D.C. 20546

OFFICIAL BUSINESS
PENALTY FOR PRIVATE USE $300

SPECIAL FOURTH-CLASS RATE BOOK

POSTAGE AND FEES PAID
NATIONAL AERONAUTICS AND SPACE ADMINISTRATION
451

U.S.MAIL

POSTMASTER : If Undeliverable (Section 158 Postal Manual) Do Not Return

"The aeronautical and space activities of the United States shall be conducted so as to contribute . . . to the expansion of human knowledge of phenomena in the atmosphere and space. The Administration shall provide for the widest practicable and appropriate dissemination of information concerning its activities and the results thereof."

—NATIONAL AERONAUTICS AND SPACE ACT OF 1958

NASA SCIENTIFIC AND TECHNICAL PUBLICATIONS

TECHNICAL REPORTS: Scientific and technical information considered important, complete, and a lasting contribution to existing knowledge.

TECHNICAL NOTES: Information less broad in scope but nevertheless of importance as a contribution to existing knowledge.

TECHNICAL MEMORANDUMS: Information receiving limited distribution because of preliminary data, security classification, or other reasons. Also includes conference proceedings with either limited or unlimited distribution.

CONTRACTOR REPORTS: Scientific and technical information generated under a NASA contract or grant and considered an important contribution to existing knowledge.

TECHNICAL TRANSLATIONS: Information published in a foreign language considered to merit NASA distribution in English.

SPECIAL PUBLICATIONS: Information derived from or of value to NASA activities. Publications include final reports of major projects, monographs, data compilations, handbooks, sourcebooks, and special bibliographies.

TECHNOLOGY UTILIZATION PUBLICATIONS: Information on technology used by NASA that may be of particular interest in commercial and other non-aerospace applications. Publications include Tech Briefs, Technology Utilization Reports and Technology Surveys.

Details on the availability of these publications may be obtained from:

SCIENTIFIC AND TECHNICAL INFORMATION OFFICE

NATIONAL AERONAUTICS AND SPACE ADMINISTRATION

Washington, D.C. 20546